DEVELOPMENT OF AN *IN VITRO* MODEL OF NEUROINFLAMMATION FOR STUDYING SECONDARY INJURY MECHANISMS IN TRAUMATIC BRAIN INJURY

A Thesis
Presented to
The Academic Faculty

By

James Thomas Shoemaker

In Partial Fulfillment
Of the Requirements for the Degree
Doctor of Philosophy in Biomedical Engineering

Georgia Institute of Technology

August 2015

DEVELOPMENT OF AN *IN VITRO* MODEL OF NEUROINFLAMMATION FOR STUDYING SECONDARY INJURY MECHANISMS IN TRAUMATIC BRAIN INJURY

Approved by:

Dr. Michelle LaPlaca, Advisor
School of Biomedical Engineering
Georgia Institute of Technology

Dr. Malú Tansey
School of Physiology
Emory University

Dr. Ravi Bellamkonda
School of Biomedical Engineering
Georgia Institute of Technology

Dr. Shean Phelps
Georgia Tech Research Institute
Georgia Institute of Technology

Dr. Edward Botchwey
School of Biomedical Engineering
Georgia Institute of Technology

Date Approved: April 20, 2015

ACKNOWLEDGEMENTS

I wish to thank my thesis advisor, Dr. Michelle LaPlaca for her guidance and mentorship throughout this long process. I would like to thank the members of my thesis committee: Dr. Ravi Bellamkonda, Dr. Edward Botchwey, Dr. Malú Tansey, and Dr. Shean Phelps for their advice and critical evaluation of my research. Their input has shaped this document into a better presentation of the fruits of this work. Current and former members and affiliates of the LaPlaca lab have provided valuable assistance and input throughout this journey. I would, in particular like to thank Dr. Brock Wester for teaching me to use the CAD software which was instrumental in the manufacture of the systems used in this research. Dr. Jelena Vukasinovic has often provided insight resulting in much needed changes in perspective.

I wish to thank Dr. Andrés García and the members of his lab for their generosity and assistance with ROS and NO imaging experiments. In particular, I would like to thank Dr. Shivaram Selvam for his aid in generating infrared dyes and in using the imaging instrumentation. I wish to thank Dr. Steve Potter and the members of his lab for their generosity and support. I would like to thank all of the past and current members of the Neurolab for participating in what I consider to be a fantastic environment of collaboration that truly elevates the quality of research for everyone involved.

I would like to thank Dr. Gregory Ford, Dr. Byron Ford, and Monique Surles from Morehouse School of Medicine who performed the mRNA gene chip analysis that greatly helped to characterize the response of the system designed here. I wish to thank Dr. Malú Tansey and Dr. Jae-Kyung Lee from Emory University who generously

contributed animals and resources that permitted the incorporation of adult microglia into the 3-D cultures, revealing the developmental effects on the inflammation response in this system.

I would like to thank the Biomedical Engineering department support staff for their tireless work that helps students navigate the graduate school process. I also wish to thank the staff of the Physiological Research Laboratory for the care and support they provide for the animals used in research.

I wish to thank my previous mentor Dr. James Lah for opening the door for me to pursue scientific research. To him, as well as to Dr. Allan Levey and Dr. Howard Rees, I owe a debt of gratitude for giving me the exposure to the laboratory environment that I have grown to love so much.

I would like to thank the many friends I have made during my time at Georgia Tech and in my previous life at Emory. Particularly to Dr. Kristen Cincotta and her husband Mike, you have saved my sanity with your friendship. Thank you for always being there.

Finally, I would like to thank my family. My sister Jocelyn and her husband Jay have always provided support for my educational endeavors. Their son, Hollon, while too young to appreciate the magnitude of this process has been a welcome distraction in recent years. My sister Bridget and her husband Billy have been there for all of my successes and failures throughout graduate school. Without the cheering and prodding from them and their daughters, Isabelle, Grace, and Sophia, I don't know if I would have successfully accomplished this goal. Lastly, and most importantly, I would like to thank my parents, Tim and Janet Shoemaker, for putting up with this process for so long. They

have supported me in every aspect of my life and have always endeavored to support me and the path I have chosen to follow. I owe them everything, and the completion of this degree was only possible because of their supportive efforts.

TABLE OF CONTENTS

LIST OF TABLES

LIST OF FIGURES

LIST OF SYMBOLS AND ABBREVIATIONS

2-D	two-dimensional
3-D	three-dimensional
AD	Alzheimer’s disease
ATP	adenosine triphosphate
BzATP	benzoylbenzoyl-ATP
BBB	blood-brain barrier
CCD	cell shearing device
CCI	controlled cortical impact
CNS	central nervous system
CSD	cell shearing device
CTE	chronic traumatic encephalopathy
DI	deionized
DIV	days *in vitro*
DPBS	Dulbecco’s phosphate-buffered saline
E#	embryonic day #
ECM	extracellular matrix
GFAP	glial fibrillary acidic protein
GFP	green fluorescent protein
H-ICG	hydro-indocyanine green
HBSS	Hank's balanced salt solution
HSPG	heparan sulfate proteoglycan
Iba1	ionized calcium binding adaptor molecule-1
ICE	interleukin converting enzyme

IFN-γ	interferon-gamma
IL	interleukin
IL-1ra	interleukin-1 receptor antagonist
iNOS	inducible nitric oxide synthase
LDH	lactate dehydrogenase
LPS	lipopolysaccharide
M-CSF	macrophage colony stimulating factor
MAP2	microtubule-associated protein 2
NO	nitric oxide
P#	postnatal day #
PBS	phosphate-buffered saline
PDL	poly-D-lysine
PDMS	polydimethylsiloxane
PIC	protease inhibitor cocktail
ROS	reactive oxygen species
TBI	traumatic brain injury
TLR4	toll-like receptor 4
TNF-α	tumor necrosis factor-alpha
TGF-β	tumor growth factor-beta

SUMMARY

A novel cell culture system was designed to serve as a model of neuroinflammation. Neurons, astrocytes, and microglia derived from embryonic and perinatal rat cortical tissue were combined in a three-dimensional hydrogel utilizing a method that facilitated cell maturation and viability. Chemical challenge of the cultures with a broad pro-inflammatory stimulus resulted in the production of inflammatory cytokines and other associated molecules commensurate with the response observed *in vivo* and in other *in vitro* systems. It was hypothesized that mechanical deformation of the multitypic neural cell cultures would produce a similar response and thus validate the system as an *in vitro* model of traumatic brain injury-induced neuroinflammation. Mechanical injury delivered using custom-manufactured culture chambers and injury devices successfully imparted a moderate level of cell death to the cultures. It was determined that a mechanically-induced inflammatory response required chemical stimulation prior to the injury. The research presented here describes the generation and characterization of a novel *in vitro* culture system and its implementation in experiments designed to model secondary injury mechanisms associated with injury-induced neuroinflammation. The findings of these studies, applications of the culture system, and future research avenues are discussed.

CHAPTER 1

INTRODUCTION

1.1 Motivation

Traumatic brain injury (TBI) is a major public health concern due to its incidence (1.7 million cases in the U.S. annually [1]) and lack of treatment options. Despite the development of promising therapies using animal models, none have translated successfully into clinical trials [2, 3]. The difficulty likely stems from the complexity of the response to an injury with causes that are highly variable. Numerous biochemical processes are triggered in response to TBI. The signaling cascades associated with inflammation are integral components of the secondary injury mechanisms that result in long-term deficits post-injury. Many of these cascades are initiated through microglial activation, which can be induced through post-injury death of, or cytokine release by other cell types, and propagated by the same mechanisms as well as by signaling from other microglia [4]. The activation of members of the family of purinergic receptors appears to play a key role in the response of microglia to injury.

Although *in vivo* models have the inherent advantage of using an intact animal in which the all of the systems involved in the injury response are present, they lack the controllability of cell culture models. *In vitro* tissue models provide a highly tunable environment in which *in vivo*-like phenomena can be simulated in a controlled, reproducible fashion. Further, three-dimensional (3-D) cell culture systems provide an environment in which cellular function is closer to *in vivo* than is observed using traditional two-dimensional (2-D) culture methods. Such models are ideally suited for studying and deciphering a complex tissue response such as that observed in TBI. The

first goal of this research was to generate a novel 3-D culture system that models the rodent brain *in vitro* and that is responsive to inflammatory stimuli. The cultures were comprised of primary neurons, astrocytes, and microglia derived from pre- and post-natal rat central neural tissue. Following optimization for cellular survival and confirmation of the inflammatory potential, the cultures were used to generate a model of mechanically-induced neuroinflammation. The goal of this step was to create a reproducible inflammatory response from a prescribed mechanical injury. Further, the system was utilized to study some of the underlying molecular mechanisms which contribute to the progressive inflammatory secondary injury mechanisms following TBI.

1.2 Background

1.2.1 TBI

1.2.1.1 Introduction

Injuries to the head by various means have long been a problematic occurrence, leading to lasting effects that manifest days, weeks, and even years after the insult. Clarification of the underlying processes responsible for the observed symptoms of TBI have only come in the last century as the field of neuroscience has developed. While the mechanics of injury in terms of the forces experienced by the skull and brain have been described using Newton's laws and the material properties of the affected tissues [5, 6], they only account for the gross tissue damage in the acute phase of injury. This is crucial for predicting survival and disability as a result of TBI, but a complete picture of the factors in play requires an understanding of how processes at the cellular level are affected by mechanical injury. As the field of neurotrauma has advanced, it has become clear that the long-term effects of TBI are caused by factors beyond cell death caused by

tissue damage. Rather, signaling cascades initiated in diverse cell types contribute to the complexity of the response.

The primary cellular components of the central nervous system (CNS) are neurons, astrocytes, microglia, and oligodendrocytes. Neurons are responsible for receiving, processing, and transmitting encoded information throughout the nervous system. Consisting of a cell body, signal-receiving dendrites, and signal-transducing axons, they have diverse morphologies that are dependent on function as well as anatomical location. Within the CNS, oligodendrocytes are the myelinating cells that provide axonal insulation for electrical signal transduction. The majority of the neuronal cell volume is contained outside of the cell body in the elaborate arborization of their processes which gives them a very high surface-area-to-volume ratio. While this allows for synaptic connections with other cells numbering orders of magnitude more than the number of the neurons themselves, it makes them a particularly vulnerable cell population due to the increased exposure to external stresses. Additionally, as they are post-mitotic cells, replacement of neurons can only be achieved through the differentiation of neuronal progenitor cells. In the acute phase following TBI, the mechanical loading can lead to increased membrane permeability and neuronal cell death. Subsequent effects include: diffuse axonal injury, cerebral ischemia, disruptions in ion homeostasis, and oxidative stress [7]. Astrocytes not only provide structural and nutritional support to neurons, but also participate in synaptic function [8] and blood-brain barrier (BBB) formation. TBI induces reactive astrogliosis which is characterized by cellular hypertrophy, increased proliferation, and an upregulation in cytokine production [9]. Microglia (discussed in detail in Section 1.2.3) act as the immune

effectors of the CNS, actively sampling the environment and becoming activated upon sensing that an insult such as TBI has occurred. Similar to astrocytes, they have a reactive phenotype characterized by proliferation and increased cytokine production. The differential responses of these cell types and the accompanying disruption of the cerebral vasculature contribute to the complex tissue response following TBI.

Perhaps the most confounding issue in the study of TBI is the heterogeneity of injury and injury response across the population. Modeling TBI is a difficult proposition due the variable severity and causes of injury, which include falls, vehicular accidents, concussive blasts, and sports-related injuries, among others. Cell and tissue-level events including cell death, astrogliosis, glial scar formation, BBB disruption, microglial activation, and inflammation can occur to varying degrees depending on injury severity. Further, the complexity of the cellular mechanisms underlying these events makes it difficult for a single model to be representative of all of the facets of the injury response [7, 10]. As such, many models isolate certain aspects of problem by either simplifying the injury mechanics or by targeting specific cellular populations. Unfortunately, no treatments that have shown promise *in vitro* or in animal models have translated to clinically effective therapies [2, 3, 11, 12]. No system can fully represent the injury responses encountered in the clinical setting, but given the prevalence of TBI, research continues to push forward to develop a translational model.

1.2.1.2 Epidemiology

TBI continues to be an ever-growing cause of morbidity and mortality throughout the developed world. With 1.7 million TBI events occurring every year in the U.S. alone, TBI is a major public health concern [1]. This includes severe, moderate, and mild TBI

(concussion) events. The CDC estimates that nearly one-third of injury-related deaths are at least partially caused by TBI, averaging 138 per day. Concussions, caused mostly by falls and motor vehicle collisions, make up the overwhelming majority of events and affect upwards of 600 out of 100,000 people worldwide annually [13]. This number includes an estimate of undiagnosed/untreated concussions which more than doubles the assessment based on hospital data [13]. The fact that so many people fail to seek medical attention following a TBI not only limits the data for epidemiological study, but also exposes one of the major barriers to successful TBI therapy. The symptoms associated with a mild TBI, particularly sports-related concussions, may not be deemed serious enough to seek medical care [14]. Thus, accurate assessment and diagnosis represents a critical need in the field of TBI research as increasing evidence implicates the long-term effects of injury in delayed dysfunction.

The effects of TBI are not limited to the acute tissue damage that occurs as a result of the injury. The long-term effects of TBI have come to national attention as they have manifested in soldiers returning from war [15, 16] and in former football athletes [17, 18]. Research has shown that underlying these long-term effects are secondary injury mechanisms rooted in inflammation that can contribute to deficits later in life [19-21] and to predisposition to neurodegenerative diseases such as Alzheimer's disease (AD) [22, 23]. These developments are exacerbated by repeated insults, leading to a condition known as chronic traumatic encephalopathy (CTE) [17, 20, 23]. According to the CDC, CTE is defined as a progressively degenerative tauopathy that is distinct from AD, but that similarly involves tau protein and relies on postmortem assessment for definitive diagnosis. Recent research utilizing diffusion tensor imaging has suggested the CTE may

be the link between TBI and AD [24]. Although the bulk of media attention has focused on soldiers and athletes, the chronic inflammatory processes induced by TBI can affect any patient. Indeed, given that most TBIs result from falls and car accidents, the long-term effects are a growing concern for the entire population and require increased research attention for the development of treatments.

1.2.1.3 Clinical trials

Many clinical trials have focused on the protection of the vulnerable population of neurons in the acute phase after TBI. However, due to the variability of injury severity and BBB involvement, the time window in which therapeutic intervention is feasible is very narrow. Since any primary necrotic tissue damage directly caused by the initial insult is difficult to address in the acute phase of injury, efforts to curb secondary injury mechanisms such as edema, intracranial pressure increase, excitotoxicity, and inflammatory cascades have been the primary goal. Phase III clinical trials from decades ago that included administration of drugs such as mannitol, barbiturates, nimodipine, PEG-SOD, and Selfotel showed no effect or overall benefit as a result of treatment [11, 12]. Physical methods of intervention such as induced hypothermia, while promising in Phase II trials, did not significantly affect outcome in Phase III trials [3]. More recently, progesterone administration following injury showed promising early results [25, 26], but failed to demonstrate clinical benefit in large-scale human trials [27, 28]. Clinical trials are ongoing for various treatments, but it is clear that there is a chronic issue of translational failure of TBI therapies.

The lack of success in the development of effective clinical therapies for TBI stems from a number of issues. First, there is the perennial problem of translation of

successful *in vitro* and *in vivo* therapies to the clinic due to the inherent differences in physiological response between small mammals and humans. Second, the heterogeneity of TBI and the response-based clinical assessment measures make for a murky picture of the underlying physiological dysfunction requiring treatment [29, 30]. Third, the narrow therapeutic window of TBI limits the feasibility of early intervention. Thus, some pharmaceutical treatments may have failed due to improper timing of administration [2]. This leads the need for an increase in the number of TBI clinical trials as they are far outpaced by those for related diseases such as stroke [31]. Finally, the design of translational studies needs to be based on sound pre-clinical *in vitro* and animal studies to maximize the potential for success [31]. Such a need could be addressed using systems that more accurately model the tissue environment following injury.

1.2.1.4 Pre-clinical experimental research

Recreating TBI in an *in vivo* animal model is a difficult proposition due to the complexity of the injury parameters. The forces experienced by a human body upon falling or during a motor vehicle collision are proportional to body mass. In order to generate forces upon an animal that are commensurate with those that impart injury to human brain tissue, the deceleration to impact would have to be of substantially greater magnitude. Therefore, most animal models of TBI tend to isolate a component of the injury mechanism and to deliver the insult such that comparable injury results in the animal. Typical animal models of TBI are controlled cortical impact (CCI), fluid percussion, and weight drop [32, 33]. Of these, the latter is the simplest, relying on gravitational acceleration of a weight through a guidance tube to deliver a closed-head diffuse injury to the animal [34]. Variation in applied force is achieved by changing the

initial height of the weight. Closed-head injuries are particularly difficult to characterize due to the heterogeneity introduced by the intact skull and head position. For this reason, a more recent injury model utilizing pneumatic impact of the unconstrained heads of mice incorporates high-speed imaging in order fully define the kinematics of closed-head injuries [35]. CCI is a more focused method of injury that utilizes a pneumatically-driven piston to injure the exposed brain [36]. Different levels of injury severity can be achieved by adjusting the velocity of the piston or the depth to which it impacts the tissue. Fluid percussion is the most well-characterized injury method and is an open-head injury that uses a pendulum to strike a piston adjacent to a fluid reservoir to generate a hydraulic pulse [37]. Injury severity is adjusted by the height of pendulum release. Fluid percussion injury can be used to model both focal and diffuse brain injury. While these as well as other methods of injury [33] have generated successful results in animals, there is concern as to what processes they are truly capable of modeling and how these translate to TBI events in humans [38, 39].

TBI has also been modeled *in vitro* using organotypic slice cultures as well as in 2-D and 3-D cell culture systems [40]. A major advantage of using slice cultures rather than dissociated cells is that the anatomy of the tissue is preserved. Organotypic slice cultures are simply thin sections of intact mouse or rat CNS tissue maintained in a culture environment for a period of time. The slices are most commonly hippocampal, but whole coronal, cortical, and thalamic slices have also been used [40]. Injuring tissue slices can be accomplished using a weight drop or impactor but can also be achieved by culturing the slices on a silicone membrane to which a prescribed biaxial strain can be applied [41, 42]. Implementation of this model has been shown to yield an injury response that was

comparable to *in vivo* injury [43]. The major disadvantages associated with organotypic slice cultures are maintaining cell viability and cellular organization. A study comparing mouse whole brain slices from neonatal and adult animals showed that although the neonatal tissue exhibited greater viability, there were significant structural changes in the neuronal and glial populations [44]. Thus, neonatal tissue is typically favored for slice cultures although it may not maintain its anatomical structure which is the major advantage of this method.

Dissociated primary cells can be cultured in 2-D or 3-D applications for the purpose of modeling TBI *in vitro*. In 2-D culture systems, injury to neurons or to neuron-astrocyte co-cultures can be achieved by applying uniaxial or biaxial strain to cells cultured on a flexible membrane similar to that described for the hippocampal slice cultures [45, 46]. This and similar flexible membrane-based methods are by far the most common for 2-D *in vitro* TBI models as cells cultured as a monolayer on a rigid substrate require an injury method such as fluid shearing [47]. Culturing primary neural cells in 3-D matrices greatly expands the options for mimicking TBI *in vitro* as the hydrogel in which they are cultured creates a tissue-like environment to which compression and shear can be applied. The choice of matrix depends on the desired mechanical properties and can also dramatically affect cell survival and morphology. Examples of biologically inert scaffolds include: agarose [48], alginate [49], self assembling peptide nanofibers [50-53] (e.g. RADA16), and silk fibroin [54, 55]. Examples of bioactive scaffolds include: extracellular matrix (ECM) proteins such as collagen and laminin [56], biologically-derived matrices such as Matrigel™ [57], and functionalized scaffolds that have had binding domains (such as RGD) covalently attached to otherwise inert structures to

promote cellular interaction [58]. The scaffold most commonly used in our lab is Matrigel™, which is derived from EHS tumors grown in mice and consists primarily of laminin, collagen IV, and heparan sulfate proteoglycan (HSPG) [57]. Neurons as well as neuron-astrocyte co-cultures grown in Matrigel™ scaffolds have been subjected to bulk shear [59-61] and compression [62] injuries using custom-made injury devices. The *in vivo*-like geometry afforded by 3-D culture more accurately reproduces the mechanical loading experienced by tissue *in vivo*.

Modeling TBI *in vitro* rather than *in vivo* has the advantages of higher throughput, increased homogeneity within samples, and consistency between samples. The downside is that it is even more difficult to capture the complexity of the full cell and tissue response since the system has been stripped down to one or two cell types. It is certainly debatable whether sacrificing complexity for control is a worthy exchange. However, if specific cell signaling pathways of interest can be accurately replicated, *in vitro* models can be powerful tools for studying diseases such as TBI.

1.2.2 Neuroinflammation

1.2.2.1 Introduction

Inflammation in the CNS shares many of the same characteristics as the innate immune response in the rest of the body in terms of the signaling pathways that are involved [63]. However, the CNS is literally set apart by the presence of the BBB. This complex interface regulator renders the CNS "immune privileged," meaning that if the integrity of the BBB is maintained, passage is limited to nutrients and molecules small enough to enter. Since the BBB is not readily permeable to antibodies and tightly regulates lymphocyte transport, the CNS remains largely sequestered from the

mechanisms of acquired immunity. It therefore falls to resident cells to carry out an inflammatory response to an insult.

Astrocytes, comprising the highest proportion of cells in CNS, become reactive in response to injury and contribute to the inflammatory response through the release of cytokines, proliferation, and scar formation [64]. It is microglia, however, that act as the sentinels of the brain. They achieve this role by constantly sampling their environment for signals indicating any form of injury [65, 66]. If detected, they can rapidly respond by releasing cytokines, acting as macrophages, or even by mobilizing to the injury site and proliferating [67]. As such, they are considered to be the immune system of the CNS. Astrocytes and microglia are also key players in a BBB-breaching event. Both cell types attempt to create a barrier around the insult to mitigate the damage caused by the presence of blood and the resulting infiltration of lymphocytes. In the case of severe infection, microglia can additionally act as antigen presenting cells to the invading lymphocytes [68]. Although isolated from the rest of the body, the CNS has the means of mounting an innate immune response to an insult as well as the ability to interact with the acquired immune system in the event of a BBB breach.

1.2.2.2 Cytokines and other signaling molecules

At the heart of inflammatory signaling are cytokines, polypeptides that are rapidly released after insult to stimulate a response from other cells. Included in this class of molecules are interleukins, interferons, tumor necrosis factors, chemokines, and certain growth factors [69]. Cytokine release can induce pro- inflammatory or anti-inflammatory responses in an autocrine or paracrine manner. Key pro-inflammatory cytokines include interleukin 1 (IL-1), IL-6, and tumor necrosis factor-α (TNF-α), while key anti-

inflammatory cytokines include IL-10 and tumor growth factor-β (TGF-β). It should be noted that both pro- and anti-inflammatory activities are known to be exhibited by cytokines such as IL-1 [70] and IL-6 [71] depending upon the location in the body and the nature of the signaling trigger. Cytokine release is a rapid process as many exist as immature molecules that are cleaved into mature, active forms in response to injury [69]. Inflammatory cytokines appear to be integral to the pathophysiology of TBI [72], and are attractive candidates for biomarkers [73] as well as for therapeutic intervention [74].

One of the most well studied cytokine families is that of IL-1. This group of proteins consists of IL-1α and IL-1β as agonists of the IL-1 receptor and IL-1 receptor antagonist (IL-1ra) as a competitive inhibitor of the IL-1 receptor [74]. Il-1β is of particular interest in the study of neuroinflammation as it is released in response to a variety of insults. The immature, pro-form of IL-1β is activated by enzymatic cleavage by interleukin converting enzyme (ICE, also known as caspase-1), which produces a mature, active molecule that is released from the cell [69]. While release of mature IL-1β has been triggered by exposure to the bacterial endotoxin lipopolysaccharide (LPS) in both *in vivo* [75] and *in vitro* [76] studies, the role of ATP signaling mediated by purinergic receptor transmission has expanded the understanding of the control of this mechanism [77-79]. However, this is not the sole mechanism by which activation can occur. IL-1β plays a major role in the innate immune response and its immature form has been shown to be cleaved extracellularly by a neutrophil enzyme [80]. In the context of neuroinflammation, the caspase-1-mediated cleavage pathway is of particular interest as it is the primary mechanism activated by acute infection as well as by injuries such as stroke or TBI [81] and is commonly studied *in vivo* [82, 83]. This method of IL-1β

release is dependent upon the formation of an inflammasome, a large multi-protein complex that forms in response to microbial presence, injury, or metabolic disruption, and recruits caspase-1 [63].

Additional pro-inflammatory species released primarily by microglia are reactive oxygen species (ROS) and nitric oxide (NO) [9]. Both are free-radical molecules, but whereas ROS such as superoxide bear their lone electron on an oxygen atom, NO bears it on a nitrogen atom. Superoxide and NO are generated by the enzymes NADPH oxidase and inducible nitric oxide synthase (iNOS), respectively. While they do not fall into the category of cytokines, they are key players in the more toxic cascades of neuroinflammation [84]. Neurotoxicity has been observed as a result of the presence of both superoxide [85] and NO [86] induced by TBI *in vivo* and by a combination of LPS and interferon gamma (IFN-γ) *in vitro*, respectively. However, another *in vitro* study found that increased neuronal death in neuron-glia co-cultures required paired stimulation of both NADPH oxidase and iNOS [87]. These varied outcomes indicate that neuroinflammation is a complex interplay of cellular signaling that is highly dependent on the system used for study.

1.2.2.3 In vivo and in vitro models

Neuroinflammation in response to TBI has been studied for decades in the clinical setting as well as in animal models [72]. The importance of cytokine signaling in the secondary injury mechanisms following TBI have made them prime targets for study in both *in vivo* and *in vitro* systems. In particular, IL-1β has been the focus of TBI-induced inflammation in animal models [64]. The effect of TBI on IL-1β release in rats has been extensively studied using various injury methods including: weight drop [88], controlled

cortical impact (CCI) [89], fluid percussion [82, 90], and long-term probe implantation [75]. With the weight drop and fluid percussion models, levels of IL-1β protein and mRNA increased within hours after injury, while a delayed release (24-48 hours) of IL-1β protein was observed in the milder probe implantation model. Time points earlier than 24 hours were not reported for the CCI model. Compared to the abundant *in vivo* studies of neuroinflammation, there is a relative paucity of *in vitro* studies. Chemical stimulation with a combination of LPS and IFN-γ-induced increases in TNF-α, IL-6, and NO in co-culture models consisting of primary neurons and either primary microglia or a microglia cell line [91]. A weight drop injury model of mouse organotypic slice cultures was found to cause an increase in IL-1β mRNA expression that peaked 4 hours after injury [92]. Exposure of various astrocyte, microglia, and brain endothelial cell lines to IL-1β caused an increase in mRNA levels of IL-6 and a number of chemokines [93], demonstrating the downstream pro-inflammatory activity of IL-1β. Although there are many fewer *in vitro* studies, one important comparison to make with the *in vivo* results is the timeline of cytokine release. The *in vivo* weight drop and fluid percussion methods of TBI demonstrated detection of elevated IL-1β protein between 3 and 8 hours after injury [82, 88] and IL-1β mRNA as early as 1 hour after injury [90]. The 4 hour peak of IL-1β mRNA in injured hippocampal slice cultures agrees with these data [92]. Regardless of the specific timeline for each study, cytokines were detected within the first 24 hours after injury. This information is critical to the design of future *in vitro* systems.

As with any inflammation, the case of neuroinflammation brings up the question as to whether the response is ultimately helpful or harmful to the damaged tissue. Indeed, this question extends to microglia. Both their macrophage-like scavenging ability [94]

and their release of anti-inflammatory cytokines [4, 95] promote healing pathways. However, their pro-inflammatory signaling and cytotoxicity mediation can promote further damage. Neuroinflammation, and specifically microglia, represent an enticing target for therapeutic intervention, but methods for achieving this remain elusive due to the poor understanding of the graded injury response. An ideal treatment would permit the initial beneficial inflammation, while limiting the prolonged, potentially chronic inflammation. In order to reach this point, the complex nature of microglia must first be better understood.

1.2.3 Microglia

1.2.3.1 History

Microglia are small, dynamic cells of the CNS with diverse immune-related function. Since first described by Pío del Río-Hortega in 1919, microglia have become an increasingly popular subject for biomedical research. The function, and consequently the origin of microglia has been studied since their identification. Although they carry the term "glia" in their name, determination of their origin has confirmed del Río-Hortega's assertion that they arise from the mesoderm, rather than from the ectoderm [68, 96]. They exhibit characteristics and markers of various cell types arising from the middle germ layer including dendritic cells and macrophages [97, 98]. Recent research has traced the lineage of microglia to primitive macrophages in the yolk sac [99], and more recently, a specific erythromyeloid precursor has been identified [100]. Due to the developmental disparity between microglia and the other cells of the CNS, questions quickly arose as to how and when they appear in the brain. Studies have determined that very early in embryogenesis, the cells migrate into the neuroectoderm and take up permanent residence

as a self-maintaining population [99, 101, 102]. Despite the extensive research focused on microglia, a complete understanding of their function is still lacking.

1.2.3.2 Function

Microglia compose approximately 10-20% of the adult glial cell population [103]. They are capable of multiple functions, such as macrophage-like scavenging, antigen presentation, and rapid proliferation and cytokine release (IL-1, IL-6, TNF-α, TGF-β1, etc) in response to various insults [68, 76, 95]. Microglia exhibit both neuroprotective and cytotoxic characteristics depending upon the biological context [104, 105], rendering their role in the CNS paradoxical. Microglia exist in one of at least two morphologically and functionally distinct states *in vivo*, known as the ramified (quiescent) and the amoeboid (activated) states. In the ramified state, the microglia are characterized by a small soma and an extensive network of processes. Although considered "quiescent," it has been shown that ends of the processes of these cells are highly motile and are actively sampling the local environment [65, 66, 96]. In response to stimuli (ATP from dying cells, ROS, pro-inflammatory cytokines, etc.), microglia release cytokines and chemokines, extend processes toward an area of insult [65], or retract their processes and transition to the activated, amoeboid morphology. In the amoeboid state, microglia can migrate along chemokine gradients towards an injury site and rapidly proliferate [96]. Their extensive expression throughout neural tissues and their diverse ability to sense and respond to environmental cues ideally place microglia in the role of sentinels of the CNS.

1.2.3.3 Purinergic receptors in microglia

Purinergic receptors are a large class of ubiquitously expressed surface receptors for which members of the purine class of molecules such as adenosine, ADP, and ATP as

well as pyrimidine derivatives such as UDP and UTP are agonists [106]. The many members of this receptor family are subdivided into three main groups. The P1 receptors are metabotropic and stimulated by adenosine. The P_2X receptors are ionotropic and mostly stimulated by ATP. The P_2Y receptors are metabotropic and are stimulated by ADP, ATP, UDP, or UTP, depending on the subtype. Due to their extensive expression throughout the body and the availability of their agonists, purinergic receptors are responsible for a very diverse array of functions.

Of particular interest is the role that purinergic signaling plays in microglial function. The G-protein coupled P_2Y_6 and P_2Y_{12} receptors are integral to microglial phagocytic activity [107] and to the mechanism of process extension [108], respectively. However, one of the most studied purinergic receptors in microglia is the P_2X_7 receptor. Expressed in microglia, astrocytes, and debatably in neurons [109], the receptor functions as a cation channel with ATP-stimulated ion channel opening [106]. Typically, the cation channel is composed of a homotrimeric conformation of P_2X_7 receptor subunits and it is particularly permeable to calcium under normal stimulation conditions [110]. Upon chronic activation with ATP, pore dilation occurs, reducing the selectivity of the channel and allowing molecules up to 900 Da to pass through [111]. The role of this large pore formation is not well understood. It can lead to apoptosis, resulting in it being referred to as a "death receptor" [112, 113]. However, there is debate as to whether stimulation conditions sufficient to induce cell death occur *in vivo* [114, 115].

Perhaps the most studied aspect of the P_2X_7 receptor is its role in the processing and release of IL-1β [77-79, 116]. This is a key function of microglia as IL-1β release is one of the first inflammatory responses of these cells to insult [117]. Activation of the

P_2X_7 receptor results in conversion of IL-1β from an immature to a mature form by caspase-1, followed by its release from the cell. This process is inflammasome-mediated, and involves signaling through pannexin-1, a protein which has also been implicated in P_2X_7 pore formation [118, 119]. Due to the high level of expression in microglia [120] and its involvement with ion transport, cytokine release, and cell death, the P_2X_7 receptor represents a potential therapeutic target in diseases involving neuroinflammation [121, 122]. Indeed, purinergic signaling has recently been shown to play a role in TBI through calcium wave propagation in astrocytes [123]. A better understanding of the role this receptor plays in microglia and how alteration of its signaling may affect the cells could lead to promising new treatments for TBI.

1.2.3.4 Studying microglial injury

Performing studies on microglia *in vivo* and *in vitro* each presents its own set of challenges. Because many microglia responses can be transient, the typical method of exposing animals to a particular treatment and subsequently sacrificing them at various time points only provides a glimpse into the dynamic characteristics of these cells. This traditional method has been used to study the early development of microglia [124] as well as to assess cellular response to *in vivo* injury [125]. However, *in vivo* imaging provides a much better picture of how these cells respond in real-time. Using a thinned-skull preparation on mutant mice to image GFP-positive cortical microglia with two-photon confocal microscopy, it has been demonstrated that the processes of microglia are highly motile in the resting state and that they rapidly extend to surround the focal region of a laser ablation injury [65, 126]. Additionally, it was shown that application of ATP to the cortical tissue via a craniotomy also induced microglia process extension [65].

Further study of resting microglia using a similar method revealed that the processes make contact with synapses and that the contact duration is dependent on the functional state of the synapse [66]. All of these microglial responses were rapid (on the order of minutes), thus elucidating previously hidden cellular behavior.

The difficulty underlying *in vitro* studies of microglia centers around maintaining their dynamic nature once isolated from CNS tissue. As evidenced by the constant movement of their processes and potential for rapid response to insult, removing microglia from their cellular and matrix signaling sources may limit their ability to exhibit *in vivo* function *in vitro*. Primary microglia in mixed cortical cultures from embryonic rats are initially few in number with a mostly rounded morphology, but later proliferate and exist as a mixed population of both rounded and process-bearing cells [127]. Isolation of primary rat microglia can be achieved by agitating confluent mixed neonatal glial cultures in which microglia are loosely adhered to the dense lawn of astrocytes [128]. This harvesting process has been performed repeatedly on the same cultures of mouse mixed glia without the loss of phenotype [129]. However, once isolated, the proliferation rate of microglia is very low compared to when co-cultured with mitogen-producing astrocytes. Other options for *in vitro* study include immortalized cell lines (such as BV-2), adult microglia, and organotypic slice cultures. However, each method carries its own inherent advantages and disadvantages [130].

In vitro studies have further implicated ATP in pro-inflammatory microglia responses. Primary rat mixed glial cultures treated with ATP exhibit increased IL-1β release and endogenous astrocyte-derived ATP is a key factor for inducing microglial release of IL-1β [131]. In neuron-microglia co-cultures derived from rat tissue,

stimulation with either ATP or benzoylbenzoyl-ATP (BzATP) (a highly potent P_2X_7 receptor agonist) resulted in neuron-specific cell death [115]. Isolated microglia have also been studied *in vitro* to explore the mechanisms underlying process retraction following insult. Using isolated primary GFP-positive mouse microglia grown on a thin layer of Matrigel™, real-time imaging has shown that LPS-treated microglia were repelled by ATP stimulation while untreated microglia were attracted to it [132]. Further, it was determined that process retraction of activated microglia was mediated by the adenosine A_{2A} receptor, a process that was confirmed to also occur in human microglia [132]. ATP-induced process extension by rat microglia into collagen gels has also been demonstrated *in vitro* [133]. While these studies have provided a deeper insight into the mechanisms underlying characteristic microglial behavior, there remains a great deal of work to capture the complexity of the *in vivo* injury response in an *in vitro* system.

Microglia are the key immune effectors of the CNS, and are therefore a potential target for the therapeutic intervention in neurodegenerative diseases, and particularly in TBI [20, 134, 135]. From the initial release of both pro-inflammatory and anti-inflammatory cytokines to proliferation and clearing of dead cells and debris, the microglial response to TBI is critical to recovery [67]. As microglia have been shown to exhibit these functions in culture [91, 129, 136], an *in vitro* model of neuroinflammation must include these cells in order to fully capture the events that may lead to the long term effects of TBI.

1.3 Research outline

The goal of developing an *in vitro* model of neuroinflammation for studying secondary injury mechanisms associated with TBI was addressed through a series of

specific aims. This section of the dissertation is the conclusion of the introductory chapter. Aims 1A and 1B describe the development and characterization of a novel 3-D multitypic neural cell culture system and its ability to model neuroinflammation. These aims are presented in Chapters 2 and 3, respectively. Aims 2A and 2B describe the adaptation of an *in vitro* mechanical injury model for these cultures and its implementation in studies of mechanically-induced neuroinflammation. These aims are presented in Chapters 4 and 5, respectively. A discussion of the injury model and its limitations as well as of the future directions for the novel culture system is presented in Chapter 6.

1.3.1 Specific Aim 1A. Develop a robust neural 3-D culture system to generate an *in vitro* representation of rat cortical tissue

1.3.1.1 Objective

Develop and characterize a 3-D multitypic culture system which incorporates primary microglia in addition to neurons and astrocytes.

1.3.1.2 Approach

Mixed glial cultures from neonatal rats were grown in a manner that favors the proliferation of both astrocytes and microglia. These cells were combined with embryonic rat-derived neurons and dispersed in a 3-D gel of ECM proteins to generate a culture which was representative of the *in vivo* rat cortex. Specific phenotypic markers were used to verify the presence of a mature cell types. Assessment of cell viability at various time points established the health of the baseline cultures as they developed and matured.

1.3.2 Specific Aim 1B. Demonstrate induced inflammation in 3-D multitypic neural cell cultures

1.3.2.1 Objective

Use a pro-inflammatory stimulus to induce the release of known markers of inflammation *in vitro*.

1.3.2.2 *Approach*

Chemical stimulation of the 3-D cultures in the form of LPS was used to induce a pro-inflammatory microglial phenotype, the achievement of which was assessed by changes in cell morphology, changes in levels of mRNA expression of key cytokines, the release of pro-inflammatory cytokines such as IL-1β, and the generation of NO.

1.3.3 Specific Aim 2A. Adapt an *in vitro* mechanical injury model of TBI for 3-D multitypic neural cell cultures

1.3.3.1 Objective

Subject 3-D multitypic neural cultures to mechanical deformation to recreate the effects of cortical injury *in vitro*.

1.3.3.2 Approach

Custom-made shear and compression devices were used to injure the 3-D cultures. Shear injury was imparted at a range of strains and strain rates with the goal of reducing the viability of a subpopulation of cells within the culture. Compression injury was imparted with a piston traveling at a range of velocities to specified depths in order to produce consistent, spatially graded injuries within the culture.

1.3.4 Specific Aim 2B. Demonstrate mechanically-induced neuroinflammation in 3-D multitypic neural cell cultures

1.3.4.1 Objective

Subject multitypic neural 3-D cultures to a mechanical insult to model TBI *in vitro* to induce an inflammatory response by the microglia and compare this to the chemically-induced response.

1.3.4.2 Approach

Intracellular and extracellular protein levels of the pro-inflammatory cytokine IL-1β were assessed by various immunological methods to determine the state of inflammation in the culture at various time points post-injury. mRNA levels of IL-1β as well as other inflammatory cytokines were determined to obtain a more detailed picture of the mechanical injury response at the genetic expression level. Additionally, the generation of NO and ROS in response to injury was measured. The outcome measures of these studies were compared to the response of the cultures to chemically-induced inflammation which was a positive control for the expected inflammatory response.

CHAPTER 2

DEVELOPMENT OF A 3-D MULTITYPIC NEURAL CELL CULTURE SYSTEM

2.1 Introduction

The initial goal of this research was to generate a neural cell culture system that better approximated the composition of living cortical tissue than previous models through the inclusion of neurons, astrocytes, and microglia. Creating a reliable *in vitro* representation of living mammalian tissue is a difficult task in which many compromises must be made. Physical limitations of a synthetic system and the absence of other interacting organs and organ systems contribute to the artificiality of the construct. At the most basic level, *in vitro* research utilizes primary or immortalized cells grown in a monolayer on a rigid plastic or glass surface. Atmospheric oxygen levels are required to overcome diffusion limitations which must be addressed due to the lack of a circulatory system for oxygen transport. Specifically, the atmospheric partial pressure of oxygen limits its diffusion rate through the cell culture medium thereby limiting the available oxygen for cellular respiration. Carbon dioxide is delivered at a concentration much higher than atmospheric levels to maintain pH balance through the bicarbonate buffering system present in living mammals. Again, the lack of active transport in the system necessitates this condition. These issues are further compounded with increasing cell density as the demand for oxygen and nutrients increases proportionally. However, to achieve a more physiologically relevant *in vitro* model, closer approximations of cell density and the ECM environment must be created.

3-D cell culture models have the distinct advantage of providing a support matrix that permits cells to grow and interact in a more natural geometry. However, with this

advantage come further diffusion limitations for oxygen and nutrient delivery. In the case of neuronal cultures, this is a critical problem. Culturing neurons *in vitro* requires a host of medium additives to ensure cellular survival and function. Unlike dividing cells such as fibroblasts or even astrocytes, the number of primary neurons grown in a dish will not increase. As such, the goal is to slow the decline and death of the cells in the population for as long as is necessary for experimentation. This can be a very difficult task since neurons *in vivo* have an extensive support network composed of other cell types.

Co-culturing neurons with astrocyte feeder-layers has long been a common method for improving neuronal survival and function [137, 138]. Typically, neurons and astrocytes are grown on separate 2-D surfaces closely apposing each other. The separation is required since the dividing astrocytes could overwhelm the neurons were they to be grown together on the same surface. 3-D culture systems allow for multiple cells types to be grown together and for them to interact in a manner that more closely resembles the *in vivo* brain in terms of geometry and connectivity. 3-D co-cultures have been used in our lab to study TBI *in vitro* [60, 62]. However, while a co-culture model used in this field can aptly reproduce the *in vivo* injury response of neurons and astrocytes, it is limited in scope as there is minimal representation of injury-induced inflammation which leads to secondary tissue damage and potential long-term injury effects.

Absent from previously studied 3-D culture systems containing neurons and astrocytes are microglia, the myeloid-derived immune effectors of the CNS. As discussed in Chapter 1, microglia not only play a crucial role in mounting an inflammatory response to various insults, they are vital for tissue protection and maintenance in the

normal brain. Therefore, a cell culture model of neural tissue must necessarily contain microglia if it is to accurately represent the brain in both resting and injured states. The goal of the work presented here is to produce such a representation through optimization of methods to generate viable, 3-D multitypic cultures consisting of neurons, astrocytes, and microglia.

2.2 Neuron and astrocyte 3-D co-culture model

The previous co-culture model utilized by our lab was intentionally designed to eliminate microglia due to their unfavorable reputation as a confounding presence in neural cell culture studies [139]. The neurons for these cultures were generated from the cortical tissue of embryonic day 18 (E18) rat fetuses. These cells were combined with purified astrocytes generated from postnatal day 0 or 1 (P0 or P1) rat pups. The purification procedure was adapted from a protocol published by McCarthy and deVellis [140]. Briefly, the mixed glial cultures were grown to confluence with agitation manually applied at each feeding to dislodge microglia and oligodendrocytes. Cells were passaged a minimum of four times prior to use in co-cultures and were not maintained beyond the tenth passage. The cells were combined at specified ratios, suspended in Matrigel™, and plated in 3-D to a thickness of between 0.5 and 1.0 mm. Complete culture methods can be found in Appendix A.

These co-cultures were used in mechanical injury studies using custom-made devices discussed in Chapter 4. These studies were designed to examine the effects of injury type (shear or compression) and severity (strain and strain rate) on outcome measures such as cell viability [60, 62], induced astrogliosis [60], and membrane disruption [62]. It was demonstrated that these acute injury effects in this co-culture

model were strain and strain rate dependent. These findings provided insight into some of the mechanisms underlying the acute cell response to mechanical injury.

As with any *in vitro* system, the co-culture model has limitations. Although many aspects of the acute mechanical injury response are effectively represented, the absence of microglia in the culture eliminates the major inflammatory component. Microglia not only play a role in the acute injury phase, but are central players in the chronic phase of injury which leads to initiation of secondary injury cascades and potential long-term ramifications such as neurodegenerative disease. Therefore, in order to more fully model injury-induced mechanisms *in vitro*, it is necessary to include these cells.

2.3 Neuron, astrocyte, and microglia 3-D multitypic culture model

The overall goal of developing a 3-D multitypic neural cell culture system is to create an *in vitro* representation of cortical brain tissue that can effectively model the *in vivo* responses to injurious stimuli. With that in mind, the specific objectives for the culture model must be established. First, all three cell types: neurons, astrocytes, and microglia must be present throughout the range of time points from which data will be taken (7-14 days). Second, the viability of the cells in the culture must be high at these same time points. If there is a preponderance of cell death in naïve cultures, this would certainly confound the assessment of cellular response post-injury. Finally, the culture should be responsive to stimuli that elicit inflammation in other models. The first two objectives will be addressed in the next sections. The latter will be addressed in Chapter 3. In order to achieve these objectives, an iterative process of culture development and testing was implemented wherein various cell harvesting and plating methods were used.

2.3.1 Initial method: augment previous co-culture model with the addition of microglia

The first 3-D multitypic cultures ultimately required three separate dissections of cortical tissue to generate neurons, astrocytes, and microglia. The initial step in the development of the culture system was to become proficient at the established techniques for generating 3-D co-cultures of neurons and astrocytes. As previously mentioned, and described in detail in Appendix A, neurons were acquired from dissociated cortical tissue from E18 rat embryos. Astrocytes were acquired from dissociated cortical tissue from P0-P1 rat pups and were purified through agitation and passaging a minimum of four times and a maximum of ten. The mechanical agitation serves to remove "contaminating" microglia and oligodendrocytes to produce a pure population of astrocytes. These cell types tend to grow loosely attached to the surface of astrocytes. Microglia, in particular, will begin to proliferate once a confluent bed of astrocytes has been established. It is this characteristic that was exploited in the first attempt at generating the multitypic cultures.

For many years, published research has described a simple method for harvesting microglia from mixed glial cultures derived from neonatal rats [76, 128, 140, 141]. Briefly, mixed glial cultures from rats aged P0-P4 were maintained for up to two weeks and subsequently shaken to remove the loosely adherent cells to the medium. These detached cells were then plated separately as a purified population of microglia. Thus, the first method to incorporate microglia in the neuron-astrocyte co-cultures was to generate a parallel set of glial cultures from which the microglia could be harvested. P0-P1 pups were used to generate a colony of purified astrocytes. P0-P4 pups were used to generate glial cultures from which the microglia were harvested. Finally, E18 embryos were used as an enriched source of neurons. The latter harvest was carried out just prior to 3-D

plating to ensure a high viability of neurons. Thus, the timing of the microglia dissection and the expansion of the astrocytes was critical to ensure sufficient cellular material was available.

On the day of 3-D plating, the neurons were harvested from E18 embryos, microglia were shaken from the mixed glial cultures, and astrocytes were trypsinized and collected from enough flasks to give the desired number of cells. Neurons, astrocytes, and microglia were combined at a ratio of 5:5:1, respectively. The cells were then suspended in high-concentration, growth factor-reduced Matrigel™ to a final matrix protein concentration of 7.5 mg/mL and to a final total cell concentration of 4,000 cells/mm^3. The cultures were then plated into either custom-made 3-D culture chambers (see Section 4.2.2.1) or into commercially available multiwell plates to a thickness of either 0.5 or 1.0 mm. Regardless of the chamber used, the surface was coated with 100 μg/mL poly-D-lysine (PDL) (Sigma-Aldrich, St. Louis, MO) for 24-48 hours. This is a higher concentration and longer coating time than typically used for 2-D cultures, but it was observed that the gel remained more adherent after two weeks *in vitro* using these conditions. While the astrocyte and mixed glial cultures were fed with DMEM/F12 (Life Technologies, Carlsbad, CA) containing 10% fetal bovine serum (Atlanta Biologicals, Norcross, GA), the medium for the 3-D multitypic neural cultures was serum-free to inhibit glial proliferation. 3-D cultures were maintained in Neurobasal medium supplemented with L-glutamine as well as with B-27 and G-5 supplements (all from Gibco®/Life Technologies/Invitrogen). B-27 supplement promotes the survival of primary neurons *in vitro* [142] and G-5 supplement is conducive to glial survival in the absence of serum [143].

The limiting factor in the number of 3-D cultures generated using this method was the yield of microglia. While more mixed glial cultures could be plated to produce more microglia, the resulting cost of maintenance would not have been justified by the modest increase in yield. Rather, the method was modified to incorporate exposure to macrophage colony stimulating factor (M-CSF) (Life Technologies), a secreted cytokine that, among other functions, promotes macrophage and monocyte proliferation and has been shown to induce proliferation in adult mouse microglia *in vitro* [144]. As microglia develop from a monocyte lineage, they also proliferate in response to stimulation with this cytokine. When mixed glial cultures were exposed to M-CSF (100 ng/mL), the increase in the number of loosely adherent, phase-bright microglia atop the astrocyte monolayer was easily observed after just 24 hours. The effect peaked around 48 hours and was not substantially enhanced with exposure to fresh M-CSF. Treatment of mixed glial cultures with M-CSF 48 hours prior to harvest for 3-D plating resulted in a sufficient yield for 3-D culture experiments.

Immunocytochemistry performed on the 3-D cultures after 13 days *in vitro* (DIV) revealed that the cultures indeed contained neurons, astrocytes, and microglia as indicated by positive labeling with antibodies against microtubule-associated protein 2 (MAP2) (1:400, Chemicon/EMD Millipore, Billerica, MA), glial fibrillary acidic protein (GFAP) (1:1,000, Chemicon/EMD Millipore), and ionized calcium binding adaptor molecule-1 (Iba1) (1:1,000, Wako Chemicals USA, Inc., Richmond, VA), respectively. At 13 DIV, the cultures were fixed with paraformaldehyde, embedded in optimal cutting temperature compound (OCT™, Sakura Finetek USA, Inc., Torrance, CA) and cut into 30 μm sections using a cryostat. The sections were mounted on gelatin coated microscope

slides and processed for immunocytochemistry. Fluorescent images were acquired using a Nikon Eclipse 80i upright microscope (Nikon Instruments, Melville, NY) equipped with a MicroFIRE camera (Optronics®, Goleta, CA). Most of the positively labeled cells appear to be astrocytes and microglia as evidenced by the colocalization of the nuclear counterstain with the GFAP and Iba1 immunolabeling (Figure 2.1). This is a qualitative assessment indicating that despite the majority of the cells being neurons at the time of plating, the culture developed into one that contains a higher proportion of glial cells. This is likely due to both cell death from the freshly dissociated E18 tissue as well as from some proliferation occurring in the glial population. The latter would presumably be occurring at a rate far below that of a serum-containing culture, but would nonetheless contribute to the shift in cellular ratio. This "stabilized" ratio of neurons to glia is consistent with what one would expect in cortical tissue *in vivo* [145].

In addition to confirming the cell types present in the 3-D cultures, the viability of the cultures was also assessed. This was achieved either by labeling live and dead cells with calcein AM and ethidium homodimer (Sigma-Aldrich), respectively, or by labeling the nuclei of all cells present as well as those of dead cells using Hoechst 33342 and propidium iodide (Molecular Probes®/Life Technologies), respectively. Fluorescent images of intact rather than sectioned cultures labeled with these reagents were acquired. Cell counts were determined by first generating thresholded images in Adobe Photoshop CS4 (Adobe Systems, Mountain View, CA) and subsequently counting cells or nuclei using ImageJ. Cell viability using calcein AM and ethidium homodimer was assessed on cultures at 26 DIV (Figure 2.2A-C). Assessment with Hoechst 33342 and propidium iodide was carried out on a separate group of cultures at 21 DIV (Figure

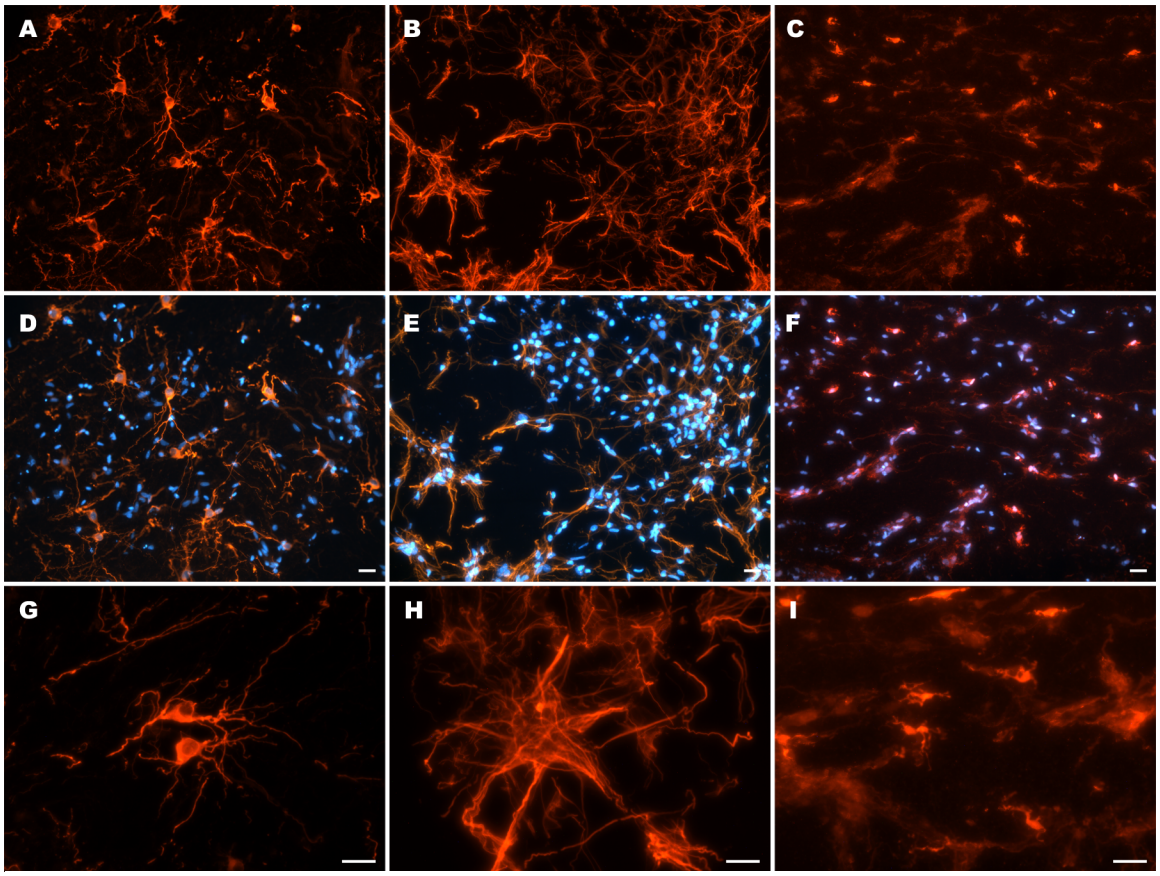

Figure 2.1. Confirmation of the presence of all three cell types in 3-D multitypic neural cell cultures. Cultures were maintained for 13 DIV. (A,D,G) The neurons stain positively with MAP2, a marker for developing neurons. (B,E,H) The astrocytes stain positively for GFAP, an intermediate filament protein. (C,F,I) The microglia stain positively for Iba1, a calcium-associated protein that is expressed in macrophages and microglia. The low power images (A-C) give a broad view of the distribution of cells in the section of culture. Most of the positively-staining cells appear to be astrocytes and microglia as evidenced by the concentration of nuclear staining with GFAP and Iba1 labeling (D-F). The high power images (G-I) show the detail of the cellular morphology in the 3-D culture. Scale bars: 25 μm.

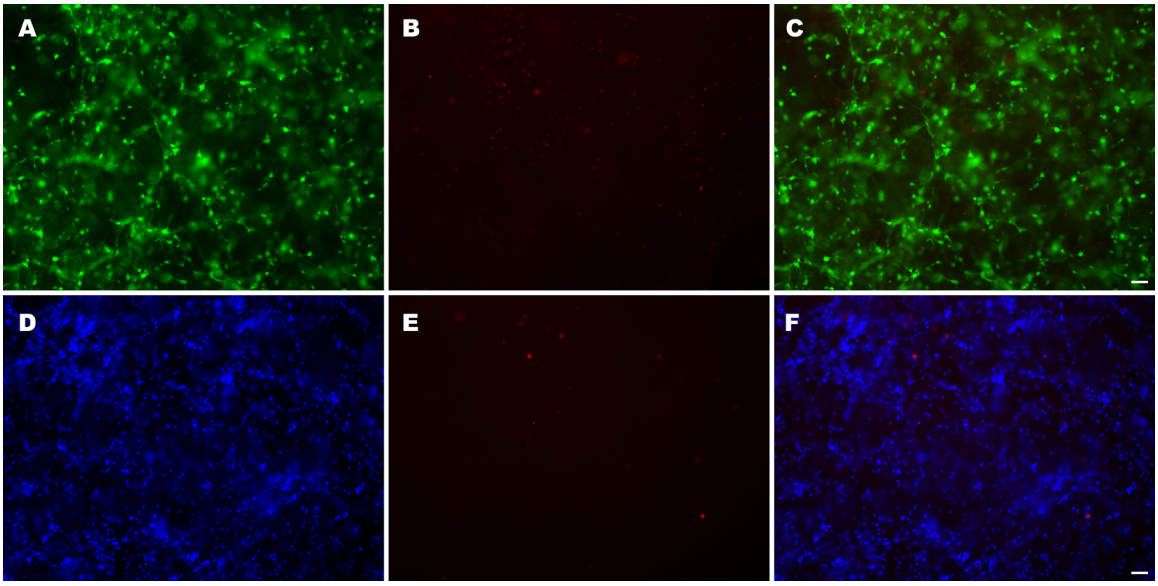

Figure 2.2. Cell viability assessment using two different methods. (A-C) A Live-Dead assay using Calcein AM (A) and ethidium homodimer (B) to label viable and dead cells, respectively was performed on 3-D cultures (26 DIV). (C) A merged image of A and B. (D-F) Cell viability using Hoechst 33342 (D) and propidium iodide (E) to label the nuclei of all cells and dead cells, respectively was determined for 3-D cultures (21 DIV) . (F) A merged image of D and E. Scale bars: 50 μm.

2.2D-F). In both cases, the cultures were rinsed with Dulbecco's phosphate-buffered saline (DPBS), exposed to the specified reagents (in DPBS) for 30 minutes and subsequently imaged using a Nikon Eclipse 80i upright microscope equipped with a MicroFIRE camera. Both methods showed a cell viability of approximately 90%.

Although these early assessments of the 3-D multitypic cultures were promising, there were a number of issues that needed to be optimized. First, the cultures would frequently retract and ultimately delaminate from the substrate after approximately one week. This could be attributed to either astrocyte contraction within the culture or some sort of astrocyte-mediated gel degradation. It was apparent that some astrocyte proliferation was occurring and that once a substantial portion of the cell population was astrocytic, the contraction of the cells would have a dominant effect on the gel geometry. Unpublished data supported this assertion as the problem of contraction was exacerbated with the inclusion of a higher proportion of astrocytes at the time of plating. Another priority in the development of the culture model was to find a way to improve microglial yield without the use of M-CSF. One of the goals of the culture system was for it to be responsive to inflammatory stimuli. The use of a treatment that induced the proliferation of microglia may have confounded attempts to induce inflammation experimentally as microglial proliferation occurs as a result of inflammation. Finally, the use of astrocytes after having maintained them between passages 4 and 10 became a concern. Although this resulted in a purer population, phenotypic drift is known to occur as cultured cells are maintained. Indeed, as the passage number increased, the astrocyte morphology was noticeably different and the proliferation rate decreased. Since other changes may occur concomitantly with these easily observable differences, using cells closer to when they

were harvested became a design priority. In order to address these concerns, a number of modifications were made to the generation and maintenance of the 3-D multitypic cultures.

2.3.2 Improved method: medium modification and the use of mixed glial cultures as a single source of all non-neuronal cells

The issue of gel retraction and delamination did not seem to affect the health of the cell culture as live-dead assessments were carried out on adherent and floating cultures with no significant variation in cell viability. However, processing adherent cultures for endpoint assays was far more expedient than if they were floating. Additionally, with the intention of subjecting the cultures to bulk mechanical injury in the future, having a culture that remained affixed to the substrate was necessary. As mentioned previously, the increased presence of astrocytes as the culture developed was assumed to be the source of the gel retraction. The medium formulation used throughout the maintenance of the 3-D cultures included G-5 supplement, which contains growth factors such as FGF and EGF among other components. As the supplement is designed to favor astrocyte growth in the absence of serum, its continued presence may have contributed to the gel retraction issue. It was decided that complete removal of the supplement was not logical as it may hinder the initial survival of the astrocytes following the trauma of trypsinization and 3-D plating. The cultures were initially plated and twice fed with G-5-containing medium. The subsequent feedings were with medium lacking G-5. All medium used for 3-D culture feedings was pre-warmed and pre-conditioned with CO_2 by placing an aliquot in a flask fitted with a filter cap into the incubator. Since medium replacement consisted of exchanging half of the medium

volume, the cultures were weaned from G-5, rather than completely deprived of it. This modification to the culture protocol delayed gel retraction to two weeks. This is the time point to which the manufacturer tests gel stability at 37 ºC. No ill effects in terms of viability or cell development and morphology were observed as a result of weaning the cultures off of G-5. The potential effects of the absence of G-5 on the *in vitro* inflammation response are addressed further in Chapter 6.

The concern about the method of inducing microglial proliferation was also ultimately addressed by changing a culture feeding procedure. It has been reported that frequent medium changes inhibits the proliferation of microglia [139]. The glia used to generate microglia for the 3-D cultures were fed every 2-3 days until the microglia were harvested. In an attempt to boost microglial yield without M-CSF treatment, the protocol was modified so that the mixed glial cultures were fed every 2-3 days until they reached confluence (~1 week). The subsequently unfed cultures were shaken to harvest microglia a week later. This method produced a microglial yield that was equal to, if not higher than, that obtained when using M-CSF treatment. As such, this became the standard method for generating microglia for the 3-D multitypic cultures.

The culture system was modified to limit the use of cells that had undergone multiple passages. The issue of using passaged astrocytes brings up a perennial debate about the validity of *in vitro* models in scientific research. While the population of cells is purer with passaging, the artificial selection and phenotypic changes that may occur during the cell culture process result in a subset of astrocytes which may be substantially functionally different from their primary progenitors. The flipside of this argument is that *in vitro* research affords the investigator both homogeneity and control. Although

passaged cells may differ greatly from those *in vivo*, the consistency of a pure population of cells is conducive to more mechanistically-targeted experiments. Since the goal of this model was to mimic cortical tissue as closely as possible, passaged cells were no longer used.

The culture method was modified to harvest both astrocytes and microglia from a single mixed glial culture. Since one of the main reasons for using passaged cells was to produce a pure astrocyte population, the presence of microglia in the early passage glial cultures had to be assessed. Estimation by visual inspection of the culture was confounded by the fact that microglia grow both loosely adhered on the surface of confluent astrocytes and to a lesser extent within the astrocyte layer. The former are easily identified as they are phase bright spheres on a lawn of phase dark cells whereas the latter are difficult to discern amid the surrounding astrocytes. It was determined that the best method for estimating the contribution of microglia from the astrocyte cultures would be to plate 3-D cultures consisting of neurons and early passage (two or fewer) astrocytes with and without additional microglia from the separate harvest. After immunolabeling the 3-D cultures for Iba1, it was qualitatively difficult to determine which cultures had been plated with additional microglia. This suggested that despite agitation and passaging, the astrocyte cultures still contained a substantial population of microglia. It was determined that rather than harvesting astrocytes and microglia from separate dissections and cultures, both cell types would be collected from the mixed glial cultures initially used for microglial harvest. Rather than shaking the cells for hours to enrich the medium with loosely adherent microglia, the cultures were trypsinized and plated with neurons in 3-D with at a neuron to total glia ratio of 2:1. This new method not

only incorporated astrocytes at their first passage, it also greatly shortened the experimental lead time and simplified the culture process.

Cultures generated using the new method were maintained for 11 DIV and processed for immunocytochemistry as described in the previous section. However, in lieu of cutting cryostat sections, the cultures were processed intact and imaged at low power using the same epifluorescence microscope setup as in the previous section. Cultures were labeled with a combination of MAP2 and GFAP or with Iba1. The immunolabeling reveals significant process extension of neurons and astrocytes (Figure 2.3A-D). While the astrocytes appear somewhat clustered, the microglia are quite equally spaced and many are exhibiting process extension as well (Figure 2.3E-G).

These changes in medium composition, feeding schedule, and cell harvest protocol resulted in cultures that could be plated and ready for experimentation (14 DIV) in less than a month. Additionally, much less tissue and fewer cell culture materials were required for production. While these were certainly not the last modifications made to the 3-D culture protocol, this streamlined process provided a sound foundation for 3-D culture experimentation. Later chapters will explore further improvements to the culture system ranging from the development of custom chambers to the use of a more defined medium composition.

2.4 Conclusions

This chapter has detailed the incremental development of a novel *in vitro* representation of rat cortical tissue. This 3-D multitypic neural culture model began as an expansion of previously described methods to incorporate an underrepresented cell type. Optimizing the addition of microglia to the neuron-astrocyte co-culture model proved to

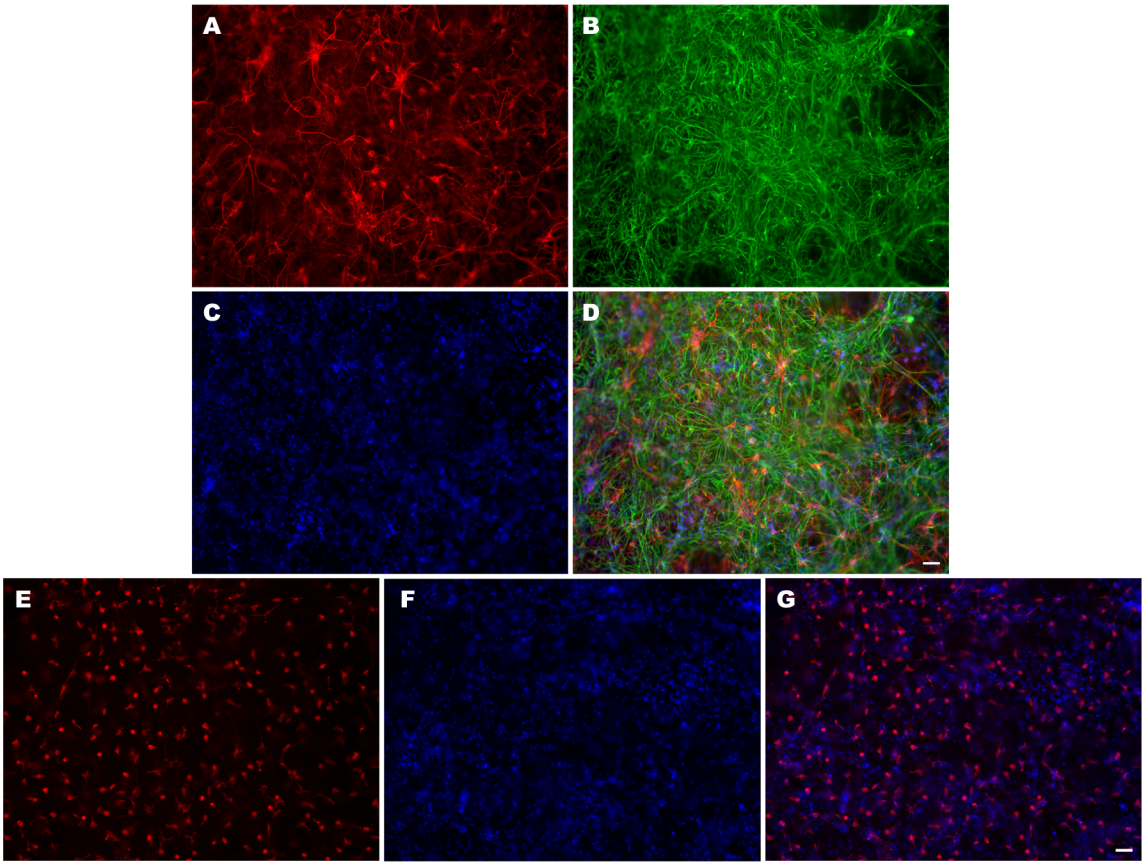

Figure 2.3. 3-D multitypic neural cell cultures contain neurons, astrocytes, and microglia with healthy morphology. 3-D cultures (11DIV) were incubated with antibodies against MAP-2 to label neurons (A) and GFAP to label astrocytes (B) as well as with a Hoechst nuclear counterstain (C). (D) A merged image of A, B, and C. Separate cultures were incubated with an antibody against Iba1 to label microglia (E) and also counterstained with Hoechst (F). (G) A merged image of E and F. Scale bars: 50 μm.

be more challenging than anticipated in terms of obtaining sufficient yield so that the microglial population would reflect that of the *in vivo* model. In the process of developing this culture system, modifications were made to earlier methods such that all cells used would be closer to the primary state rather than being a blend of primary and secondary cells. Specifically, the mixed glial cultures undergo a single passage at the time of plating when they are combined with primary neurons to generate the final 3-D cultures. Further adjustments to maintenance medium protocols resulted in more stable, adherent gels at 14 DIV. This proved to be critical in the characterization of inflammatory response of these cultures.

Although the increased complexity gained through the addition of microglia brings the 3-D culture model closer to what can be achieved using an *in vivo* model, it clearly remains far removed from living tissue. This is perhaps the greatest weakness of *in vitro* research. Many may argue that in the absence of vasculature a complete picture of the inflammatory response to injury cannot be represented. This is true. However, this next generation of 3-D neural culture is simply another step toward creating an ideal *in vitro* model of brain tissue. Despite the absence of many of the key players involved in the injury response, much can learned about isolated cellular behaviors. The distinct advantage afforded by this system is control. By creating homogeneous primary cultures with tissue from multiple animals, variability is reduced, and some subtle effects which may be lost in statistical noise *in vivo* may be elucidated. This is not to suggest that the model presented here should be implemented in lieu of *in vivo* models. Rather, just as animal models are used as a precursor to clinical research, so too can *in vitro* systems provide an efficient launching pad for pre-animal testing. To be sure, the 3-D multitypic

neural cell culture system could further be augmented by the introduction of more cell types. However, characterization of the system as developed here provides insight into the translation of cellular function from *in vivo* to *in vitro*.

CHAPTER 3

CHARACTERIZATION OF THE 3-D MULTITYPIC NEURAL CELL CULTURE SYSTEM AS A MODEL OF NEUROINFLAMMATION

3.1 Introduction

The driving force behind developing the 3-D multitypic neural cell culture system was ultimately to use it to study the neuroinflammatory responses induced by injury. Although neurons and particularly astrocytes can participate in inflammatory signaling cascades, the main cells that fill this role are microglia. Incorporating these cells into the culture system was a critical step in creating an *in vitro* model of neuroinflammation. As research in the area of neuroinflammation has progressed, it has become clear that inflammation plays a key role in the secondary and long-term responses to a number of neurological insults. As such, it is a prime target for therapeutic intervention. However, inflammation has both ameliorative and deleterious effects, and it is this duality that makes understanding its underlying mechanisms so crucial. No pre-clinical studies for therapeutic intervention following TBI have successfully translated to humans. Using an *in vitro* neuroinflammation model as the basis for therapeutic research may clarify new avenues of study that lead to successful treatments.

Since the study of microglia began almost a century ago, a great deal has been learned about their function. There exist many protocols for their isolation and maintenance *in vitro* [76, 128, 129, 140, 141], but their use in the unique system presented here requires that their growth and behavior be characterized in this new milieu. As discussed in Chapter 1, microglia can exist in at least two different functional and morphological states *in vivo*: the inactive, ramified state and the activated, amoeboid

state. Although they extend processes and can be activated, microglia *in vitro* do not exhibit the ramified phenotype associated with "resting" microglia *in vivo* [96, 146]. They do, however, extend processes and morphological changes toward a more rounded phenotype can be induced with LPS treatment [147]. Ideally, the cells plated into the 3-D cultures will initially grow as quiescent cells and be inducible into an activated state in response to insult. In tandem with the incorporation of microglia into the 3-D multitypic neural cell culture model, some isolated microglia were maintained in 2-D in order to get a sense of their behavioral characteristics (morphology, proliferative capacity, etc). Visualization of microglia in 2-D cultures can more easily be achieved than in 3-D cultures as there is no interference from multiple cellular layers. When plated into fresh flasks after isolation from the mixed glial cultures, the microglia adhered to the uncoated tissue culture plastic within minutes. At this point, they exhibited a rounded morphology. When maintained in the same serum-containing medium in which the mixed glia were grown, they did not noticeably change or proliferate over the course of a week, even when exposed to M-CSF. Rather, after a week they would shrink and ultimately die. However, when the serum was replaced with G-5, the microglia began to extend processes after 2-3 days. They still did not proliferate, even with M-CSF exposure. Given these observations, clear critical factors to consider in developing an *in vitro* model of neuroinflammation were that microglia would only proliferate in the presence of astrocytes and that the use of G-5 was preferable to serum to induce process extension. In the culture model presented in Chapter 2, the microglia are generated from mixed glial cultures and the 3-D cultures are maintained in a serum-free, G-5 supplemented

environment. This design meets the criteria, making the method for 3-D multitypic neural cultures a candidate for a neuroinflammation model.

Prior to any mechanical injury testing (Chapter 4), the system was characterized using LPS as a positive control for inflammation. It was expected that exposing the cultures to LPS would induce a broad inflammatory response detectable by many different outcome measures. The expected outcome was for the LPS stimulation to cause: cytokine release, upregulation of inflammatory molecules at the mRNA and protein level, nitric oxide release, generation of ROS, morphological changes in the microglia from an inactive to an active state, and possibly cell death. An induced inflammatory response would be the first step in validating the 3-D multitypic neural cell culture system as a model of neuroinflammation.

3.2 LPS-induced neuroinflammation

3.2.1 LPS as a positive control

The gram-negative bacteria surface molecule, LPS is known to stimulate the innate immune response across many species [148-150]. It binds to toll-like receptor 4 (TLR4), a highly conserved molecule expressed on the surface of macrophages and dendritic cells. Along with CD14, TLR4 mediates the inflammatory response to LPS, in particular, the release of cytokines such as the pro-inflammatory IL-1β. As microglia are derived from a dendritic cell lineage, they are stimulated by LPS through the same TLR4-mediated pathway. Since cytokines such as IL-1β are also released by microglia in response to traumatic injury, stimulation of these cells with LPS was used to demonstrate that the cells could be potentiated into a state of inflammation. It therefore represents a positive control for the induction of inflammation in the 3-D culture system. Thus, it was

utilized with each of the outcomes measures to be used in mechanical injury experiments to confirm the inflammatory potential of the model.

3.2.2 General experimental methods

3-D multitypic neural cell cultures were generated as discussed in Chapter 2 and as described in detail in Appendix A. All data presented in this chapter were acquired from 3-D cultures grown in reusable, custom-made culture chambers described in Section 4.2.2. Cells were generally maintained in a 37 ºC incubator at 5% CO_2 and 95% relative humidity for either 7 or 14 days prior to LPS stimulation, although other time points were sometimes used where indicated. LPS (Sigma-Aldrich) was delivered as part of a complete medium change. 3-D cultures were exposed to medium containing LPS at either a concentration of 10 μg/mL or at a higher concentration to compensate for the dead volume of the culture (as the primary constituent of the hydrogel is water). The latter is indicated as a "final" LPS concentration of 10 μg/mL.

For experiments in which released factors were being measured, conditioned medium was collected at time points ranging from 1 to 24 hours. For outcome measures requiring cellular material, the gels were degraded using BD™ Cell Recovery Solution (BD Biosciences, San Jose, CA) according to the manufacturer's protocol. Live cell imaging for NO was carried out *in situ* using an NO-sensitive dye diluted in DPBS. Cells processed for immunocytochemistry were fixed with 2% paraformaldehyde in phosphate-buffered saline (PBS), permeabilized with 0.1% Triton X-100, incubated with primary antibody overnight at 4 ºC and with secondary antibody for 1-2 hours at room temperature. All solutions for immunolabeling (including rinse buffer) contained 0.05% saponin, a mild, reversible detergent. Culture viability was assessed either by using

fluorescent markers as discussed in Chapter 2 or by the use of a lactate dehydrogenase (LDH)-based *In Vitro* Toxicology Assay Kit (Sigma-Aldrich). Methods pertinent to individual experiments are detailed in the subsequent sections.

3.2.3 Changes in cytokine mRNA levels

Levels of mRNA expression were measured via microarray following treatment of cultures with LPS. After 14 DIV, 3-D neural cultures were treated with LPS at a final concentration of 10μg/mL (n=6) or with Hank's balanced salt solution (HBSS) vehicle (n=6) for 4 hours. This time point was chosen as both mRNA [88] and protein concentrations [73] of a number of cytokines have been shown to be elevated at 4 hours. The Matrigel™ matrix was degraded by treating the cultures with BD™ Cell Recovery Solution for 2 hours on ice with agitation on an orbital shaker. Two cultures were pooled to represent a single sample (pooled n=3). The sample pooling was determined in preliminary experiments to be necessary to generate enough RNA for the microarrays.

Total RNA was extracted with TRIzol Reagent (Life Technologies), quality controlled, and quantified by Agilent 2100 Bioanalyzer (Agilent Technologies, Santa Clara, CA). Microarrays were completed according to manufacturing guidelines (Affymetrix® Inc., Santa Clara, CA), with cRNA hybridized to an Affymetrix Rat Genome 1.0 ST GeneChip® array (Affymetrix Inc.). The chips were hybridized at 45°C for 16 hours, washed, stained with streptavidin-phycoerythrin, and scanned according to manufacturing guidelines. Three chips were used for each experimental group: with and without LPS treatment. Table 3.1 shows some of the notable species that had a significantly (ANOVA) elevated message level, namely cytokine iNOS and the cytokines: IL-1α, IL-6, TNFα, and IL-1β. These data indicate that the 3-D neural cultures

Table 3.1.

Molecule	Average Signal (log2)		Fold Change (linear)	ANOVA p-value
	without LPS	with LPS		
IL-1α	4.15	11.08	121	2.48E-07
IL-6	4.39	11.12	106	1.05E-08
TNFα	6.27	11.72	44	2.81E-07
iNOS	5.85	10.82	31	1.68E-08
IL-1β	7.08	11.51	22	1.47E-08

Levels of mRNA expression of pro-inflammatory molecules are elevated in 3-D multitypic neural cell cultures in response to LPS stimulation. Cultures (14 DIV) were exposed to a final concentration of 10 µg/mL LPS or to HBSS vehicle for 4 hours. The matrix was disintegrated to isolate the cells and the RNA was extracted from the cells using TRIzol Reagent. Microarrays (Affymetrix Rat Genome 1.0 ST GeneChip®) were completed and the data were statistically analyzed by ANOVA (without LPS, n=3; with LPS, n=5). LPS treatment produces a significant increase in the levels of many molecules. Those presented in the table are representative of the molecules expected to have increased expression in inflammation.

are chemically inducible to an inflammatory state. However, an increase in gene transcription does not always correlate to an increase in translation into protein. As such, the next step was to assess cytokine production at the protein level.

3.2.4 Effects on IL-1β protein levels

Based on the microarray data as well as the known mechanistic relationship between LPS exposure and IL-1β release, this cytokine was chosen for outcome testing at the protein level. Prior to release from the cell, a pool of immature IL-1β is present near the cell surface, ready for rapid signaling. Upon insult, the immature molecule is cleaved into its mature form by caspase-1 and is released from the cell to deliver its pro-inflammatory signal. Assuming this mechanism is present and functional in this culture system, it was expected that mature IL-1β would be detectable by ELISA in the culture medium in response to LPS stimulation. The microarray data demonstrated that the levels of IL-1β mRNA were increased in response to LPS stimulation. It was expected that this elevation would correspond to an increase of intracellular IL-1β protein levels upon LPS stimulation as detected by Western blot and immunocytochemistry.

3.2.4.1 LPS-induced IL-1β release

After 7 DIV, 3-D cultures were exposed to normal medium or to medium containing 10 μg/mL LPS. The medium was collected 24 hours later and centrifuged at 1,000 rcf to remove any contaminating cells. The supernatant was collected (n=3 per condition) and analyzed with a rat IL-1β ELISA kit (R&D Systems, Minneapolis, MN). It is clear that after 24 hours of LPS exposure, the concentration of IL-1β in the medium is substantially higher than that in the medium of untreated cultures (Figure 3.1). The means are significantly different as determined by an unpaired t-test using Welch's correction

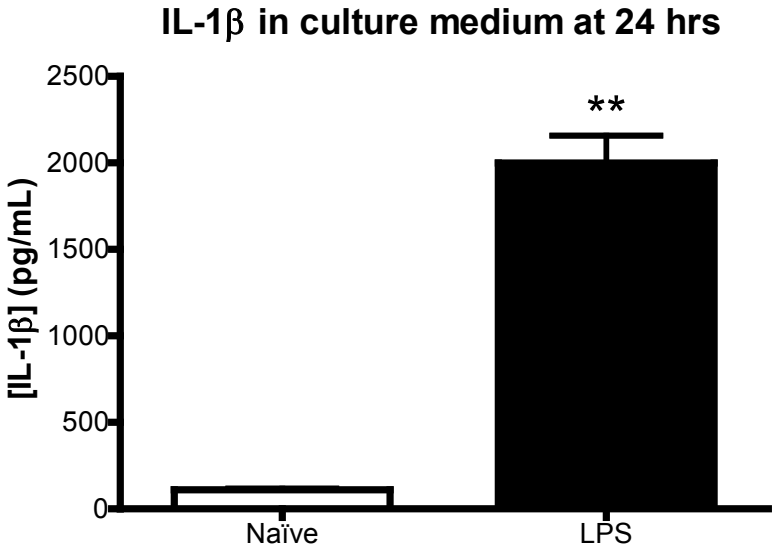

Figure 3.1. 3-D multitypic neural cell cultures release IL-1β in response to LPS stimulation. Cultures (7 DIV) were exposed to 10 μg/mL LPS or to HBSS vehicle for 24 hours. The medium was collected and assayed for IL-1β by ELISA. LPS treatment produces a significant increase in the levels of IL-1β ($p<0.01$, $n=3$) Data were statistically compared using a one-tailed, unpaired t-test with Welch's correction for unequal variances. Bars are means plus SEM.

for unequal variances ($p<0.01$). The correction was applied after the variances were determined to be significantly different using an F-test. Despite the small sample size, these data indicate that the 3-D cultures can be induced to produce a characteristic inflammatory response upon exposure to the LPS positive control.

3.2.4.2 LPS-induced upregulation of IL-1β protein expression

Following the quantitative analysis of released IL-1β by ELISA, the question remained as to whether LPS stimulation caused a concomitant upregulation of intracellular protein expression. To address this, both Western blot and immunocytochemistry methods were employed. At 13 DIV, 3-D cultures were given normal medium containing HBSS vehicle (n=3) or medium containing 10 μg/mL LPS (n=3). After 4 hours, cultures from each experimental condition were rinsed with cold PBS containing a "cOmplete" protease inhibitor cocktail (PIC) (Roche Life Science, Indianapolis, IN), collected with BD™ Cell Recovery Solution containing PIC, and pooled into Eppendorf tubes (pooled n=1 per condition). As with the sample preparation for the microarrays, sample pooling was necessary to ensure sufficient protein for loading the SDS-PAGE gel. The tubes were kept on ice for one hour with frequent inversion to facilitate the disintegration of the gel. The samples were centrifuged at 1,000 rcf at 4 ºC for 5 minutes and the pellets were resuspended with a protein extraction solution containing NP-40, deoxycholate, and PIC. The tubes were kept on ice and vortexed periodically during protein extraction. The samples were centrifuged at 1,000 rcf at 4 ºC for 5 minutes and the supernatants were transferred to clean Eppendorf tubes. Protein content was determined by BCA protein assay (Pierce™/Life Technologies) and the samples were diluted to equal protein concentrations with SDS-PAGE sample loading

buffer. The reduced and denatured samples were separated in 8-16% Tris-Glycine gradient SDS-PAGE gels (Invitrogen™/Life Technologies) and wet-transferred to PVDF membrane (EMD Millipore, Billerica, MA) for antibody detection. The membrane was exposed to anti-rat IL-1β antibody (R&D Systems) overnight at 4 ºC. The membrane was incubated with secondary antibody conjugated to IR Dye 800 (Rockland Immunochemicals Inc., Pottstown, PA) and scanned using an Odyssey® infrared scanner (LiCor, Lincoln, NE).

The Western blot data reveal a clear upregulation of intracellular IL-1β protein (Figure 3.2). The immature form of the cytokine is expected to migrate at an apparent molecular weight of 31 kD, while the mature form is expected at 17 kD. The immature form is clearly detectable in the untreated sample, but the mature form is not. LPS stimulation causes a large increase in intensity of the band representing immature IL-1β and makes the band representing the mature form detectable. The weaker band migrating slightly higher than 31 kD likely represents a posttranslationally modified (e.g. glycosylated) form of IL-1β. Even with LPS exposure, the mature IL-1β band is fairly weak. This is likely due to the release of this form from the cell in response to the insult. These data reveal that treatment with LPS causes a substantial increase in intracellular levels of IL-1β after only a 4 hour exposure.

To visualize the expression of IL-1β in response to LPS stimulation, 3-D cultures maintained for 21 DIV were exposed to LPS at a final concentration of 10 μg/mL or to medium containing and equivalent amount of HBSS vehicle for 24 hours. The cultures were subsequently fixed with paraformaldehyde and processed for immunocytochemistry as described in Section 3.2.2 using the same antibody against rat IL-1β that was used for

Figure 3.2. Intracellular levels of IL-1β are upregulated in response to LPS stimulation. Cultures (13 DIV) were exposed to 10 μg/mL LPS (n=3, pooled n=1) or to HBSS vehicle (n=3, pooled n=1) for 4 hours. At 4 hours post-injury, Western blot data indicates there is a substantial upregulation of the intracellular production of IL-1β. The 31 kD band represents the immature form of IL-1β. LPS stimulation induces the production of a small amount of mature IL-1β present which is indicated by the 17 kD arrow. The latter was not detectable in untreated cultures.

Western blotting. Fluorescent images were captured using the same epifluorescence microscope and camera setup described in Section 2.3.1. The vehicle-treated cultures show only low-intensity, fibrillar labeling that is likely nonspecific (Figure 3.3A,B). When treated with LPS, however, the signal is much more intense and is present in cells with morphology that is characteristic of microglia (Figure 3.3C,D). Based on the Western blotting data, it is likely that the observed signal increase is due to the upregulation of immature IL-1β in the cells. The immunocytochemistry data suggest that microglia are the primary contributors to the LPS-driven IL-1β response in the 3-D cultures.

3.2.5 Effect on NO production

Along with the increased levels of cytokine mRNA determined by microarray as presented in Section 3.2.3, the mRNA level of iNOS was also increased. Thus, it was expected that stimulation with LPS would produce a detectable increase in NO levels in the culture medium. NO is a toxic free radical generated in response to pro-inflammatory cytokines released in response to an insult. As is the case with any free radical species, the molecule is unstable and thus, difficult to detect experimentally. Thus, levels of NO are most often determined by assaying for nitrite, a stable breakdown product of NO. Developed in 1858, the Griess test is a simple, commonly used colorimetric method for the determination of nitrite in biological fluids and cell culture media. Additionally, in order to directly determine the level of NO production in response to LPS stimulation, a NO-specific infrared hydrocyanine dye was used [151].

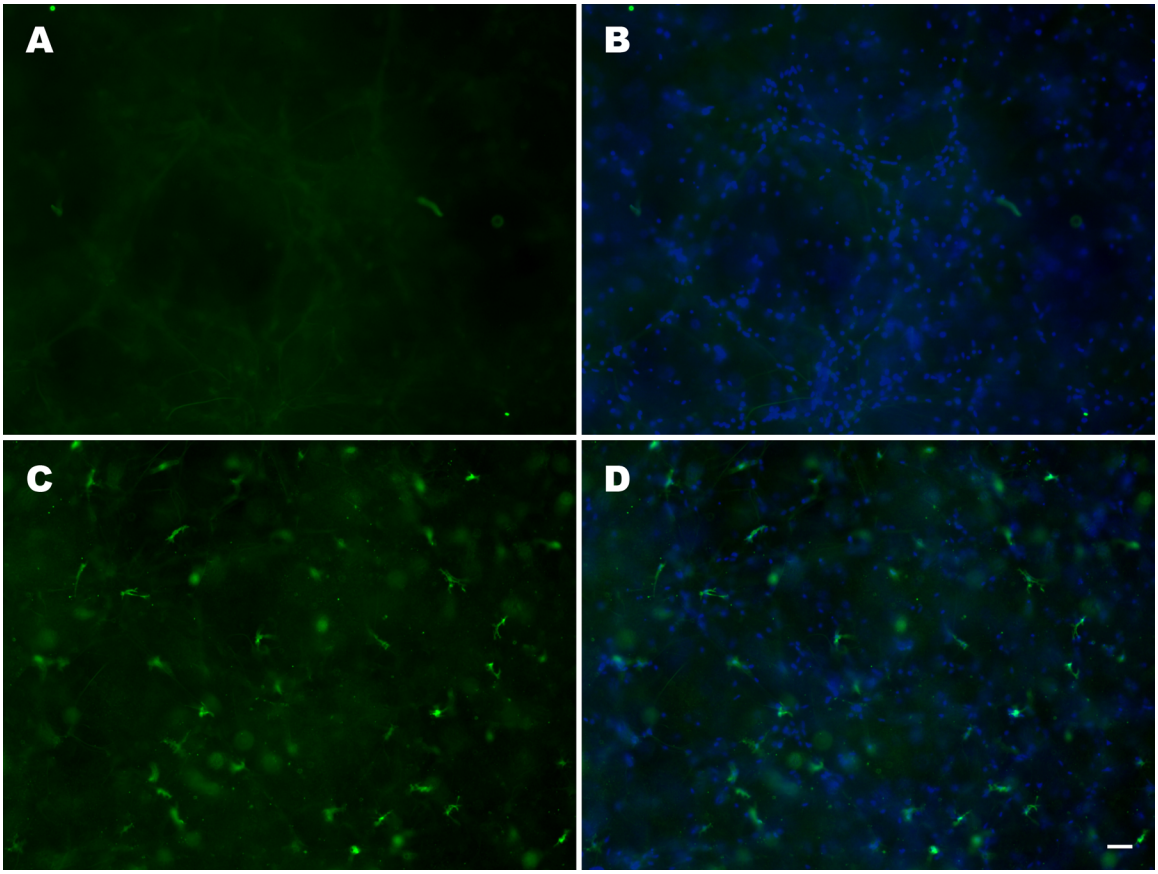

Figure 3.3. Immunocytochemical visualization of LPS-induced IL-1β expression. Cultures (21 DIV) were exposed to a final concentration of 10 μg/mL LPS or to HBSS vehicle for 24 hours. Fixed cultures were incubated with antibody against IL-1β as well as with a Hoechst nuclear counterstain. (A) IL-1β labeling in vehicle-treated cultures appears nonspecific and fibrillar. (B) IL-1β in vehicle-treated cultures with nuclear counterstain. (C) IL1β in LPS-treated cultures labels cells with morphology consistent with microglia. (D) IL-1β in LPS-treated cultures with nuclear counterstain. Scale bar: 50 μm.

After 11 DIV, 3-D cultures were exposed to LPS at a final concentration of 10 μg/mL (n=3) or to HBSS vehicle (n=3) for 24 hours. The cultures were rinsed with DPBS and subsequently exposed to the NO-sensitive hydrocyanine dye for one hour. Three of the cultures for each condition were rinsed with DPBS and imaged using an IVIS Lumina® near-infrared imaging system (PerkinElmer, Waltham, MA). The raw data from the *in situ* labeling with the infrared NO sensor dye showed an increase in fluorescent signal after LPS stimulation (Figure 3.4A). This difference was determined to be statistically significant by an unpaired t-test using Welch's correction for unequal variances ($p<0.01$) (Figure 3.4B). After 7 DIV, similar cultures were exposed to medium containing 10 μg/mL LPS or to HBSS vehicle. The media from three samples per condition was collected at 24 hours and the level of nitrite present was determined using a Griess assay (Promega, Madison, WI). Without LPS stimulation, there is no detectable nitrite in the culture medium as the signal from the Griess assay is outside the range of the standard curve. The presence of LPS caused nitrite levels to elevate to an average of nearly 6 ng/mL after 24 hours (Figure 3.4C). Although it is a bit misleading to run a statistical analysis on these data as it is essentially comparing a detectable signal to the absence of a signal, the means are significantly different as determined by an unpaired t-test using Welch's correction for unequal variances ($p<0.01$). Thus, the *in situ* NO data and the measure of nitrite from separate cultures are in agreement that LPS exposure increases levels of NO in the cultures.

3.2.6 Effect on 3-D culture viability

LPS stimulation failed to induce process retraction or any morphological change of the microglia (not shown). This unexpected outcome led to the question of whether

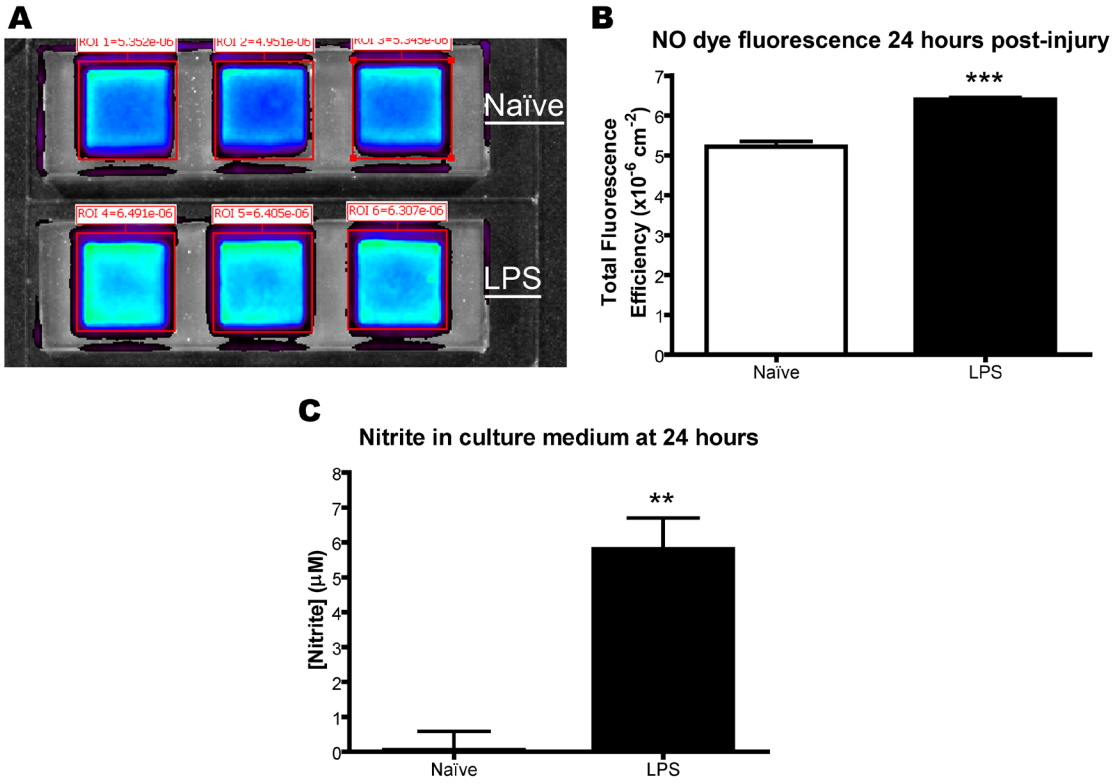

Figure 3.4. 3-D multitypic neural cell cultures release NO in response to LPS stimulation. (A) Cultures (11 DIV) exposed to a final concentration of 10 µg/mL LPS for 24 hours show an increased fluorescence signal using an NO-sensitive infrared dye. (B) Quantification of this signal reveals a significant difference in the level of NO ($p<0.001$, $n=3$). (C) Medium collected from cultures (7 DIV) treated with the same conditions contains significantly higher levels of nitrite at 24 hours ($p<0.01$, $n=3$). Data were statistically compared using a one-tailed, unpaired t-test. Bars are means plus SEM.

microglial activation in response to LPS would ultimately be toxic to the cultures as was expected based, in particular, on the induced NO release [152-155]. To determine the effect of LPS on culture health, cell viability was assessed by both fluorescent live-dead assay and by measuring LDH release. As described in Section 2.3.1, two methods of determining cell viability by fluorescence were implemented. The first, a "live-dead" assessment using calcein AM and ethidium homodimer to label live and dead cells, respectively, was performed 24 hours after cultures (25 DIV) were subjected to 10 μg/mL LPS stimulation (n=4) or to a medium change (n=2). The results showed that LPS induced a small, but statistically significant reduction in cell viability in the cultures ($p<0.05$) (Figure 3.5A). However, a subsequent experiment in which Hoechst 33342 and propidium iodide were used to label the nuclei of all cells and dead cells, respectively, was performed 48 hours after cultures (19 DIV) were subjected to 10 μg/mL LPS stimulation (n=4) or to a medium change (n=4) as before. The results did not reveal any difference in cell viability due to LPS exposure (Figure 3.5B).

The fact that the two methods yielded different results can be attributed to the method of cell count determination. As described in Section 2.3.1, this was achieved by thresholding the images and determining counts by defining cell geometry parameters. Since epifluorescent images of intact 3-D cultures were captured, signal from multiple focal layers was detected. As calcein causes the entire cellular cytoplasm to fluoresce, determining cell boundaries was challenging despite the use of a broad range of threshold levels. As a result, multiple cells may have been counted as a single cell. Thus, the number of viable cells using this method may have been underrepresented, and given the small *n* for each experimental condition, the effect may have been substantial. This was

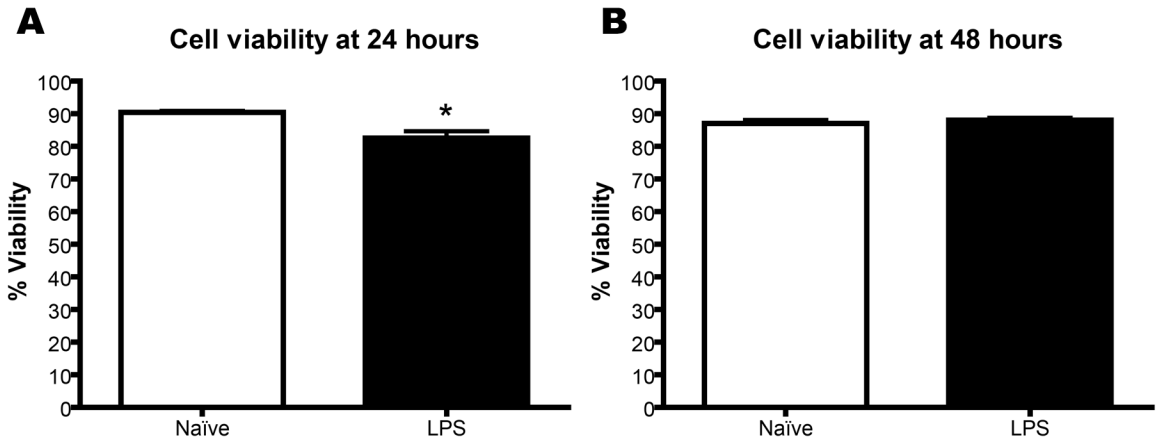

Figure 3.5. Determination of cell viability in response to LPS stimulation using fluorescent markers. (A) 24 hours after cultures (25 DIV) were exposed to 10 µg/mL LPS (n=4) or to HBSS vehicle (n=2), a Live-Dead assay was performed using Calcein AM and ethidium homodimer to label viable and dead cells, respectively. LPS treatment significantly reduces cell viability ($p<0.05$). (B) 48 hours after cultures (19 DIV) were exposed to 10 µg/mL LPS (n=4) or to HBSS vehicle (n=4) viability was assessed using Hoechst 33342 and propidium iodide to label the nuclei of all cells and dead cells, respectively. This method shows no significant difference between the naïve cultures and the LPS-treated cultures. Data were statistically compared using a one-tailed, unpaired t-test. Bars are means plus SEM.

the primary reason that the second method exclusively using nuclear stains was employed. It was expected that sequestration of signal to the nucleus would improve the ability to accurately separate individual cells. Indeed, the total cell count using this method was higher using the same experimental conditions. Although this appeared to be more consistent, the presence of clustered and overlapping cells still posed a problem for acquiring accurate cell counts. Thus, cell death was next assessed by measuring LDH release in response to LPS exposure.

LDH is an enzyme that is broadly expressed in the cells of nearly all organisms. It reversibly catalyzes the conversion between pyruvate and lactate in the glycolysis pathway. Due to its ubiquity and high expression level, it is an easily detected marker for cell damage and its release is often used as an indicator of cell death. 3-D cultures maintained for 13 DIV were exposed to medium containing 10 μg/mL LPS (n=6) or to normal medium (n=2) for 23 hours. At this point, the medium was collected and LDH was measured colorimetrically using an *In Vitro* Toxicology Assay Kit. The acquired data were compared to that from cultures given normal medium and treated with 0.1% Triton X-100 for 1 hour prior to media collection. The permeabilization of all cell membranes with this detergent gives data that represents maximum LDH release. The data show that LPS has no significant effect on the viability of the cells (Figure 3.6). These data corroborate that obtained from the viability assessment using the nuclear markers. The lack of LPS-induced toxicity was a surprise given the expectations based on the effects of LPS on cytokine levels in the 3-D cultures. Coupled with the lack of morphological changes in the microglia, these data certainly call into question the parity between this system and an *in vivo* model. However, given that the cultures responded to

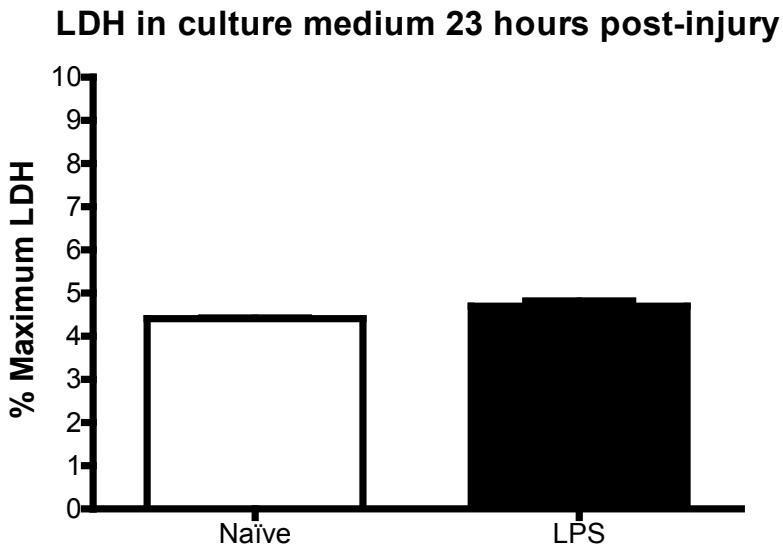

Figure 3.6. Determination of cell viability in response to LPS stimulation by LDH release. 23 hours after cultures (13 DIV) were exposed to 10 µg/mL LPS (n=6) or to HBSS vehicle (n=2), LDH levels in the medium were determined using an *In Vitro* Toxicology Assay Kit. No significant difference in cell viability is evident using this method. Data were statistically compared using a one-tailed, unpaired t-test. Bars are means plus SEM.

LPS as expected in terms of cytokine expression and release, the 3-D multitypic neural cell cultures certainly have viable uses for *in vitro* research.

3.3 Culture system applications

The added layer of complexity introduced to these cultures by the incorporation of microglia provides a platform on which *in vitro* inflammation studies can be based. Whereas previously studied culture systems have included two of the three cell types present here, they lacked the more complete picture of cellular interaction offered by this system. The fact that the microglia are inducible into an inflammatory state demonstrates that these cultures could be used in the study of any disease in which inflammation plays a role. The ever-increasing body of research into this topic has revealed that this spectrum of disorders is expanding. Inflammatory processes are continually being implicated in the development and exacerbation of disease states affecting cells throughout the human nervous system, including AD, Parkinson's disease, multiple sclerosis, and amyotrophic lateral sclerosis [156, 157]. This system models cortical neural tissue and is thus applicable to the study of diseases in which these cell populations are particularly vulnerable such as AD. Presumably, this culture system would be a viable candidate for studying both pro-inflammatory and anti-inflammatory mechanisms that occur in disease. One field of study in which such mechanisms are of particular interest is TBI. The neuron-astrocyte co-cultures previously described by our lab were indeed designed and used for TBI experiments. The utilization of 3-D cultures allows for mechanical loading that is closer to what occurs *in vivo*. The implementation of this culture system in mechanical injury studies is presented in Chapters 4 and 5.

In the same vein as traumatic injury, the 3-D multitypic neural culture system could also be used to study the inflammatory effects of foreign bodies in CNS tissue. This would be appropriate for the optimization of electrode or device implantation in which limiting the host response is a major concern. Brain injury resulting from stroke or aneurysm could be modeled by incorporating this culture system into hypoxia and anoxia studies. Blast injury could also potentially be modeled using this system and is discussed further in Chapter 6. Finally, given that the cells used in these cultures are from early stages of development, diseases such as fetal alcohol syndrome or other maladies stemming from drug exposure *in utero* could effectively be modeled. The true strength of an *in vitro* model of neuroinflammation is that once the baseline response to the insult of choice has been established, methods of clinical intervention to enhance neuronal survival can readily be tested. Further, by scaling up the number of cultures generated in a particular experiment, high-throughput studies could also be carried out. This 3-D culture system has the potential to provide the foundation of powerful *in vitro* disease models in which inflammation-mediated secondary injury mechanisms can be studied.

3.4 Conclusions

This chapter has provided support to the assertion that the 3-D multitypic neural culture model is a viable model of neuroinflammation. Multiple studies in which an inflammatory response was induced revealed that cytokine expression at both the mRNA (microarray) and protein (ELISA, Western blot, and immunocytochemistry) level are increased in response to LPS. Further, the release of NO as measured both directly (infrared dye imaging) and indirectly (nitrite levels) was demonstrated, which suggests that LPS should ultimately result in a cytotoxic response in the cultures [153-155].

However, this was not corroborated by cell viability and LDH release studies. Also concerning was the lack of a morphological shift in the microglia in response to LPS which has been reported to be accompanied by increased NO production [152, 158]. It was expected that this shift would occur as it precedes microglial migration and proliferation in response to an inflammatory stimulus *in vivo*. However, this morphological change is not directly caused by LPS. Rather, signaling molecules such as ATP may be absent due to the lack of LPS cytotoxicity. Despite the absence of these responses to LPS stimulation, it can be argued that this system still represents a valid model as the cultures exhibit a cytokine expression profile consistent with neuroinflammation.

Aside from the lack of cytotoxicity, comparison with other *in vitro* models of LPS-induced neuroinflammation shows parity with the system presented here. Treatment of primary rat microglia with LPS has been shown to elevate levels of nitrite in the culture medium at 24 hours [159, 160] as well as to increase levels of TNF-α, IL-1β, and IL-6 within the same time frame [160]. Treatment with a combination of LPS and IFN-γ has also been shown to elevate levels of nitrite at 24 hours for both primary rat microglia and BV-2 cells [91]. In a cerebellar granule cell neuron-glia co-culture model, treatment with LPS/IFN-γ resulted in an increase in nitrite after 48 hours [87]. The model that most closely relates to that presented here is the aggregating neural cell culture model. This culture method generates spheroids composed of multiple cell types that can be maintained as a 3-D aggregate supported by ECM derived from the primary cells. Aggregating spheroids derived from E16 rats treated with LPS/IFN-γ for 24 hours exhibited elevated gene expression of IL-6, TNF-α, iNOS, and IL-1β as measured by

PCR [161]. The elevation of pro-inflammatory species at the mRNA and protein level as well as the increase in NO production as measured by nitrite levels corresponds well to the data acquired using the system described here. Although IFN-γ was never included with LPS stimulation, its use has been described as a means to augment the LPS response [162]. As such, it is reasonable to compare these models with the 3-D multitypic neural cell culture model. Where this system differs is in the lack of LPS-induced morphological changes in microglia [146] and in the absence of cytotoxicity. Decreased neuronal viability in response to LPS treatment has been described in transwell insert-separated and direct co-cultures of primary rat neurons and microglia [163]. Additionally, neuronal cell death in response to LPS/IFN-γ has been shown in cerebellar granule cell neuron-glia co-cultures enriched with microglia [87] and in co-cultures of primary mouse neurons with either primary mouse microglia or BV-2 cells [91]. Thus, although this model exhibits many of the expected responses to LPS stimulation, it does not demonstrate decreased cell viability.

There are a number of possible explanations as to why the expected increase in cell death was not observed. First, the cultures may simply not have been incubated with LPS long enough for the neurotoxic mechanisms to initiate. The longest time point prior to medium collection post LPS exposure was 24 hours. It is possible that extending the exposure beyond this time point may elicit the expected cell toxicity. Second, the concentration of LPS used for these experiments was quite high. Since this stimulation induces a broad innate immunity response from the microglia consisting of the release of many different cytokines, the cultures may have been overwhelmed to the point that no specific signaling pathways could be activated. Similarly, it is possible that some

neuroprotective pathways may have been concomitantly activated, effectively resulting in offsetting mechanisms. Specifically, this system differs from most of those discussed previously due to its inclusion of astrocytes. Astrocytes can be neuroprotective as they have mechanisms to alleviate oxidative stress [164]. However, they have also been demonstrated to have neurotoxic effects in response to LPS stimulation *in vitro* [165]. Whether their presence in this system is helpful or harmful cannot readily be determined, but their potentially ameliorative effect cannot be ruled out.

A final possibility for the lack of cell death is that some technical aspects of the culture method may be unfavorable to the initiation of neurotoxic signaling cascades. The cell density of the 3-D cultures (4,000 cells/mm^3) is high relative to typical 2-D plating densities (50,000-100,000 cells/cm^2)—the 2-D density equivalent of these cultures if the same number of cells were plated would be 400,000 cells/cm^2. Despite the increased cell density afforded by the 3-D geometry, the cultures still have densities that are more than an order of magnitude lower than the *in vivo* rat cortex [166]. The resulting intercellular distances in these cultures are relatively large and released cytokines may diffuse in such a way that no gradients can effectively be established. Additionally, the 3-D gel is covered with a volume of feeding medium which is more permissive to diffusion than the gel itself. Therefore, cytokine density is further diluted, perhaps preventing the expected signaling. Indeed, each of the cytokine-based outcome measures presented in this chapter detects output from cells in direct response to the LPS stimulation. Induction of cell death would require intercellular signaling as microglia are the primary effectors of the LPS response and neurons would be the cells most vulnerable to toxic signaling pathways.

The absence of a morphological shift in response to LPS can be explained with similar reasoning. The TLR4-mediated innate immune response mounted by the microglia upon LPS stimulation is, again, a broad response in the sense that many cytokines are upregulated and released. As with the explanation for lack of cell death, signaling molecules that would induce a morphological change may be effectively diluted to the point that their signals are not transmitted. Alternatively, the composition of the Matrigel™ ECM may be affecting the microglial response. This will be explored further in later chapters. The lack of cell death itself may be the reason that the shift is not observed. Many of the mechanical aspects of microglial behavior, including morphological shift and chemotaxis, rely on ATP gradients which typically result from dying cells. In the absence of dying cells or exogenous ATP, the cultures may lack the necessary signals to induce microglia to assume a rounded morphology. This brings up the question of the efficacy and validity of LPS as a positive control for neuroinflammation in this system.

In subsequent chapters, the 3-D multitypic neural cultures are subjected to various mechanical insults with the intent of modeling the secondary injury mechanisms associated with TBI. In order to assess the ability of the cultures to be induced into a state of inflammation, LPS was chosen as a positive control as it has classically been used to induce inflammation in both *in vivo* and *in vitro* models [167]. However, given that the TLR4-mediated inflammation pathway activated by LPS is part of the innate immune response, it is perhaps not the best control for a TBI model. Although microglia are certainly activated in response to injury *in vivo* [65, 125, 126], the mechanisms by which cytokine expression is upregulated and through which the microglia change from a

quiescent to an active state are different than those of innate immunity. Additionally, LPS has been described as an "incomplete stimulus" that requires another factor such as ATP since LPS generates a large pool of intracellular immature IL-1β, but is less effective at inducing cleavage and release [77].

The presence of ATP from dead or dying cells is crucial for the activation of microglia signaling pathways. This signaling occurs through purinergic receptors on the microglial cell surface. This large family of receptors includes ionotropic and metabotropic members which have been shown to be responsible for cellular responses ranging from chemotaxis [133, 168] to induction of IL-1β release [131]. The latter is associated with activation of the P_2X_7 purinergic receptor by ATP [79]. Based on this information, stimulation of the 3-D cultures with ATP would likely be a more relevant positive control for the injury mechanisms associated with TBI. The introduction of a modified form of ATP to these cultures is explored further in Chapter 6. However, LPS stimulation demonstrated that the microglia in these cultures can be induced into a state of inflammation which was the primary goal of these experiments. The next step of the research presented here is to develop a mechanical injury protocol for these cultures that is consistent with the parameters of TBI.

CHAPTER 4

IMPLEMENTATION OF THE 3-D MULTITYPIC NEURAL CELL CULTURE SYSTEM IN THE DEVELOPMENT OF A MECHANICAL INJURY MODEL OF TRAUMATIC BRAIN INJURY

4.1 Introduction

The development of an *in vitro* model of TBI requires a system in which the mechanical deformations that occur *in vivo* can be mimicked. Mechanical injury of cultured cells has long been studied in 2-D using methods such as scratching cells on a rigid substrate and stretching cells on a flexible membrane. The former method lacks consistency, but the latter has been successful with slice cultures [41] in addition to 2-D cultures [46, 169]. In our lab, delivery of the mechanical load that produces the stretch injury is achieved using a circular tube piston driven by a linear actuator at specified velocities and displacements to achieve the desired strains and strain rates. While injuries carried out in this manner can reproduce some of the forces experienced by cells in TBI *in vivo*, the 2-D geometry of the culture system certainly affects the subsequent cellular response. Such studies are effective for modeling the acute effects of injury, but may not adequately represent secondary injury mechanisms. In our lab, these experiments at most included neurons and astrocytes. As discussed in Chapter 2, were microglia to be included in a 2-D culture system, many of them would grow as rounded cells, loosely adhered to astrocytes. As such, the microglia would not experience the same strain as the neurons and astrocytes which would be in direct contact with the flexible membrane. Using a 3-D culture system results in a more "tissue-like" environment in which all of the cells present can grow in a natural morphology and will experience more uniform strains

when mechanically injured. As previously discussed, the 3-D cultures described in Section 2.2 have been extensively utilized in both shear and compression injury studies.

In the initial development of a mechanical injury model using the 3-D multitypic neural cultures, a similar approach was used as with the development of the cultures themselves. Specifically, previously defined injury methods were implemented wherein 3-D cultures containing neurons, astrocytes, and microglia were used in place of the neuron-astrocyte co-cultures. The first goal was to confirm that the new cultures could be injured in a manner that yielded a consistent level of cell death in the cultures. Since the ultimate goal of this research was to create a model of mechanically-induced neuroinflammation, the establishment of a method that resulted in the death of a significant population of cells without killing the entire culture was critical. Too mild an injury might not be sufficient to trigger an inflammatory response. Too severe an injury might kill far too many cells (including the microglia) or overwhelm the system to the point where the outcome measures are washed out. In essence, the goal was to produce an injury severe enough to substantially affect the most vulnerable cell population (neurons), while sparing the cell populations involved in the inflammatory response (astrocytes and more importantly, microglia). As detailed in this chapter, this proved more difficult to achieve than expected. It ultimately required an overhaul of the culture method as well as a complete shift in the mechanism of injury delivery. However, such changes were necessary to create a consistent injury model that would ultimately be the test-bed for inflammation studies.

4.2 Improvement of custom-manufactured 3-D culture and injury chambers

4.2.1 Previously-developed injury devices

The initial method employed to impart mechanical deformation to the 3-D multitypic neural cell cultures was a custom-made 3-D cell shearing device (CSD) [61]. This system utilized custom-made, silicone-walled dual culture chambers adhered to glass coverslips set in a polycarbonate frame for interface with the cell shearing mechanism. For injuries, the chamber was held fixed while a polycarbonate top plate with silicone pads made contact with the 3-D cultures and delivered a prescribed shear deformation via an attached PID-controlled actuator. While this well-designed system delivered consistent shear injuries, it was not without limitations. Most of these stemmed from the method of manufacture. The machined polycarbonate components were milled in such a way that only matching pairs of top and bottom plates would sufficiently align for use in the device. This led to generating 3-D cultures in standard multiwell plates and transferring them to the custom chambers for injury followed by transfer back to the multiwell plates. While this did not present an experimental problem in the properly controlled experiments in which this system was employed, it was far from streamlined.

Ideally, the 3-D cultures would be grown and injured in the same chamber, eliminating the need for transfer of the delicate cell-seeded matrices. While this could be achieved using the existing chambers, the need to match the top plate to its bottom mate would require attachment of the appropriate top plates to the actuator for each injury. Additionally, preparing the chambers for culture use proved difficult as the mixed composition of the chambers (silicone, glass, and plastic) led to incompatibility with one or more typical methods for cleaning and sterilization. The logical solution was to create

separate culture chambers consisting solely of silicone and glass that could be inserted into the plastic assembly at the time of injury. This would eliminate the need to physically transfer the cultures as well as require only a single plastic assembly to carry out all injuries. Producing such a modular design using available milling machines was not feasible due to the grooves necessary to allow insertion of the culture chamber into to injury frame. In the interest of enhancing the reproducibility of *in vitro* injury experiments, and due to the availability of the resource, the redesigned injury system was generated using 3-D printing technology.

In addition to the CSD, *in vitro* injury was also imparted using a 3-D cell compression device (CCD) [62]. This system delivered mechanical load to 3-D cultures by means of a 10 mm diameter piston driven by a linear actuator controlled by the same PID controller as the CSD. The strains and strain rates possible with the CCD were comparable to those achievable using the CSD. While the CCD did not have the same limitations as the CSD, it was also modified to be compatible with the improved chamber slides using 3-D printed parts. Additionally, rapid prototyping allowed for simplified generation of pistons with different diameters.

4.2.2 Manufacture of *in vitro* chamber slides, CSD chambers, and CCD components

4.2.2.1 Culture chamber slides

The silicone walls of 3-well chamber slides were made of Sylgard 184® (Dow Corning, Midland, MI) polydimethylsiloxane (PDMS) cast in reusable 3-D printed molds made of Objet FullCure® 950 Tango Gray material (printed by RedEye, Eden Prairie, MN). All CAD files for the culture as well as the injury components were created using Pro/ENGINEER® Wildfire 5.0 (PTC, Inc., Needham, MA). To complete the chamber

slide, the silicone walls were adhered to 75mm x 25mm plain glass slides using Dow Corning® 734 flowable sealant (Figure 4.1). Although the use of glass coverslips with the previous model allowed for the use of high-power microscope objectives with short working distances, glass slides provided the durability required for insertion into and removal from the *in vitro* injury chamber.

4.2.2.2 CSD chambers

The modular shear injury chambers were generated using the same dimensions as the previous chambers so that no modifications to the injury device would be necessary. All parts of the shear injury chamber were printed using an Objet Eden 250 printer (Stratasys, Eden Prairie, MN) using Fullcure® 720 material. The complete chamber consists of three components: a **frame** into which the chamber slide can be inserted; an **insert** placed into the frame to secure the chamber slide; and a **lid** with "C"-shaped feet to which PDMS inserts are adhered such that when placed on top of the frame, gentle contact with the 3-D cultures is made (Figure 4.2). Numerous iterations of this design were manufactured to produce properly mating parts before carrying out injury experiments. This was required as working within the tolerances of the 3-D printer necessitated compensation for slight disparity in the dimensions of the printed piece versus the CAD file.

4.2.2.3 CCD components

New pistons were created using the same dimensions as the previous milled polycarbonate components. The pistons were printed using Objet Fullcure® 720 material (Figure 4.3A and 4.3B), and as with the design of the lid for the CSD chamber, PDMS

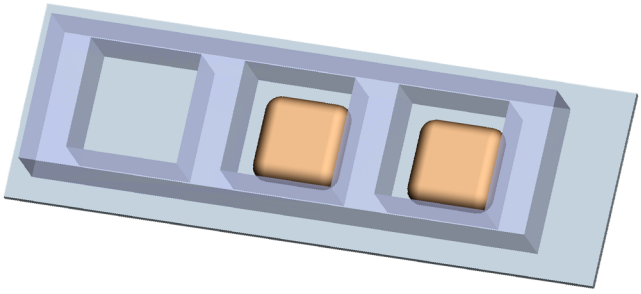

Figure 4.1. Custom-manufactured 3-D culture chamber slide.

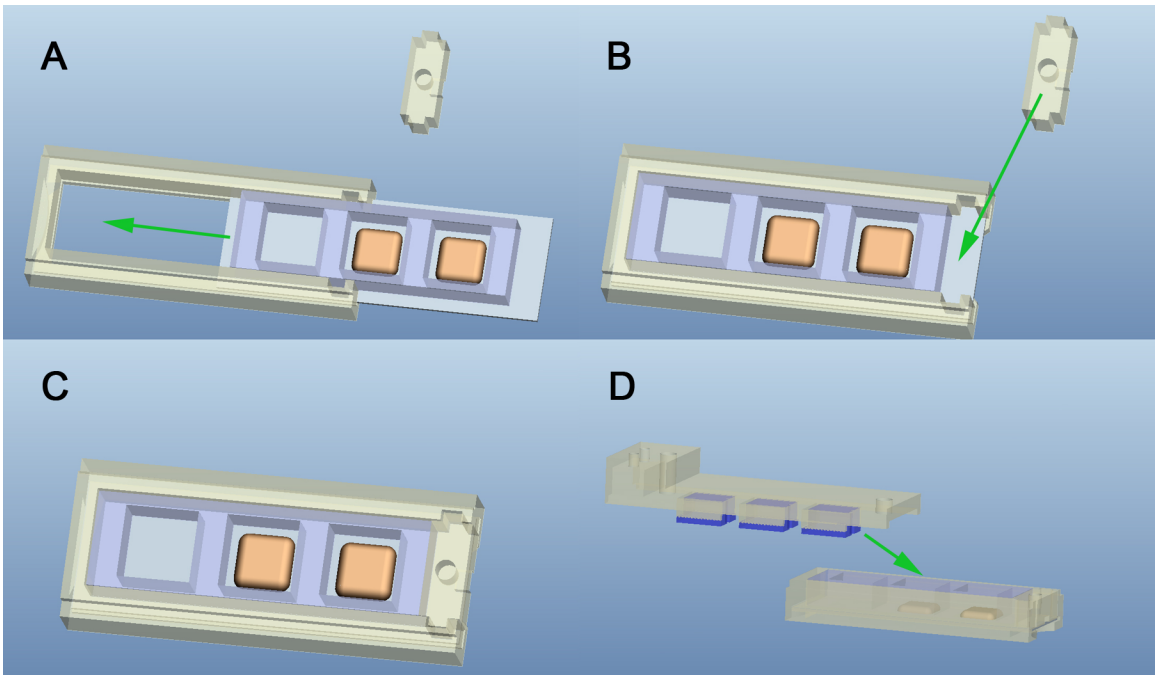

Figure 4.2. Shear injury chamber assembly. (A) The chamber slide is inserted into the injury frame. (B,C) The insert is placed into the frame to secure the chamber slide. (D) The lid is placed on top of the frame.

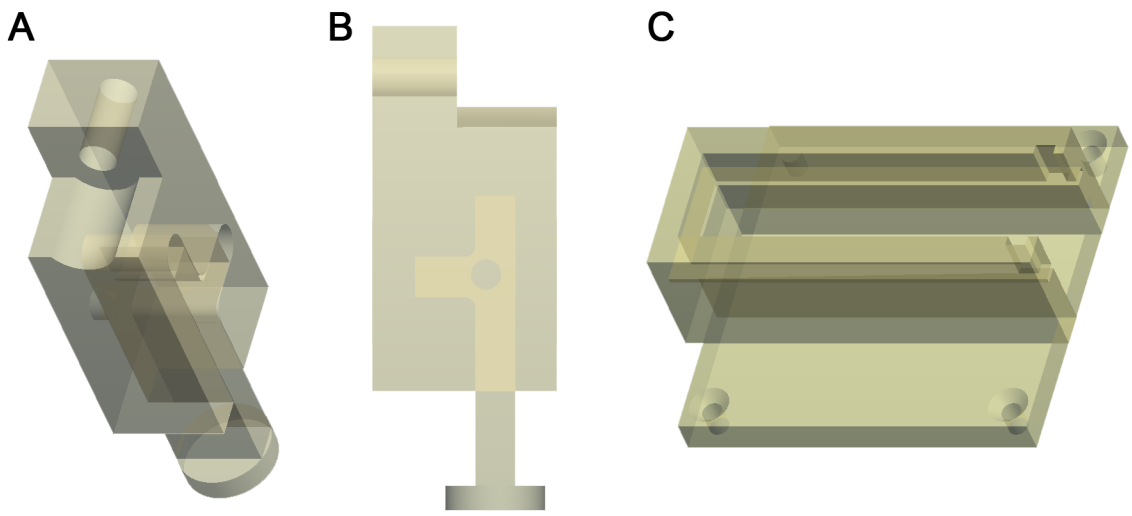

Figure 4.3. 3-D printed compression injury device components. (A) The piston assembly with 10 mm piston inserted. (B) Right profile of the piston assembly. (C) The compression injury frame for holding chamber slides.

pads were adhered to the piston surface where it made contact with the 3-D cultures during injury. An additional modification to the CCD was to print a frame to hold the culture chamber slides during injury (Figure 4.3C). The upper dimensions of this frame were identical to the CSD injury frame. It was substantially taller to facilitate inserting and removing the chamber slides and also to position them within the range of the piston stroke. Detailed methods for the manufacture and preparation of the chamber slide, shear injury chamber, and compression injury components can be found in Appendix A.

4.3 Experimental methods

4.3.1 Chamber slide preparation

The glass and silicone chamber slides were designed to be completely reusable. Prior to 3-D plating, the slides were cleaned using detergent as well as both aqueous and organic solvents. Slides were rinsed with tap water, wiped with a cotton swab, and soaked in tap water containing dissolved powdered Alconox (Alconox, Inc., White Plains, NY) for at least 30 minutes on a rotary shaker. The sides were then rinsed with fresh tap water and then exposed to sequential 10 minute soaks in: deionized (DI) water, 70% ethanol, acetone, 70% ethanol, and DI water. All of these steps were carried out on a rotary shaker. Sterilization was achieved by sealing the slides in steam sterilization pouches and autoclaving them at 127 ºC with a Tuttnauer 3850M benchtop autoclave (Tuttnauer, Hauppauge, NY). The slides were then transferred to 15 cm polystyrene culture dishes (4 slides per dish) and coated with 500 µL of 100 µg/mL PDL in DI water for 24-48 hours. On the day of plating, the PDL was removed and the wells were rinsed twice with 500 µL of sterile, DI water. The liquid from the culture chambers was aspirated to remove as much water as possible and they were then allowed to dry

completely in the laminar flow hood while tissue dissection and dissociation procedures were carried out.

4.3.2 Cell culture

3-D multitypic neural cell cultures were generated as discussed in Chapter 2 and as described in detail in Appendix A. Briefly, E18 rat cortical neurons were combined with cortical glial cells acquired from P0 rats at a 2:1 ratio of neurons to total glia. The cells were mixed with high-concentration, growth factor-reduced Matrigel™ (final plating protein concentration of 7.5 mg/mL) to a cell concentration of 4,000 cells/mm^3. The 3-D cultures were plated at a volume of 100 μL or 200 μL into the custom-made chamber slides described in Section 4.2.2. The cells were maintained in an incubator at 37 ºC and 95% relative humidity. The cultures were fed with medium containing G-5 supplement 90 minutes after the initial plating (500 μL) and 24 hours post-plating (replacing half of the medium). All subsequent half-medium exchanges were with medium without G-5. All medium used for 3-D culture feedings was pre-warmed and pre-conditioned with CO_2 by placing an aliquot in a flask fitted with a filter cap into the incubator.

4.3.3 Mechanical injury

4.3.3.1 Shear injury

Preparation of the shear injury chamber for mechanical loading of the 3-D cultures consisted of rinsing the previously mentioned parts with DI water, spraying them with 70% ethanol, patting them dry, placing them into 15 cm polystyrene dishes and exposing them to UV light in a laminar flow hood for at least 1 hour. For injury, medium was removed from the cultures; the chamber slide was transferred to the plastic frame, secured with the plastic insert, and gently compressed by affixing the lid with PDMS well

inserts. Between injuries, the PDMS pads of the lid were wiped with 70% ethanol and then dipped in sterile medium. The entire assembly was transferred to the CSD where the frame secured in place and the top was attached to the linear actuator by means of a plastic chuck. Once assembled, the shear deformation was imparted to the cultures (2 per 3-well chamber slide) by a PID-controlled linear actuator (Figure 4.4). A trapezoidal input was generated by custom code written in LabVIEW® (National Instruments, Austin, TX). The mechanical loading delivered 0.50 strain with strain rates of 10 sec^{-1} or 30 sec^{-1}. Sham controls were placed into the injury chamber and CSD but not subjected to mechanical loading. After exposure to injury or sham conditions, cultures were given fresh medium and returned to the incubator. Naïve conditions simply consisted of a medium change and were included to ensure that the sham condition did not impart injury to the cultures. Confirmation that the lid of the injury chamber was moving with the impulse of the actuator while the chamber slide remained fixed was obtained using registration marks and a microscope during device activation.

4.3.3.2 Compression injury

Chamber slides were transferred directly to the CCD for injury as the frame and piston remained affixed to the device. Prior to injury experiments, the frame and piston were wiped down with 70% ethanol and allowed to dry. Medium was removed from the cultures and the chamber slide was transferred to the device in a 10 cm polystyrene dish. Once inserted in to the CCD, the stage was moved to position each culture beneath the piston (8 mm or 10 mm diameter) for injury. The same controller and LabVIEW® software from the CSD were used to deliver the mechanical load. The piston was driven to a depth of between 0.50 mm and 1.00 mm from the surface of the culture at specified

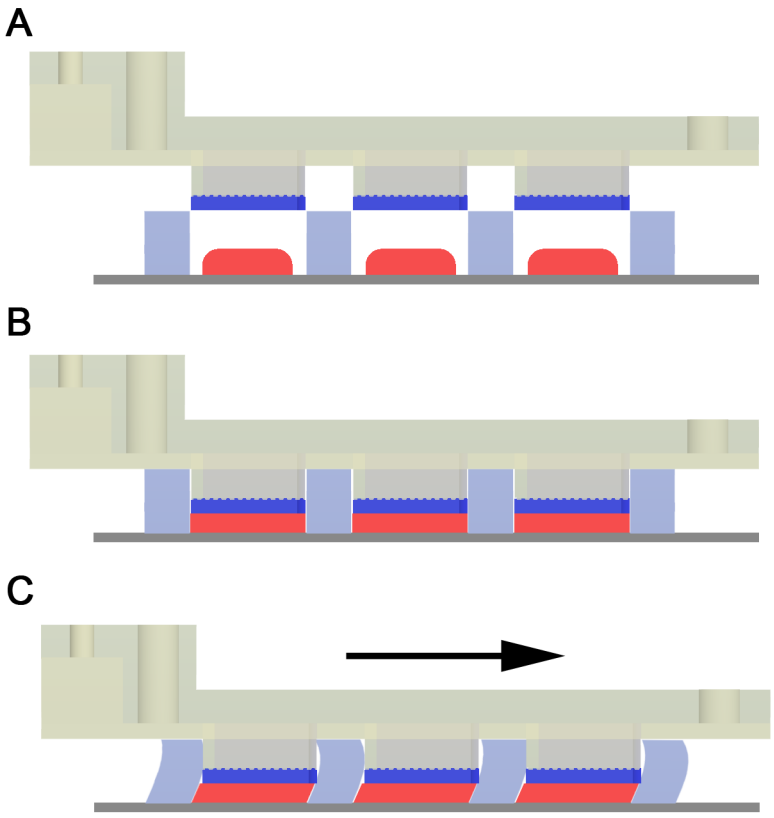

Figure 4.4. Shear injury illustration. (A) The shear injury lid is positioned above 3-D cultures. (B) The lid is lowered to gently compress the cultures to a uniform thickness. (C) A linear actuator rapidly displaces the lid relative to the fixed-position cultures, creating a shear deformation.

velocities ranging over an order of magnitude between 30 mm/s and 500 mm/s. For low velocity compression injuries (30 mm/s), the piston was lowered to make contact with the culture surface prior to device activation. For compression at all other velocities, the piston was above the culture prior to activation. For sham injuries, the piston was manually advanced to gently make contact with the culture surface and slowly retracted. Between each injury, the PDMS surface of the piston was swabbed with 70% ethanol and dried. After exposure to injury or sham conditions, the cultures were given fresh medium and returned to the incubator. Naïve conditions were the same as for the shear injury experiments.

4.3.4 Outcome measures

4.3.4.1 Cell viability

Cell viability was determined by using calcein AM and ethidium homodimer to identify live and dead cells, respectively, or by using Hoechst 33342 and propidium iodide to identify all cells and dead cells, respectively. 3-D cultures were rinsed with DPBS, exposed to the fluorescent markers (in DPBS) for 30 minutes, and imaged using a Nikon Eclipse 80i upright microscope equipped with a MicroFIRE camera. Images from three fields from each culture were captured at 10X magnification using both appropriate fluorescent filters. Each channel was individually thresholded in Adobe Photoshop CS4 and cells or nuclei were counted using defined parameters in ImageJ software. For some experiments, 3-D cultures were exposed to propidium iodide prior to mechanical injury to identify dead cells or cells with compromised plasma membranes. Imaging was carried out using the aforementioned microscope setup.

4.3.4.2 LDH Assay

Culture medium was collected at time points ranging from 1 hour to 24 hours post-injury. Levels of LDH were determined colorimetrically using an *In Vitro* Toxicology Assay Kit and a Power Wave X 340 spectrophotometer (Bio-Tek Instruments, Inc., Winooski, VT) operated using KC Junior Software (Bio-Tek). The data were compared to that from cultures treated with 0.1% Triton X-100 for 30 minutes to 1 hour prior to medium collection to establish maximum LDH release.

4.3.4.3 Immunocytochemistry

Complete cultures processed for immunocytochemistry were fixed with 2% paraformaldehyde in PBS, permeabilized with 0.1% Triton X-100, incubated with primary antibody overnight at 4 ºC and with secondary antibody for 1-2 hours at room temperature. All solutions for immunolabeling (including rinse buffer) contained 0.05% saponin. Cultures were probed using primary antibodies against MAP2, GFAP, and Iba1. Hoechst 33342 was used as a nuclear counterstain.

4.3.4.4 Statistical analysis

Data were statistically compared using one-way ANOVA followed by a post-hoc Tukey-Kramer test for multiple comparisons if ANOVA yielded a result of $p<0.05$.

4.4 Shear injury of 3-D multitypic neural cell cultures

In order to demonstrate the ability to inflict cellular damage using the improved culture and injury system, pilot experiments were performed in which cell viability was assessed after shear injury. Cultures maintained for 25 DIV were subjected to shear injury (n=8), sham injury (n=4), or no injury (n=2). Live-dead assessment using calcein AM and ethidium homodimer 24 hours after injury revealed a significant reduction in cell viability

in both the sham ($p<0.01$) and injury ($p<0.05$) conditions compared to the naïve condition (Figure 4.5A). The viability of the sham and injured cultures did not differ significantly. The accuracy of these data was questioned due to the difficulty in determining cell boundaries when processing the calcein AM data. As discussed in Section 3.2.6, the projection of 3-D fluorescent signal onto a 2-D image coupled with the cytosol-filling labeling of the calcein AM led to the decision to perform viability assessment exclusively using nuclear markers. This would allow for more discrete labeling of the cultured cells. Cultures maintained for 19 DIV were subjected to shear injury (n=8), sham injury (n=4), or no injury (n=4) as before. Cell viability determined using Hoechst 33342 and propidium iodide 48 hours after injury revealed no significant reduction in viability in response to injury (Figure 4.5B). These experiments were repeated at various time points and with minor modifications to the injury chamber, but did not consistently demonstrate that any significant cell death was occurring in response to shear injury.

4.5 Compression injury of 3-D multitypic neural cell cultures

Pilot experiments using compression injury were carried out to determine if changing the means of mechanical loading would prove more successful at delivering mechanical injury. In addition to the change in the method of mechanical injury, the method of cell viability assessment was changed to LDH release to increase accuracy and sensitivity. The initial compression injury experiments using previously employed velocity parameters (30 mm/s) did not show any increase in LDH release in response to injury. Thus, higher velocity conditions were added. Cultures maintained for 7 DIV were subjected to compression injury with an 8 mm diameter piston to a depth of 0.50 mm at 30 mm/s (n=2), 100 mm/s (n=2), and 500 mm/s (n=4) as well as to sham (n=2) and naïve

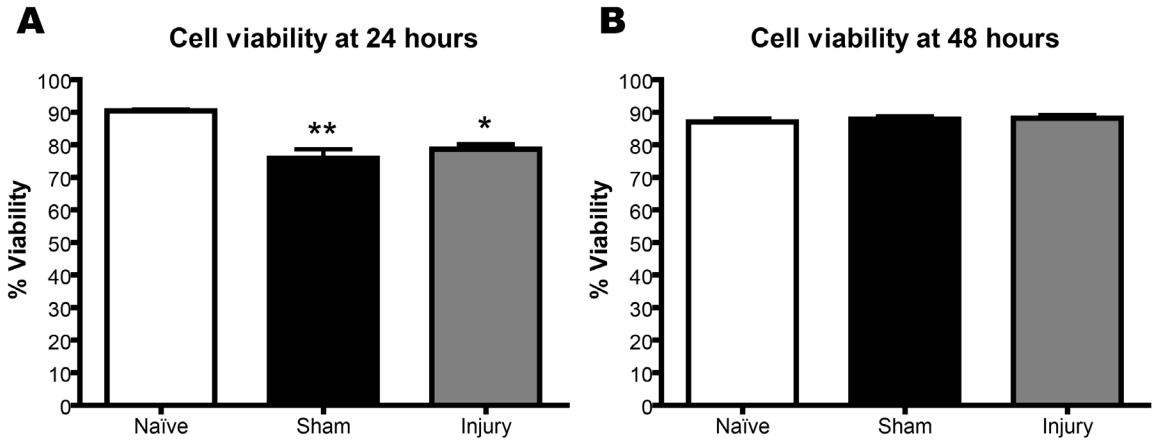

Figure 4.5. Determination of cell viability in response to shear injury using fluorescent markers. (A) 24 hours after cultures (25 DIV) were subjected to shear injury (0.50 strain, $30s^{-1}$) (n=8), to sham injury (n=4), or to no injury (n=2), a Live-Dead assay was performed using Calcein AM and ethidium homodimer to label viable and dead cells, respectively. Cell viability is significantly reduced in both the injury ($p<0.05$) and sham ($p<0.01$) conditions compared to the naïve control. The sham and injury conditions are not significantly different from each other. (B) 48 hours after cultures (19 DIV) were exposed to shear injury (0.50 strain, $30s^{-1}$) (n=8), to sham injury (n=4), or to no injury (n=4), viability was assessed using Hoechst 33342 and propidium iodide to label the nuclei of all cells and dead cells, respectively. This method shows no significant difference between any of the conditions. Data were statistically compared using one-way ANOVA followed by a post-hoc Tukey-Kramer test for multiple comparisons, if necessary. Bars are means plus SEM.

(n=2) conditions. LDH release 24 hours after injury progressively increased with increasing velocity (Figure 4.6). However, due to the small sample size, the only significant difference was between the maximum velocity (500 mm/s) and the naïve control ($p<0.05$).

Based on the promising trend of the pilot data, further compression injury experiments were conducted with a key change to the culture method. Cultures had typically been plated at a volume of 200 μL such that filling the 200 mm^2 well would result in a gel with a thickness of 1 mm. However, filling the bottom of the well to the walls caused a meniscus to form and prevented either injury method from being effective. Rather, the cultures were plated such that the gel would cover as much area as possible without making contact with the wall. The resulting cultures were thicker in the center than at the edges. Phase contrast microscopy clearly indicated that at the surface of the chamber slide, the center of the gel was nearly devoid of viable cells. As this would certainly be affecting the viability data, cultures were subsequently plated at a volume of 100 μL. These looked substantially healthier at their thickest point, which was closer to the desired thickness of 1 mm.

To assess the time course of LDH release after mechanical insult, 100 μL cultures maintained for 13 DIV were subjected to compression injury with a 10 mm diameter piston (500 mm/s velocity, 0.50 mm depth) or to sham injury. Medium was collected from injured cultures at 2, 4, and 8 hours (n=3 each) and from sham cultures at 8 hours (n=3). The LDH activity in the medium of the injured cultures increased with time and at 4 and 8 hours was significantly different from the sham conditions ($p<0.001$) (Figure 4.7).

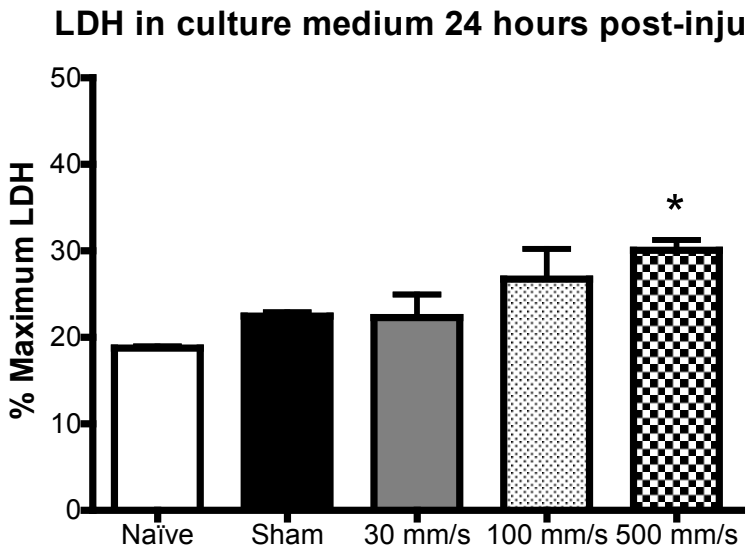

Figure 4.6. Determination of cell viability in response to compression injury by LDH release. Cultures (7 DIV) were subjected to compression injury (8 mm piston diameter, 0.50 mm depth) at velocities of 30 mm/s (n=2), 100 mm/s (n=2), and 500 mm/s (n=4), as well as to sham (n=2) and naïve (n=2) conditions. LDH release in the medium increases with increasing piston velocity. The 500 mm/s injury is significantly different than the sham condition ($p<0.05$). Data were statistically compared using one-way ANOVA followed by a post-hoc Tukey-Kramer test for multiple comparisons. Bars are means plus SEM.

The maximum actuator velocity for which the output closely matched the input was 500 mm/s. Thus, to achieve an increase in injury severity, another parameter would have to be modified. The simplest options were piston diameter and compression depth. Since the piston diameter had already been increased to 10 mm, the effect of compression depth was assessed. Cultures maintained for 12 DIV were subjected to a compression injury with a 10 mm diameter piston to a depth of 0.50 mm or 1.00 mm into the culture (n=3 each) or to a sham injury (n=3). The LDH activity in the injured culture medium 20 hours after injury is significantly higher than the sham at both injury depths ($p<0.001$) (Figure 4.8A). Further, LDH release from the 1.00 mm injury is significantly higher than that from the 0.50 mm injury, registering greater than 100% LDH activity. The compromised astroglial morphology and near absence of MAP2-positive neurons in the images collected from immunocytochemical analysis of the cultures corroborates the severity of the 1.00 mm injury (Figure 4.8F,G). However, the morphology of the cells subjected to the 0.50 mm injury (Figure 4.8D,E) does not appear substantially different from the sham (Figure 4.8B,C)

4.6 Conclusions

This chapter has described the evolution of the *in vitro* injury model for the 3-D multitypic neural cell cultures. Using the materials and parameters of the previously described model for neuron-astrocyte co-culture injury failed to produce injured cells in the microglia-containing cultures. Neither cell viability nor levels of LDH were affected when shear injuries up to 0.50 strain and strain rates up to 30 s^{-1} were delivered. Given the severity of injury that such mechanical loading was expected to impart, this result was surprising. One possible explanation is that the presence of the microglia in the cultures

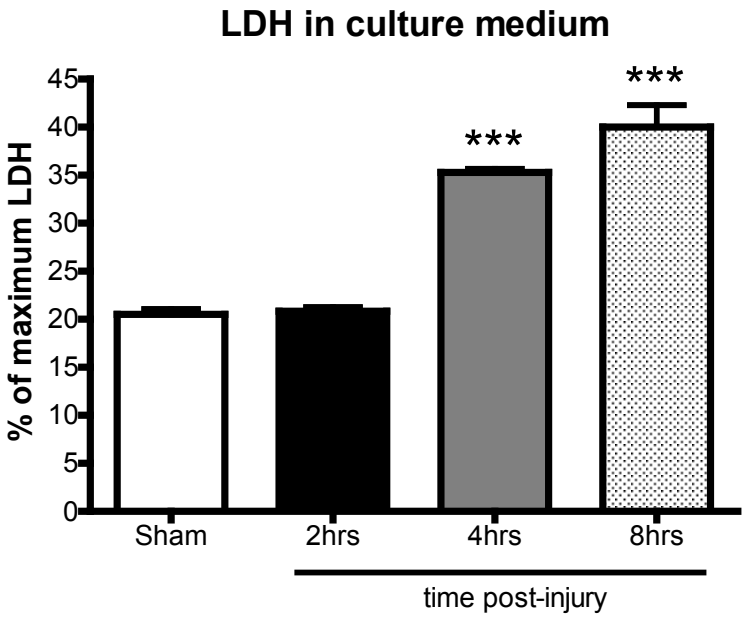

Figure 4.7. Time course of LDH release in response to compression injury. Cultures (13 DIV) were subjected to compression injury (10 mm piston diameter, 500 mm/s velocity, 0.50 mm depth) or to sham injury. The level of LDH in the medium was determined at 2, 4, and 8 hours (n=3 each) and from the sham cultures at 8 hours (n=3). LDH activity in the medium increases with time after compression injury and was significantly different from sham at both 4 and 8 hours ($p<0.001$). Data were statistically compared using one-way ANOVA followed by a post-hoc Tukey-Kramer test for multiple comparisons. Bars are means plus SEM.

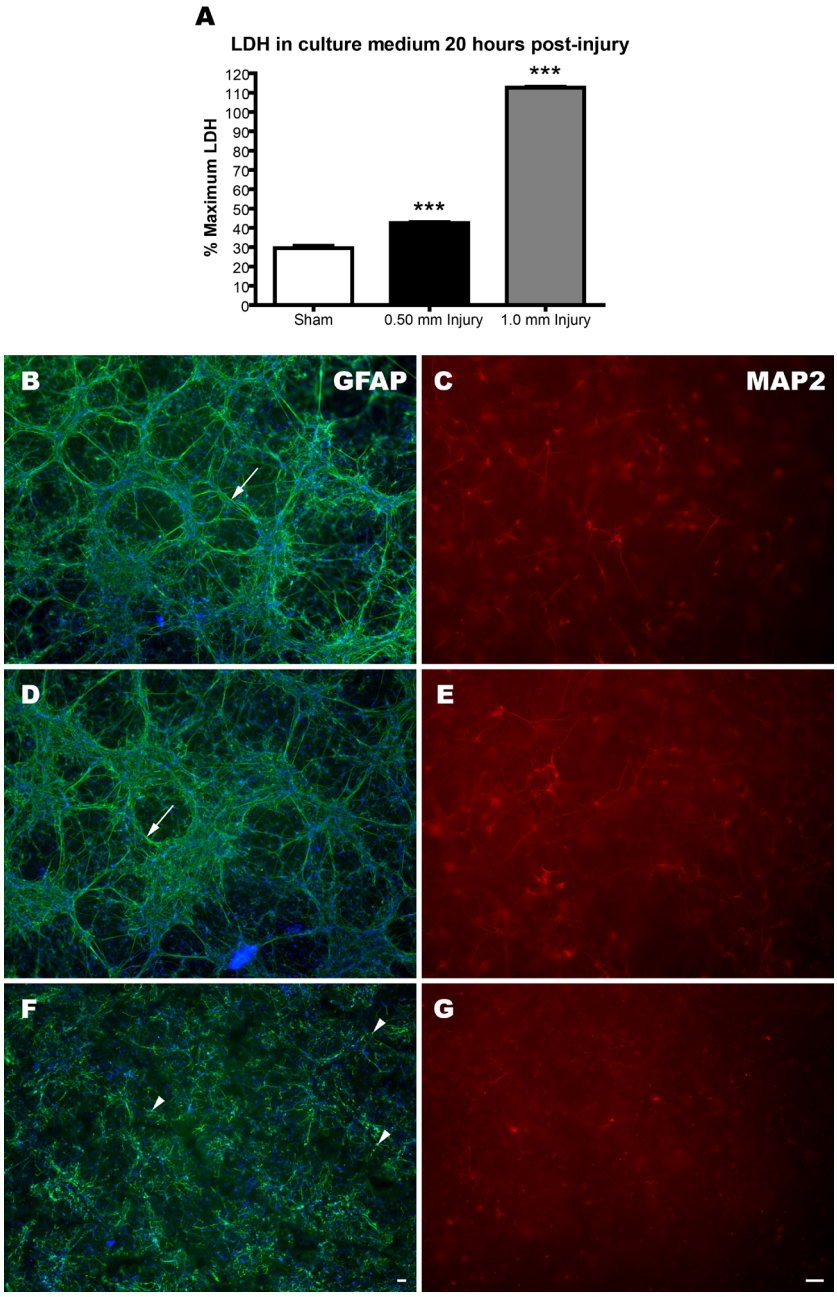

Figure 4.8. The depth of piston compression into the culture decreases cell viability and affects cell morphology. Cultures (12 DIV) were subjected to compression injury (10 mm piston diameter, 500 mm/s velocity) to a depth of 0.50 mm or 1.00 mm or to a sham injury (n=3 each). (A) LDH activity in the medium is significantly higher than sham for both injury conditions ($p<0.001$). Cultures were incubated with antibodies against GFAP (B,D,F, green) or MAP-2 (C,E,G) to label astrocytes and neurons, respectively, as well as with Hoechst nuclear counterstain (B,D F, blue). The cells do not exhibit morphological differences in the 0.50 mm injury (D,E) compared with the sham injury (B,C). GFAP fibers in both conditions are intact (arrows). There is a substantial degradation in the astrocyte fibers (arrowheads) and a near absence of neurons in the 1.00 mm injury (F,G) compared with the sham injury (B,C). Bars are means plus SEM. Scale bars: 50 μm.

was ameliorating the injury response via induction of macrophage-like activity, and after 24 hours the response was not detectable using the chosen outcome measures. However, experiments in which the cultures were pre-loaded with propidium iodide, injured, and immediately imaged also failed to show any cell death. Another explanation is that despite the advantages of the updated culture and injury chamber design, it is possible that the prescribed mechanical load was not being accurately delivered to the cultures. However, injuries carried out using the previously manufactured chambers also failed to demonstrate cell death when compared to sham controls. Further, were the new chambers posing a problem to the injury model, the implementation of compression injury should not have been affected as the chamber has no effect on the load delivery. Indeed, compression injury experiments using previously employed parameters also failed to injure the cells. Ultimately, it was found that a piston velocity of over an order of magnitude higher than previously used was required to reliably damage the cells as measured by LDH activity and confirmed with immunocytochemistry.

The optimized injury system described in this chapter is comparable to other methods of delivering mechanical trauma *in vitro*. Using the previous 3-D neuron-astrocyte co-cultures, both shear and compression injury increased cell permeability to calcein in a strain-rate-dependent manner while only high strain-rate shear injury significantly decreased cell viability [62]. Cell injury and death have been demonstrated in 2-D neuronal cultures grown on flexible substrates. Stretch injury of 2-D primary rat neurons has been shown to induce cell permeability to calcein [169]. Biaxial stretch injury of SH-SY5Y cells was demonstrated to induce both cell injury and death in a strain, but not strain-rate-dependent manner [170]. Neuron-glia co-cultures have

exhibited increased LDH activity in response to injury delivered by impact with a custom punch [171] and by stretch [172]. The latter response was shown to be enhanced by hypoxia. Although hypoxic conditions were not tested in the system presented there, they could easily be included in future studies. In hippocampal slice cultures, membrane permeability demonstrated by propidium iodide uptake has been demonstrated in response to injuries delivered by weight drop [173], by stretch [43], and by electrically-controlled cantilever [174, 175]. The compression injury model described in this chapter demonstrated injury-induced membrane permeability indicated by propidium iodide uptake as well as cell death based on the time-dependent elevation of LDH activity in the medium. The final design allows for delivery of a graded injury through modification of piston diameter, piston velocity, and penetration depth. The data presented here have shown that changing one or more of these parameters can result in injury levels ranging from nearly zero cell death to nearly complete destruction of the culture. Such a wide dynamic range allows for flexibility in designing experiments to model different severities of TBI *in vitro*.

Despite the unexpected changes to the injury parameters, the resulting protocol has a notable advantage in that it is closer to the *in vivo* CCI model. Although piston velocities used in CCI are a further order of magnitude higher than 500 mm/s, the mechanics of intact tissue (including the presence of the dura mater) are far different than those of a relatively soft hydrogel seeded with neural cells. Thus, this *in vitro* model of mechanical injury may not only serve as a standalone platform for the study of neuroinflammation, it may be directly comparable, if not translatable, to an *in vivo* system. Given the updated injury model presented in this chapter and the demonstration

of the inflammatory potential of these cultures in Chapter 3, the application of mechanical loading to the 3-D multitypic neural cell cultures should be sufficient to induce inflammation *in vitro*. This assertion assumes that the appropriate signaling pathways can be triggered in a culture model that, although it includes microglia, still lacks some of the key players in inflammation. Even in the absence of the complete picture of neuroinflammation, this model will provide insight into some facets of the microglial response to mechanical injury

CHAPTER 5

MECHANICAL INJURY-INDUCED NEUROINFLAMMATION IN THE 3-D MULTITYPIC NEURAL CELL CULTURE SYSTEM

5.1 Introduction

The ultimate goal of this research was to develop an *in vitro* model of neuroinflammation that is triggered by mechanical injury. The benefits of such a model include: consistency of the 3-D cultures, repeatability of injury delivery, and potential for high-throughput experiments. Despite the stripped-down nature of the *in vitro* system, the 3-D geometry and novel cellular composition of the cultures was believed to result in a model that captured microglia-driven inflammatory responses. Previous chapters have detailed the creation of the novel 3-D multitypic neural cell culture system, validation of the induction of inflammation in this system by chemical stimulation, and the evolution of a mechanical injury method for 3-D cultures. The next step was to attempt to produce an inflammatory response to mechanical loading *in vitro* that was on par with the response induced by the LPS positive control.

The initial choice of outcome measures used to assess the state of inflammation of the cultures was guided by the success of those that were employed for the LPS experiments detailed in Chapter 3. Some of the mechanical injury experiments presented in this chapter were performed in tandem with these LPS experiments. Specifically, IL-1β was chosen as the cytokine of interest due to its role in the injury response as well as the increased levels of the molecule at both the protein and mRNA level in response to LPS stimulation. Also, given the involvement of purinergic signaling in the activation of caspase-1, it was expected that the presence of extracellular ATP from mechanically

injured cells would provide the appropriate stimulation for IL-1β release. The release of other molecules such as superoxide and NO were also examined in order to obtain a more complete picture of the inflammatory response of the cultures.

As with the development of the mechanical injury model to sufficiently impart injury to the cultures, eliciting an inflammatory response proved to be more difficult than expected. Inconsistencies in culture geometry and related issues with mechanical injury led to minor modifications to the culture chamber slide and to the compression injury device, respectively. However, even with these modifications, the experiments were met with uneven success as the data presented in this chapter will illustrate. Despite this, the groundwork laid by these experiments provides a solid foundation for an *in vitro* model of mechanically-induced neuroinflammation.

5.2 Final modifications to the culture and injury systems

5.2.1 Medium reformulation

During the course of the experiments presented in this chapter, modifications were made to the medium used for maintaining the 3-D cultures. Standard B-27 supplement contains antioxidants, including superoxide dismutase, which could certainly interfere with inflammation processes. While the presence of antioxidants in the medium did not interfere with the detection of IL-1β and NO upon LPS stimulation, this response may have simply overwhelmed any damping effects of the antioxidants. In order to improve the detection of the potentially subtler inflammatory response to mechanical injury, antioxidant-free B-27 was used in all media formulations for the microarrays as well as for the experiments utilizing dyes sensitive to NO and ROS.

In another attempt to prevent the potential masking of mechanically-induced inflammation, the use of phenol red-free base medium was implemented for the same experiments. It has been suggested that medium preparations containing phenol red may possess estrogen-like activity [176-178] and estrogen is known to interfere with inflammatory processes in microglia [179, 180] and astrocytes [181]. A further advantage of eliminating phenol red was the removal of potential interference with colorimetric or dye-based assays. It should be noted that stock Matrigel™ preparations still contained phenol red from the gel as well as from the HBSS diluent. However, after repeated feedings with phenol red-free medium, this was reduced to a negligible level.

5.2.2 Chamber slide redesign to create flat 3-D cultures

As mentioned briefly in Chapter 4, when plating the 3-D cultures in the custom made chamber slides, the options for the culture geometry were for the gel to be thickest at the edges (meniscus effect) or at the center. In addition to the contributions of gel surface tension and the varying contact angles for wetting the PDL-coated glass and silicone surfaces, the protein content and thermal sensitivity of the Matrigel™ contributed to meniscus formation if the gel was permitted to touch the sides of the culture chamber. Rather, the alternative situation in which the gel remained as a roughly square-based dome was preferred such that the cultures would be able to make contact with the shear or compression injury devices. However, inconsistencies between cultures remained due to human variability in dispensing the gel and in the spreading of the gel on the glass surface. It was noted that despite exposure to organic solvents before reusing the chamber slides, the contact angle between the gel and the glass surface would decrease with repeated use. Thus, cultures spread more easily when plated into older chamber slides.

Beyond these concerns, the variability of thickness within a single culture would certainly cause a diffusion-dependent gradient of nutrient availability. This was the cause of the aforementioned issue with the cell death observed at the bottom of the 200 μL cultures which resulted in a shift to using a volume of 100 μL.

To address these issues, it was determined that the ideal culture geometry would be a square of uniform 1 mm thickness. However, due to the issues with meniscus formation, this proved quite difficult to achieve. Allowing for the meniscus to form and then backfilling the cavity with more cell-seeded Matrigel™ was considered, but never attempted as the geometry would likely remain inconsistent. Neither pre-heating nor pre-cooling of the chambers prior to gel prevented the meniscus from forming. As would be expected, this did affect the spreading of the gel as the warmer the substrate, the more rapidly polymerization occurred. Decreasing the surface tension of the PDL solution with isopropyl alcohol during coating was attempted to limit the height the PDL would climb the silicone wall. While this was successful for the coating phase, the stickiness of the gel due to protein content still resulted in a meniscus. Coating the walls of the wells with paraffin wax as previously described for invasion assays utilizing well inserts [182] was also unsuccessful and additionally left wax debris in the cultures. Finally, it was determined that the gel climbing the walls would be limited if the wall height was decreased. Thus, a new culture chamber was created consisting of 3 wells, each with a surface area of 150 mm^2 and a depth of 1 mm within the full size wells (Figure 5.1). Thus, the volume of each smaller culture well was 150 mm^3 so that 150 μL of cell-seeded Matrigel™ would completely fill it to the top of the 1 mm rim resulting in a flat 3-D culture. This new geometry greatly reduced plating time and no difference in cell

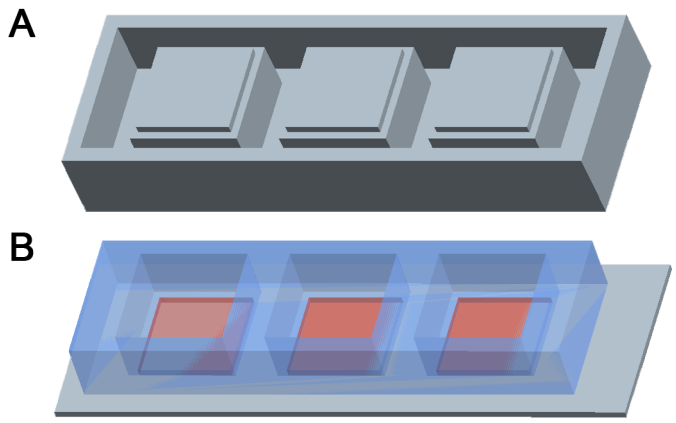

Figure 5.1. Redesigned chamber slide to facilitate the plating of 3-D cultures of uniform 1 mm thickness. (A) Molds for casting the silicone culture wells were printed in Objet FullCure® 950 Tango Gray material. (B) The completed culture chamber consists of three silicone-walled wells in a single piece adhered to a glass slide. The lip around the bottom of the well allows for the plated 3-D culture to have a flat surface.

viability was observed throughout the thickness of the culture. Additionally, the flat cultures had the advantage that a lower volume of culture medium could be used since the uniform culture thickness was not as easily exposed by the fluid meniscus. While cultures were maintained with 400 μL of medium, for injury experiments, the volume was reduced to 200 μL post-injury to concentrate any released factors for endpoint assays.

5.2.3 Change in piston diameter for compression injury device

One issue that arose with the new culture chamber was that the diameter of the compression injury piston had to be reduced. Since the sides of the culture were now constrained, compressing a square culture approximately 12.5 mm on a side with a 10 mm diameter piston caused the gel to displace upward which resulted in a devastating injury. In some cases, the culture would stick to the piston and pull away from the glass surface during retraction. Aside from this technical issue, it made sense to decrease the piston diameter from the standpoint of modeling neuroinflammation. The goal for the injury model was to cause enough cellular damage to result in the activation of pro-inflammatory pathways without causing culture-wide necrosis. Using this new flat 3-D culture and a smaller piston diameter would create a radial injury gradient. Ideally, three areas of the culture would be present post-injury: an injury umbra under the piston where cells experienced severe mechanical damage, an injury penumbra surrounding the umbra where cells experienced varying levels of compression and strain, and an uninjured region beyond the penumbra where cells experienced little to no deformation. It was in the penumbral region where the microglial response to injury was expected to be the highest. A piston with a diameter of 4 mm was designed which was large enough to still

impart compression rather than creating a cavity. This piston size would severely injure approximately 10% of the culture and hopefully generate an observable penumbra where an inflammatory response to injury could be detected. Additionally, three pistons were combined into a single 3-D printed part (Figure 5.2) so that all three cultures present on each chamber slide could be injured simultaneously, increasing throughput dramatically.

5.3 Experimental methods

5.3.1 Cell culture

3-D multitypic neural cell cultures were generated as discussed in Chapter 2 and as described in detail in Appendix A. Briefly, E18 rat cortical neurons were combined with cortical glial cells acquired from P0 rats at a 2:1 ratio of neurons to total glia. The cells were mixed with high-concentration, growth factor-reduced Matrigel™ (final plating protein concentration of 7.5 mg/mL) to a cell concentration of 4,000 cells/mm^3. The 3-D cultures were plated into custom-made chamber slides as 100 μL dome-shaped cultures or as 150 μL flat cultures, as indicated. The cells were maintained in an incubator at 37 ºC and 95% relative humidity. The cultures were fed with medium containing G-5 supplement 90 minutes after the initial plating (500 μL for dome-shaped cultures or 400 μL for flat cultures) and 24 hours post-plating (replacing half of the medium). All subsequent half-medium exchanges were with medium without G-5. All medium used for 3-D culture feedings was pre-warmed and pre-conditioned with CO_2 by placing an aliquot in a flask fitted with a filter cap into the incubator.

5.3.2 Compression injury

Between 7 and 14 DIV, medium was removed from the cultures and the chamber slides were transferred in 10 cm polystyrene dishes to the CCD for injury. Prior to injury

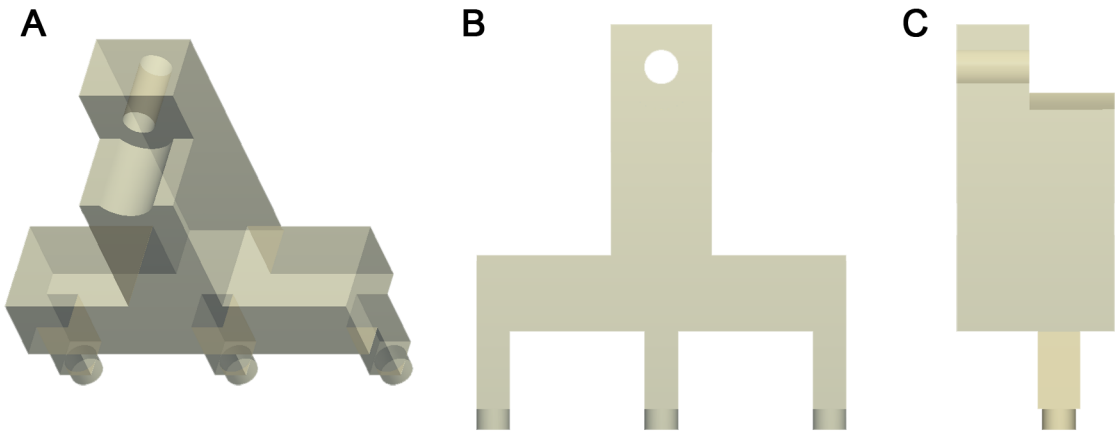

Figure 5.2. New 3-D printed compression injury pistons (A) The assembly with three 4 mm pistons. (B) Front view of the pistons. (C) Right profile of the pistons.

experiments, the frame and piston were wiped down with 70% ethanol and allowed to dry. Cultures were injured either individually using the 10 mm diameter piston or three at a time using the multiple 4 mm diameter pistons. The piston was positioned above the center of the cultures and driven to a depth of between 0.50 mm and 1.00 mm from the surface of the culture at a velocity of 500 mm/s. For sham injuries, the piston was manually advanced to gently make contact with the culture surface and slowly retracted. Between each injury, the PDMS surface of the piston was swabbed with 70% ethanol and dried. After exposure to injury or sham conditions, the cultures were given fresh medium and returned to the incubator. Naïve conditions were either transferred to the device briefly and given fresh medium or simply received a medium change.

5.3.3 Addition of adult mouse microglia

Adult microglia were harvested from C57/BL6 (heterozygous for GFP on CXCR1/Fractalkine promoter) mice according to a published protocol [183]. Briefly, whole brains were removed from adult mice and minced in cold PBS. The tissue was enzymatically dissociated using a cocktail of dispase II, papain, and DNase for 20 minutes at 37 ºC. The tissue was then rinsed and mechanically dissociated using a series of Pasteur pipets flame-narrowed to decreasing diameters. The resulting suspension was filtered through a 40 μm cell strainer and centrifuged twice for at 250 rcf for 5 minutes with a rinse in between. The pellet was resuspended in HBSS containing 37% Percoll. A density gradient was generated by layering this suspension atop a 70% Percoll solution and subsequently layering a 30% Percoll solution atop the suspension. After centrifugation at 300 rcf for 40 minutes with no brake, the microglia were concentrated at

the interface between the 70% and 37% Percoll layers. The cells were collected, centrifuged at 800 rcf for 5 minutes, and resuspended with 3-D culture medium.

The adult microglia were introduced to 3-D cultures (150 μL, flat) maintained for 7 DIV either by direct dropwise addition (15,000 cells/culture) to the medium or by mixing the cells with Matrigel™ and pipeting this gel (5,000 cells/culture) into a pocket created in the corner of the 3-D cultures at the time of their plating. The cultures were maintained for an additional 7 DIV before being subjected to LPS stimulation (0.1, 1, or 10 μg/mL final concentration) or to compression injury (4 mm piston diameter, 500 mm/s velocity, 1.00 mm depth). The latter was delivered to the center of the culture if the adult microglia had been added dropwise or adjacent to corner where the cells dispersed in Matrigel™ were plated. The response of the GFP positive microglia was followed by fluorescence microscopy over the course of 3 days, and fluorescent images were acquired using a Nikon Eclipse 80i upright microscope (Nikon Instruments, Melville, NY) equipped with a MicroFIRE camera (Optronics®, Goleta, CA).

5.3.4 Outcome measures

5.3.4.1 IL-1β ELISA

At specified time points after injury, medium was collected from each of the cultures into Eppendorf tubes and centrifuged at 1,000 rcf to remove any contaminating cells. The supernatants were transferred to fresh Eppendorf tubes and assayed immediately or frozen at -80 ºC. The samples were thawed and analyzed with a rat IL-1β ELISA kit (R&D Systems, Minneapolis, MN) according to the manufacturer's protocol.

5.3.4.2 Western blot

At specified time points after injury, cultures were rinsed with cold PBS containing "cOmplete" PIC, collected with BD™ Cell Recovery Solution containing PIC, and pooled into Eppendorf tubes. Sample pooling of three cultures was necessary to ensure sufficient protein for loading the SDS-PAGE gel. The tubes were kept on ice for one hour with frequent inversion to facilitate the disintegration of the Matrigel™. The samples were centrifuged at 1,000 rcf at 4 ºC for 5 minutes and the pellets were resuspended with a protein extraction solution containing NP-40, deoxycholate, and PIC. The tubes were kept on ice and vortexed periodically during 1 hour of protein extraction. The samples were centrifuged at 1,000 rcf at 4 ºC for 5 minutes and the supernatants were transferred to fresh Eppendorf tubes. Protein content was determined by BCA protein assay (Pierce™/Life Technologies, Carlsbad, CA) and the samples were diluted to equal protein concentrations with SDS-PAGE sample loading buffer. The reduced and denatured samples were separated in 8-16% Tris-Glycine gradient SDS-PAGE gels (Invitrogen™/Life Technologies, Carlsbad, CA) and wet-transferred to PVDF membrane (EMD Millipore, Billerica, MA) for antibody detection. The membrane was blocked with Odyssey® Blocking Buffer (LiCor, Lincoln, NE), exposed to anti-rat IL-1β antibody (R&D Systems) overnight at 4 ºC. The membrane was incubated with secondary antibody conjugated to IR Dye 800 (Rockland Immunochemicals Inc., Pottstown, PA) and scanned using an Odyssey® infrared scanner (LiCor).

5.3.4.3 Immunocytochemistry

Cultures (150 μL, flat) maintained for 21 DIV were subjected to compression injury (4 mm piston diameter, 500 mm/s velocity, 1.00 mm depth), to sham injury, to a

naïve condition, or to LPS stimulation (10 μg/mL final concentration) (n=3 each). After 24 hours, cultures were fixed with 2% paraformaldehyde in PBS for 30 minutes and permeabilized with 0.1% Triton X-100 in blocking buffer containing 10% normal horse serum. The cultures were incubated with goat anti-rat IL-1β primary antibody (R&D Systems) overnight at 4 ºC and with FITC-conjugated donkey anti-goat secondary antibody (Jackson ImmunoResearch, West Grove, PA) for 1 hour at room temperature. Antibody solutions contained 1% serum. All solutions for immunolabeling (including rinse buffer) contained 0.05% saponin, a mild, reversible detergent. Fluorescent images were acquired using a Nikon Eclipse 80i upright microscope equipped with a MicroFIRE camera.

5.3.4.4 mRNA microarray

Cultures (150μL, flat) maintained for 14 DIV were exposed to injury (4 mm piston diameter, 500 mm/s velocity, 1.00 mm depth), sham, naïve, or LPS conditions. Four hours after injury, the cultures were rinsed twice with cold PBS. The Matrigel™ matrix was degraded by treating the cultures with BD™ Cell Recovery Solution for 2 hours on ice with agitation on an orbital shaker. Two cultures were pooled to represent a single sample, which resulted in 3 samples for each treatment condition (n=3). The sample pooling was determined in preliminary experiments to be necessary to generate enough RNA for the microarrays. Total RNA was extracted with TRIzol Reagent (Life Technologies), quality controlled, and quantified by Agilent 2100 Bioanalyzer (Agilent Technologies, Santa Clara, CA). Microarrays were completed according to manufacturing guidelines (Affymetrix® Inc., Santa Clara, CA), with cRNA hybridized to an Affymetrix Rat Genome 1.0 ST GeneChip® array (Affymetrix Inc.). The chips were

hybridized at 45°C for 16 hours, washed, stained with streptavidin-phycoerythrin, and scanned according to manufacturing guidelines. Three chips were used for each experimental group.

5.3.4.5 Direct NO detection using NO-sensitive dye

Cultures (150 μL, flat) maintained for 13 DIV were subjected to compression injury (4 mm piston diameter, 500 mm/s velocity, 1.00 mm depth), to sham injury, to a naïve condition, or to LPS stimulation (10 μg/mL final concentration). After 24 hours, the cultures (n=3 for each condition) were rinsed with DPBS and subsequently exposed to an NO-sensitive hydrocyanine infrared dye (in DPBS) for 1 hour. The cultures were rinsed with DPBS and imaged using an IVIS Lumina® near-infrared imaging system (Perkin Elmer, Waltham, MA).

5.3.4.6 Griess assay for nitrite production

Cultures (150 μL, flat) maintained for 13 DIV were subjected to compression injury (4 mm piston diameter, 500 mm/s velocity, 1.00 mm depth), to sham injury, to a naïve condition, or to LPS stimulation (10 μg/mL final concentration). After 24 hours, medium was collected from each of the cultures (n=6 for each condition) and the level of nitrite present was determined. Nitrite is a stable breakdown product of NO and was detected using a two-step colorimetric diazotization reaction known as a Griess assay (Promega, Madison, WI) according to the manufacturer's instructions.

5.3.4.7 Direct ROS detection with superoxide-sensitive dye

Cultures (100 μL) maintained for 8 DIV were rinsed with DPBS and subsequently exposed to hydro-indocyanine green (H-ICG) (250 μM in DPBS), an infrared dye sensitive to the presence of superoxide [184], for 1 hour. The cultures were then

subjected to compression injury (10 mm piston diameter, 500 mm/s velocity) to a depth of either 0.75 mm or 1.00 mm or to sham injury (n=3 for each condition). Additionally, there was a set of cell-free Matrigel™-only controls (n=3) that were treated as a naïve condition would have been. DPBS was added to the cultures and each chamber slide was covered with a custom-made lid consisting of FEP membrane over a 3-D printed frame of Fullcure® 720 plastic and imaged using an IVIS Lumina® system at time points up to 13 hours post-injury. The custom-made lids prevented buffer evaporation which had been shown in a previous experiment to result in a constantly increasing fluorescent signal over the time course.

5.3.4.8 Statistical Analysis

Data from experiments comparing two treatment conditions were statistically compared using a one-tailed, unpaired t-test with Welch's correction for unequal variances where appropriate. Data from experiments comparing more than two treatment conditions were statistically compared using one-way ANOVA followed by a post-hoc Tukey-Kramer test for multiple comparisons if ANOVA yielded a result of $p<0.05$.

5.4 Effect of *in vitro* compression injury on IL-1β

5.4.1 Extracellular IL-1β release

It was hypothesized that mechanical injury of the 3-D multitypic neural cultures would initiate an inflammatory response and that IL-1β would be a marker for this induced inflammation. Cultures (100 μL) maintained for 13 DIV were subjected to compression injury (10 mm piston diameter, 500 mm/s velocity, 0.50 mm depth) or to sham injury. Medium was collected at 4 hours (n=6 for each condition). Medium was also collected from cultures stimulated with LPS (10 μg/mL) (n=2) as a positive control.

The ELISA data show that IL-1β was essentially undetectable in either the sham or injury condition (Figure 5.3). All measured absorbance values for these conditions were lower than the lowest nonzero standard. Similar cultures, from which the medium was collected at 24 hours after injury, had detectable levels of IL-1β in the culture medium but showed no significant difference among the naïve, sham, and injury conditions (not shown).

In order to develop a picture of the potential time dependence of IL-1β detection, the amount of IL-1β released in response to mechanical injury was measured in the media samples from the LDH time course experiment described in Section 4.5. Cultures (100 μL) maintained for 13 DIV were subjected to compression injury (10 mm piston diameter, 500 mm/s velocity, 0.50 mm depth) or to sham injury. Medium was collected from injured cultures at 2, 4, and 8 hours (n=3 each) and from the sham cultures at 8 hours (n=3). Medium was also collected at 8 hours from an uninjured LPS condition (n=2) as a positive control for IL-1β release. The ELISA data show that IL-1β release did not increase significantly with injury (Figure 5.4). The sham condition showed significantly higher IL-1β in the culture medium than the medium collected 2 hours post-injury. However, since the sham medium was collected at 8 hours, this is not an equivalent comparison.

5.4.2 Intracellular IL-1β protein expression

To determine if mechanical injury induced an upregulation in the intracellular protein expression of IL-1β, the cultures for which ELISA data were presented (Figure 5.3) were processed for Western blot and probed for IL-1β. Confirmation of culture injury was determined by LDH assay (Figure 5.5A). The Western blot data illustrates that the compression injury failed to increase the intracellular levels of immature IL-1β (31

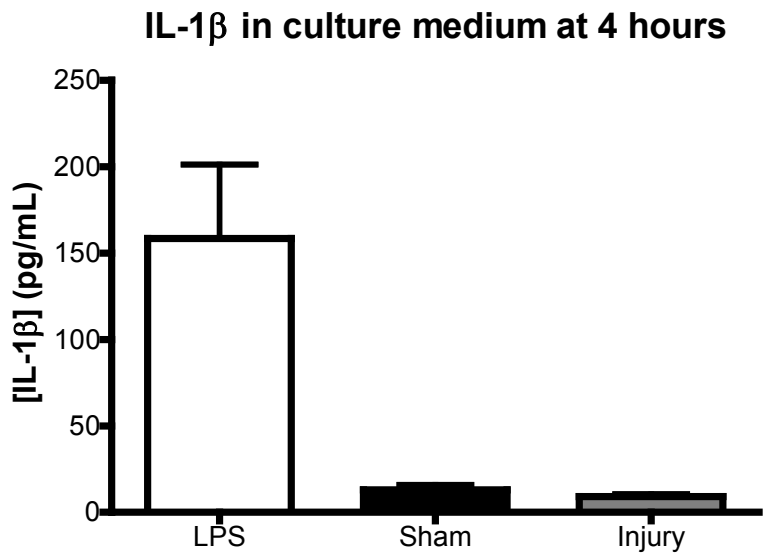

Figure 5.3. Il-1β is not released at 4 hours in response to compression injury. Cultures (100 μL, 13 DIV) were subjected to compression injury (10 mm piston diameter, 500 mm/s velocity, 0.50 mm depth) or to sham injury. Medium was collected at 4 hours (n=6 for each condition). LPS (10 μg/mL) (n=2) was included as a positive control. IL-1β is not detectable in the medium of either the injury or the sham condition. Bars are means plus SEM.

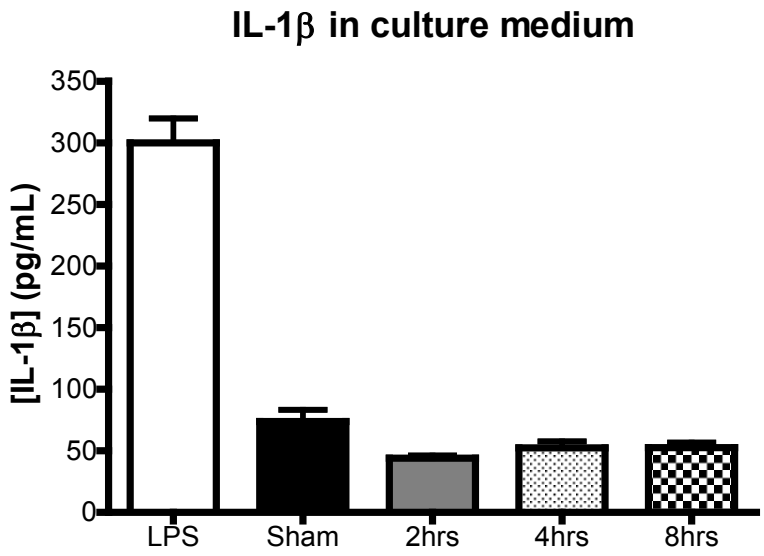

Figure 5.4. IL-1β release is not significantly increased over a time course after compression injury. Cultures (100 μL, 13 DIV) were subjected to compression injury (10 mm piston diameter, 500 mm/s velocity, 0.50 mm depth) or to sham injury. Medium was collected at 2, 4, and 8 hours (n=3 each) and from the sham cultures at 8 hours (n=3). Medium was also collected at 8 hours from an uninjured LPS condition (n=2) as a positive control for IL-1β release. There is no time-dependent increase in IL-1β release due to compression injury and no significant difference from the sham condition. Data were statistically compared using one-way ANOVA. Bars are means plus SEM.

kD band) compared to the sham condition (Figure 5.5B). There appears to be a modest increase in band intensity with injury, but without a loading control, the densitometric data cannot confidently be statistically compared. The LPS positive control substantially upregulated immature IL-1β protein expression, and was the only condition for which the mature form of IL-1β (17 kD band) was detectable.

Immunocytochemistry provided visual confirmation of the Western blot data. Immunolabeling with anti-rat IL-1β antibody revealed only background signal in the naïve condition as well as in both the sham and injury conditions in the region adjacent to piston contact point (Figure 5.6A-C). In the LPS-stimulated cultures, positive IL-1β labeling was observed in cells with morphology consistent with microglia (Figure 5.6D). The background signal also appears in the LPS cultures and based on the pattern may be labeling fibrillar structures of astrocytes. The specificity of the labeling cannot be assessed as no pre-adsorption antibody controls were included.

In order to confirm that the lack of IL-1β detection in response to injury was not simply attributable to the protein-level analysis, mRNA microarrays were used to compare injured and sham cultures. Two separate experiments on 150 μL flat cultures were carried out using two different piston sizes for compression injury. Microarray data comparing injured and uninjured cultures did not reveal any change in IL-1β at the mRNA level. Further, neither analysis showed transcriptional upregulation or downregulation of any gene of interest in response to mechanical injury despite the potentiation demonstrated in the LPS experiment described in Section 3.2.3.

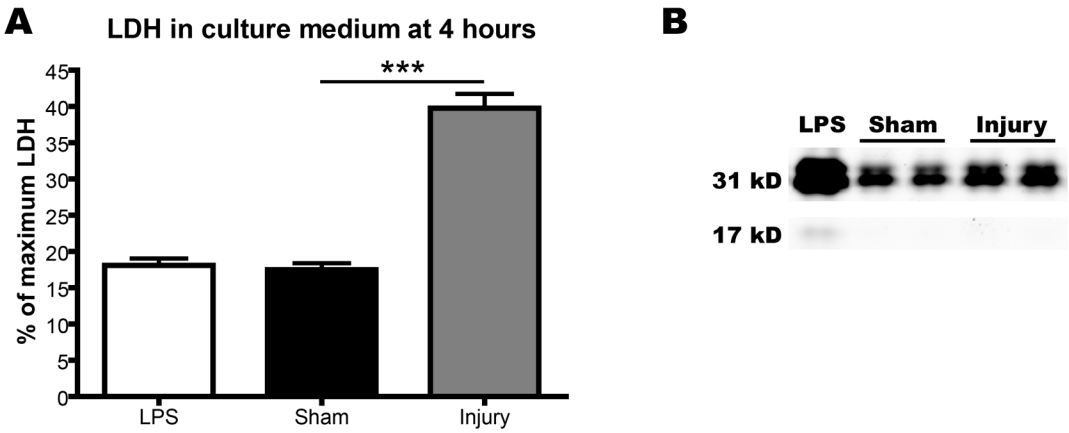

Figure 5.5. Intracellular IL-1β is not significantly increased in response to compression injury. Cultures (100 μL, 13 DIV) were subjected to compression injury (10 mm piston diameter, 500 mm/s velocity, 0.50 mm depth) or to sham injury. (A) LDH activity in the medium at 4 hours indicated successful injury ($p<0.0001$). Cultures (n=6 for each condition) were collected, pooled (3 cultures pooled per sample, pooled n=2), degraded, and protein was extracted for Western blot. LPS (10 μg/mL) (n=2, pooled n=1) was included as a positive control. (B) Western blot data for the samples reveals a small increase in intracellular, immature IL-1β in response to compression injury. This difference cannot be statistically compared due to the lack of a loading control. LDH data for sham and injury conditions were statistically compared using a one-tailed, unpaired t-test. Bars are means plus SEM.

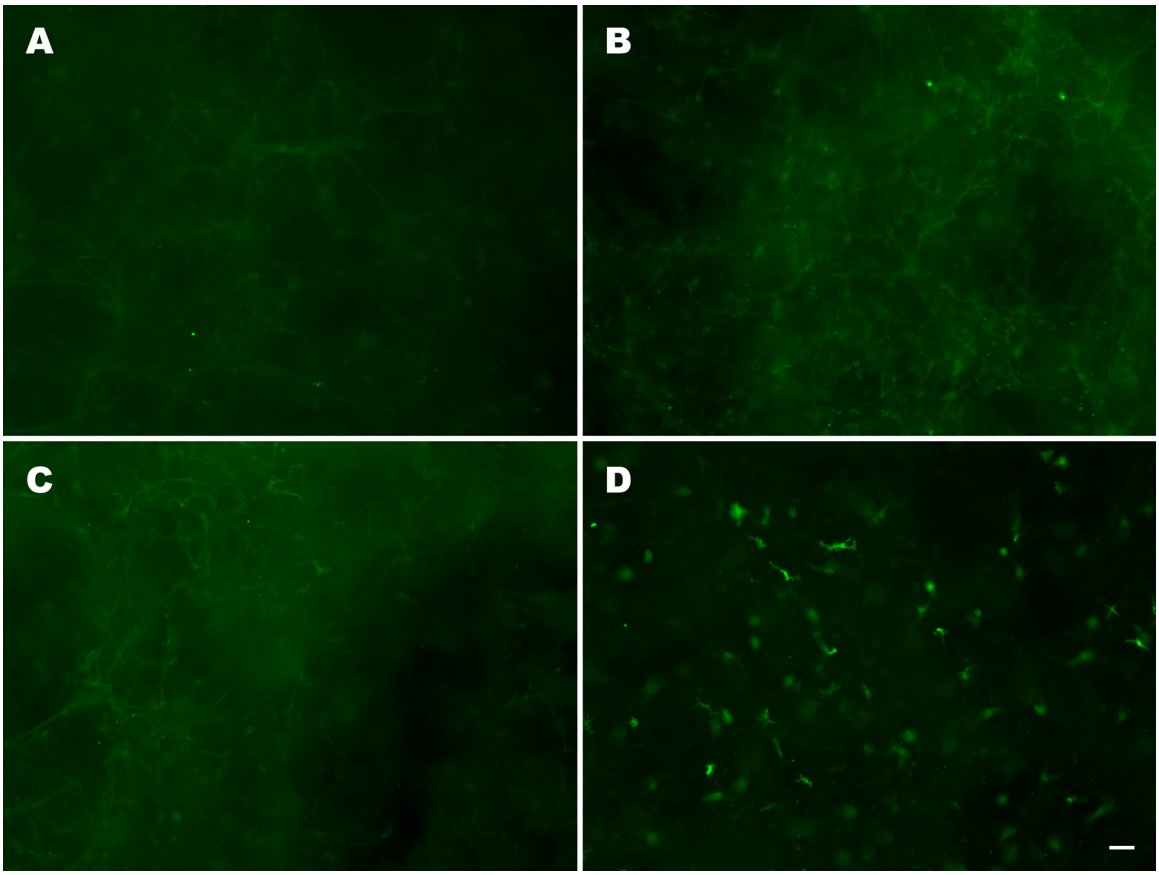

Figure 5.6. Immunolabeling for IL-1β is not detectable in response to compression injury. Cultures (150μL, flat, 21 DIV) were subjected to compression injury (4 mm piston diameter, 500 mm/s velocity, 1.00 mm depth), to sham injury, to a naïve condition, or to LPS stimulation (10 μg/mL final concentration) (n=3 each). Fixed cultures were incubated with antibody against IL-1β. IL-1β labeling appears nonspecific and fibrillar for the naïve (A), sham (B), and injury (C) conditions. The LPS condition (D) shows labeling consistent with microglia. Scale bar: 50 μm.

5.5 Effect of *in vitro* compression injury on NO production

Due to the lack of success in inducing IL-1β release, NO production in response to mechanical injury was assessed. The availability of a NO-sensitive infrared dye allowed for near real-time monitoring of NO release post-injury, potentially capturing an acute injury response that was previously undetectable. Both sham and injury conditions had significantly higher fluorescence than the naïve condition ($p<0.05$) as is visually apparent in the raw data (Figure 5.7A) and in the quantification of the fluorescence (Figure 5.7B). Neither condition was significantly different from the LPS control, nor were they significantly different from each other. It is worth noting, however, that the pattern of fluorescence observed in the injury condition exhibits precisely the desired profile for this model of neuroinflammation. There is a halo of increased signal around the piston impact site which corresponds to an injury penumbra and umbra, respectively. These direct NO measurements were not corroborated by the levels of nitrite in the medium. The only condition that gave detectable signal was the LPS positive control (Figure 5.7C). Potential explanations for this discrepancy are addressed in Section 5.9.

5.6 Effect of *in vitro* compression injury on ROS production

A time-dependent profile of superoxide production in response to injury was established using H-ICG, a superoxide-sensitive infrared dye followed by compression injury. At 20 minutes post-injury, the raw fluorescent signals from both injury conditions were noticeably higher than the sham condition (Figure 5.8A). Quantification of the data showed that both injury conditions exhibited significantly higher levels of fluorescence than the sham condition ($p<0.001$), but that they were not significantly different from each other (Figure 5.8B). The fluorescence of the sham condition was also not

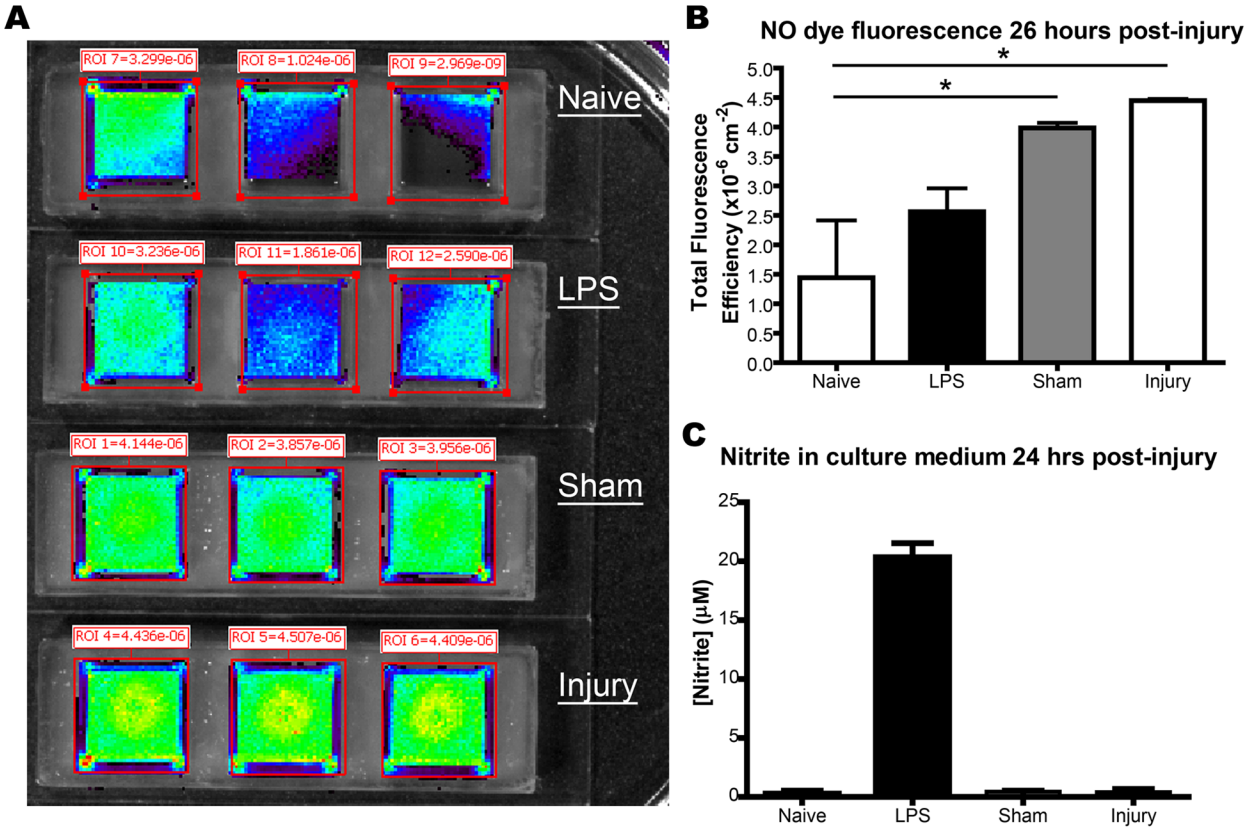

Figure 5.7. NO production in response to compression injury. Cultures (150 µL, flat, 13DIV) were subjected to compression injury (4 mm piston diameter, 500 mm/s velocity, 1.00 mm depth), to sham injury, to a naïve condition, or to LPS stimulation (10 µg/mL final concentration) (n=3 each). After 24 hours, the cultures exposed to a NO-sensitive hydrocyanine infrared dye (in DPBS) for 1 hour. The cultures were rinsed with DPBS and imaged using an IVIS Lumina® near-infrared imaging system. (A) Raw *in situ* NO dye fluorescence shows an increase in signal for both the sham and injury conditions relative to the naïve. (B) Quantification of this data confirms that these increases are statistically significant ($p<0.05$), but indicates that the injury condition is not significantly different from the sham. (C) Levels of nitrite in all but the LPS condition were undetectable. Data were statistically compared using one-way ANOVA followed by a post-hoc Tukey-Kramer test for multiple comparisons. Bars are means plus SEM.

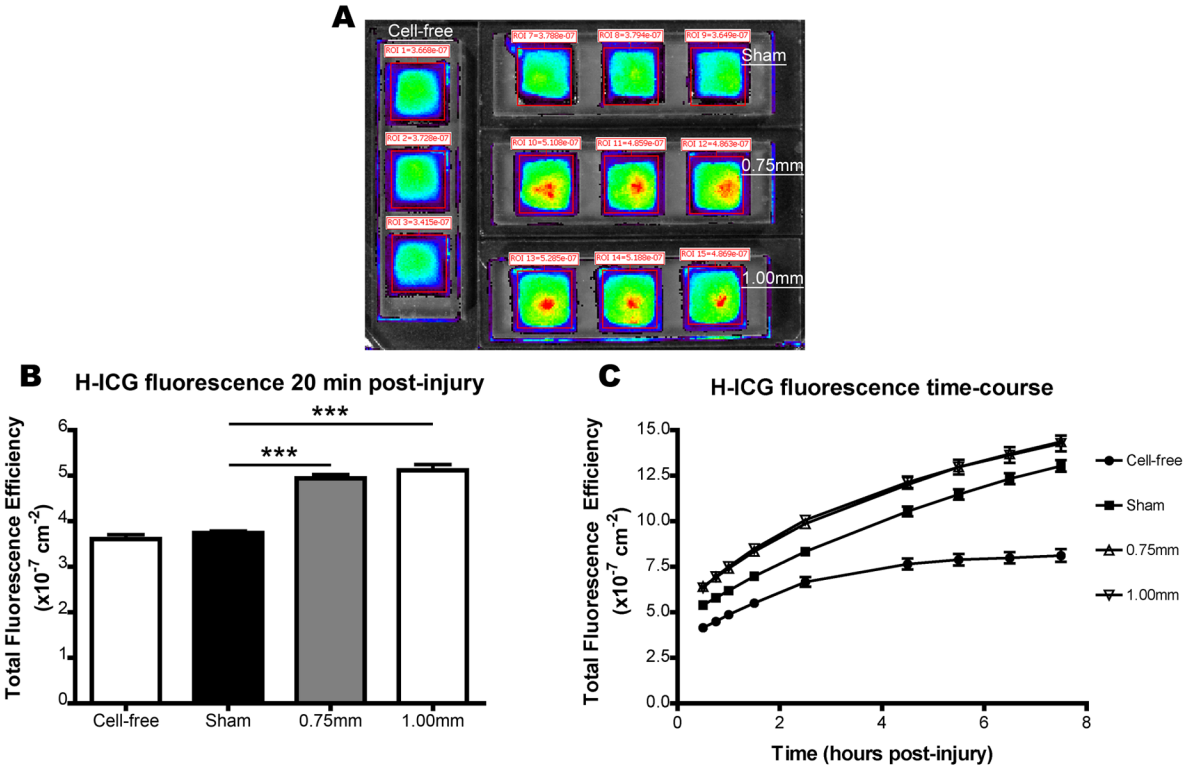

Figure 5.8. ROS production in response to compression injury. Cultures (100 µL, 8 DIV) were pre-exposed to H-ICG (250 µM in DPBS) for 1 hour. The cultures were then subjected to compression injury (10 mm piston diameter, 500 mm/s velocity) to a depth of either 0.75 mm or 1.00 mm or to sham injury (n=3 for each condition). Additionally, there was a set of cell-free Matrigel™-only controls (n=3) that were treated as a naïve condition would have been. DPBS was added to the cultures and they were imaged using an IVIS Lumina® system at time points up to 13 hours post-injury. (A) Raw *in situ* superoxide-sensitive dye fluorescence at 20 minutes post-injury shows an increase in signal for both injury conditions relative to the sham. (B) Quantification of this data confirms that these increases are statistically significant ($p<0.001$), but indicates that the injury conditions are not significantly different from each other. (C) Time course data shows that the signal for the sham and injury conditions continues to rise, while the cell-free control signal levels off. The injury and sham data remain significantly different through 5.5 hours. Data were statistically compared using one-way ANOVA followed by a post-hoc Tukey-Kramer test for multiple comparisons. Bars are means plus SEM.

significantly different from that of the cell-free Matrigel™ control. The fluorescent signal of the injury and sham conditions continued to rise over time, while the cell-free signal leveled off (Figure 5.8C). The injury and sham data remained significantly different through 5.5 hours post-injury, but began to converge after this point. The 3.5 hour time point and time points beyond 7.5 hours were omitted due to falsely high readings given by auto-exposure issues with the IVIS Lumina® system.

5.7 Effect of LPS pre-treatment on compression-injury induced inflammation

It was hypothesized that mechanical injury alone may not be sufficient to elicit the expected inflammatory response in the 3-D multitypic neural cultures. Cultures (100 μL) maintained for 7 DIV were "primed" with medium containing LPS (10 μg/mL) for 2 hours, rinsed, then subjected to compression injury (10 mm piston diameter, 500 mm/s velocity, 0.50 mm depth) (n=6) or to sham injury (n=3). Medium was collected from the cultures 4 hours later and levels of IL-1β were determined by ELISA. Significantly more IL-1β was released from the injured cultures compared to the sham cultures ($p<0.0001$) (Figure 5.9). This indicates that exposing the cultures with LPS or another pro-inflammatory reagent prior to injury may be necessary to generate a detectable inflammatory response.

5.8 Effect of adding adult mouse microglia to the 3-D multitypic neural cell cultures

Given the apparent requirement of an additional stimulus to produce an inflammatory response to *in vitro* injury, it became clear that the 3-D multitypic neural cultures may not possess the necessary components to generate the expected response. To determine if the immaturity of the microglia was affecting the outcome, adult microglia from mice were incorporated into the system. The goal of these studies was to ascertain if

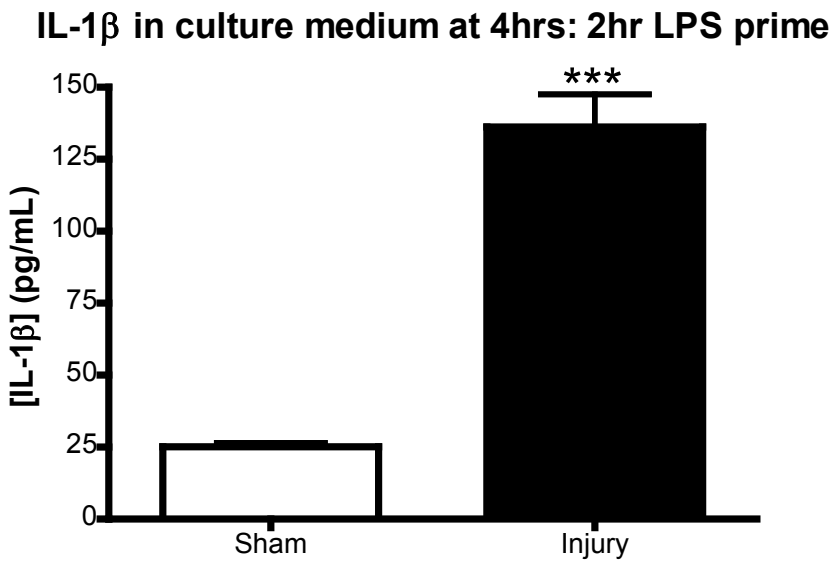

Figure 5.9. IL-1β release in response to compression injury requires LPS pre-treatment. Cultures (100 µL) maintained for 7 DIV were "primed" with medium containing LPS (10 µg/mL) for 2 hours, rinsed, then subjected to compression injury (10 mm piston diameter, 500 mm/s velocity, 0.50 mm depth) (n=6) or to sham injury (n=3). At 4 hours, levels IL-1β are significantly increased in the medium of the injury condition compared to the sham ($p<0.0001$). Data were statistically compared using a one-tailed, unpaired t-test with Welch's correction for unequal variances. Bars are means plus SEM.

the adult microglia would exhibit the expected morphological or chemotactic behaviors that had not been observed with the postnatal rat microglia. Within a few days of adding the adult microglia to the 3-D multitypic neural cultures, they exhibited significant process extension. Compression injury induced neither a morphological shift nor a chemotactic response (not shown). However, 3 days of exposure to LPS resulted in concentration-dependent process retraction (Figure 5.10).

5.9 Conclusions

This chapter has detailed the experiments designed to characterize mechanically-induced inflammation of the 3-D multitypic neural cultures. In the absence of additional stimulation, the cultures failed to consistently produce a detectable response to compression injury using the chosen outcome measures. While the *in situ* detection of NO and superoxide using the near-infrared dyes sensitive to these species appeared promising, substantial variability was encountered in subsequent experiments. The source of these inconsistencies seemed to lie with the limitations of the IVIS Lumina® system which was designed for *in vivo* imaging. Often, the signal-to-noise ratio of the acquired infrared signal was fairly low, leaving a very small window in which acceptable data could be acquired. The result was that the subtle differences between the small cell populations in these cultures (compared to *in vivo*) were sometimes washed out by background signal or by nonspecific oxidation mechanisms of the dyes. Also concerning was the disagreement between the NO detected in the cultures and the levels of nitrite detected in the corresponding media samples (Figure 5.7). While this could possibly be attributed to normal interconversion pathways within the cells [185], it still casts doubt on the reliability of the data.

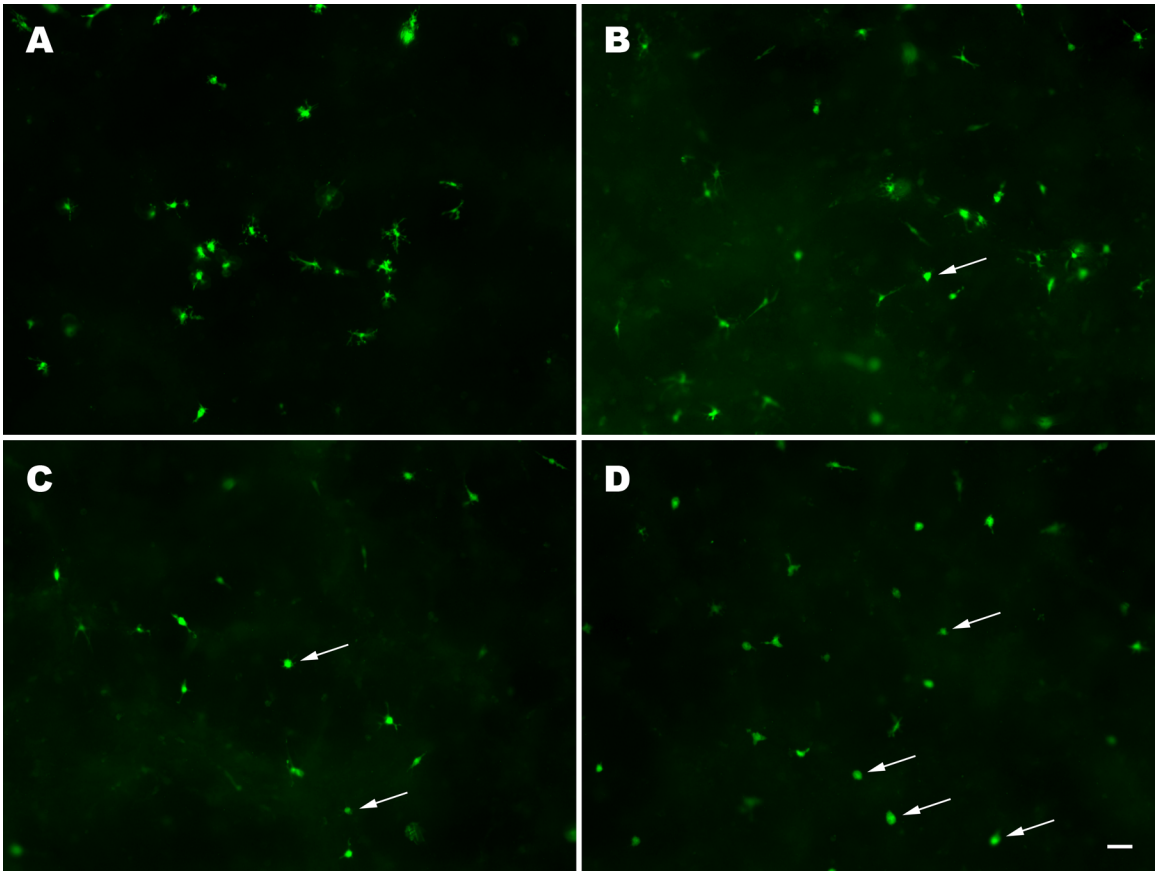

Figure 5.10. Adult mouse microglia in the 3-D multitypic neural cell cultures exhibit a concentration-dependent morphological shift in response to LPS stimulation. GFP-positive adult mouse microglia were added dropwise to cultures (7 DIV) and maintained for an additional 7 days. Live cells were imaged following 3 days of vehicle (A) or LPS treatment at final concentrations of 0.1 μg/mL (B), 1 μg/mL (C), or 10 μg/mL (D). Adult mouse microglia in vehicle-treated cultures exhibit process extension (A). The frequency of cells displaying a rounded morphology increases with increasing concentrations of LPS (B-D, arrows).

Most disappointing was the lack of detectable changes in IL-1β levels in response to injury. This cytokine was chosen as a likely marker for inflammation in this system partially based on the results of the LPS experiments presented in Chapter 2, but also because of the mechanism by which it released from cells. Release of IL-1β can occur in the acute phase following injury as it simply requires enzymatic cleavage to produce a mature protein from the pool of immature IL-1β present within the cell. Further, the known involvement of ATP signaling in this process made it an attractive candidate in a model where extensive membrane damage and cell death would be imparted. In response to compression injury alone, IL-1β was not released from the cell nor was its intracellular production upregulated at the protein or mRNA level. However, exposure of the cultures to LPS prior to compression or sham injury yielded a significant increase in IL-1β in the medium of the injured cultures. Although this is the desired outcome, this method of "priming" the cultures activates a different inflammation pathway than what would be expected in response to mechanical injury. Thus, from the standpoint of model development, it is not an ideal requirement. This once again calls into question the appropriateness of LPS as a positive control for this system, an issue that is addressed further in Chapter 6. Another concern is that although the sham cultures were exposed to LPS as well, the observed signal increase may have been the result of nonspecific IL-1β release due to direct damage to the cells rather than through a caspase-1-mediated pathway.

These concerns lead to the question of what this system is truly capable of modeling. *In vitro* systems are, by their very nature, far removed from their parent organism. As such, data gleaned from the use of such models is accompanied by many

caveats. Assuming that functionality representative of an *in vivo* model has been demonstrated, as is the case here, the data can prove invaluable in the study of disease. The 3-D multitypic neural culture model combines three cell types in a novel way and has demonstrable potential for the induction of inflammation pathways. The inability to produce a reliable TBI-like inflammation response using the injury methods described here does not completely discount this as a model of neuroinflammation. There are numerous avenues in the design of the culture system (particularly matrix and medium composition) that, if modified, could result in a representative model. These possibilities are explored in more detail in Chapter 6 along with other possible applications for this culture system beyond TBI.

CHAPTER 6

DISCUSSION

6.1 Research summary

The research presented here was designed to investigate the potential of a 3-D culture system consisting of neurons, astrocytes, and microglia harvested from rat to serve as a model of mechanically-induced neuroinflammation. Iterative development of culture and plating methods ultimately yielded a 3-D multitypic neural culture with a high viability of the cell types of interest. Stimulation of these cultures with LPS produced the expected outcomes of: upregulation of the mRNA of various pro-inflammatory cytokines, increased intracellular and extracellular levels of IL-1β protein, and increased NO production. Surprisingly, the inflammatory response did not trigger any cytotoxic mechanisms within the culture as there was no significant change in cell viability in response to LPS treatment. Also surprising was the lack of a shift in microglial morphology. Previously designed *in vitro* injury devices were adapted to suit a modular design for the 3-D culture chambers. Shear injury failed to induce cell death in the cultures and was abandoned as the mechanical injury model. Compression injury required an order of magnitude increase in the piston velocity to achieve the desired level of cell death in the 3-D cultures. However, when compared with sham conditions, this injury model failed to elicit increases in IL-1β protein expression, cytokine mRNA expression, and NO production. ROS production was significantly increased, but this result was inconsistent in subsequent experiments. When cultured were exposed to LPS prior to injury, there was a significant increase in IL-1β released into the culture medium.

6.2 Alternative culture conditions

Throughout the course of this research, variants of the previously described culture conditions and experimental parameters were implemented in attempts to elicit a mechanically-induced inflammation response. Some, such as the use of antioxidant-free B-27 supplement, became a part of the final culture protocol. Others had no effect but are discussed here to illustrate the many avenues pursued in the development of this culture system.

6.2.1 Alternative 3-D hydrogels

Although Matrigel™ has long been used in our lab to promote high primary cell viability and the development of mature neural networks, it has disadvantages. Its composition is not very well-defined since it is generated from extracts from an *in vivo* host. In addition to the controlled ratios of laminin, collagen IV, and HSPG, there are a host of growth factors present, even in the formulation in which they have been reduced. While this is helpful in supporting cellular survival, it is certainly a downside in a system designed to model secondary injury processes. Aside from the presence of growth factors, laminin has been shown to have neuroprotective properties [186, 187], even in its polymerized form [188].

Some alternative hydrogels that were considered included: collagen I, silk fibroin, and self-assembling peptide nanofibers. Type I collagen has attractive mechanical properties for an injury model, but is not a normal component of the CNS ECM. Similarly, silk fibroin would be a good choice from a mechanical perspective, but not a biological one. Indeed, a combination of silk fibroin and collagen I has been used to culture primary neurons to model cortical injury [189]. One self-assembling peptide

nanofiber, RADA16 (commercially, BD PuraMatrix®), was implemented with primary neurons. Short peptides (~12-16 amino acids) with alternating acidic and basic side chains separated by hydrophobic residues will spontaneously form beta-sheet secondary protein structure upon addition of a medium containing dissolved salts. Multiple attempts were made to seed neurons in this gel, but the cells never extended processes and the gel itself rapidly degraded by layered delamination. It has been reported that the cells from the BV-2 microglia cell line extend processes in this scaffold [190].

Regarding some of the negative attributes of Matrigel™, it should be noted that two of the growth factors present in the formulation, EGF and bFGF, are also present in G-5 supplement at concentrations 4 and 6 orders of magnitude higher, respectively. Obviously, this does not negate the potential interference of the other growth factors with the hypothesized injury response, but it indicates that their concentrations may be negligible. In terms of the neuroprotective attributes of laminin, it has been reported that laminin is produced by astrocytes in primary cultures derived from embryonic and newborn rats [191], so even in the absence of Matrigel™ there would still be plenty of laminin present. Thus, growth factor-reduced Matrigel™ was settled upon as the scaffold for these investigations.

6.2.2 Effects of ECM composition on microglial phenotype and activity

The key ECM proteins responsible for the appearance of function of microglia in culture appear to be fibronectin and laminin [192, 193]. Both proteins have been shown to increase in the penumbral region after CCI in mice [194]. 2-D preparations of prenatally-derived rat microglia extended processes on a fibronectin substrate but remained rounded on a laminin substrate [192]. However, although 2-D preparations of

postnatally-derived mouse microglia grown on laminin also exhibited a weakly adhered, rounded phenotype, cells grown on fibronectin did as well [193, 195]. In contrast to these preparations, the microglia grown in the 3-D multitypic neural cultures extended processes despite laminin being the primary constituent of the hydrogel. Based on its implication in IL-1β release from microglia [196] and astrocytes [197] in primary rat cultures, the absence of fibronectin from the Matrigel™ formulation was thought to be contributing to the lack of detection of the IL-1β in response to injury. To determine if the presence of fibronectin in the ECM would affect IL-1β release, it was added to a Matrigel™ preparation prior to 3-D cell plating. This addition did not have any effect on secreted IL-1β levels 24 hours after compression injury when compared to standard preparations. However, based on the *in vivo* CCI data [194], the microglia may only respond to a fibronectin gradient in the region surrounding the injury rather than to its addition to the bulk ECM.

6.2.3 Effects of medium supplements on microglial activity

Throughout the previous chapters, modifications to the medium used for the 3-D multitypic neural cultures have been discussed. In order to assure a healthy mix of neurons and glia without allowing the glia to overtake the cultures, G-5 supplement was included at the time of plating and at the two subsequent feedings at 90 minutes and 24 hours. Thereafter, half-medium exchanges were with medium lacking G-5. As mentioned in Chapter 2, this delayed the onset of gel contraction from 1 week to at least 2 weeks after plating. However, in order to confirm that the removal of G-5 did not affect the potential for IL-1β release, a post-injury time course experiment was run on cultures that continued to receive G-5. The IL-1β ELISA data was not significantly different from

previously presented data collected in parallel from cultures maintained without G-5 (see Figure 5.4). Since there were also no observed effects on cellular health, the weaning protocol for G-5 was continued.

The clear decision to use antioxidant-free B-27 supplement in place of the baseline formulation was immediately beneficial in the fluorescence studies with the infrared ROS sensor dye. One of the included antioxidants was superoxide dismutase which completely abolished any signal that could have been detected using the dye. However, even in the modified formulation, B-27 contains a substantial amount of bovine serum albumin (enough to be visible to the naked eye on PVDF membrane after electrophoretic transfer for Western blot), which has been reported to have antioxidant properties [198]. Additionally, the supplement contains progesterone, which has been used in clinical trials for TBI treatment. Despite the presence of these species, elimination of B-27 supplement from the culture medium in the days preceding injury did not have an effect on microglial response to injury.

6.3 ATP stimulation of cultures

Given the previously described involvement of ATP signaling in IL-1β release, as well as the demonstration of ATP-induced microglial chemotaxis both *in vivo* [65] and *in vitro* [132], it was logical to include ATP stimulation in parallel with the injury studies presented here. In lieu of the standard ATP molecule, the highly active BzATP form was used as it is a potent agonist of the P_2X_7 receptor, which is directly involved in IL-1β processing and release.

6.3.1 ATP as a positive control

The integral roles played by ATP in microglial function would possibly make it a better candidate for a positive control than LPS. Additionally, the ideal model for *in vitro* injury using this culture system would involve the formation of ATP gradients from the umbral region of injury into the penumbral region where a microglial response would be induced. Whereas LPS was an acceptable positive control for the outcome measures utilized in this research, the mechanism by which it elicits IL-1β release is through the TLR4-mediated innate immune pathway, which it not physiologically relevant to a TBI model. ATP would certainly have been more meaningful from a biochemical signaling perspective.

6.3.2 BzATP stimulation of 3-D multitypic neural cell cultures

BzATP was utilized in parallel with a limited number of experiments in an attempt to amplify the microglial response to mechanical injury. When delivered in combination with LPS, the combined treatment reduced the levels of IL-1β detected in the medium. This finding may correlate with the observed ATP-induced process retraction of LPS-stimulated microglia [132]. Combined LPS/BzATP treatment did not, however, result in a visible difference in intracellular IL-1β immunolabeling compared to LPS stimulation alone. Stimulation of cultures with BzATP after mechanical injury produced a modest, but not significant increase in immature IL-1β levels compared to the sham condition as determined by Western blot. However, there was no significant difference between this result and that obtained from the previously presented unstimulated cultures (see Figure 5.5). Finally, BzATP stimulation had no effect on NO production as measured by nitrite levels 24 hours after stimulation. Thus, although it is

not as physiologically relevant to the TBI inflammation mechanisms, LPS is a successful positive control due to the breadth of its effect on pro-inflammatory outcome measures. Stimulation with standard ATP may have produced different results since the BzATP molecule is specifically a P_2X_7 agonist. Additionally, bulk delivery in the medium may not have been the best course for exposure as there would be no gradients established.

6.4 Future directions

6.4.1 Injury model

6.4.1.1 Model limitations

The research presented here indicated that aside from inconsistently detected superoxide release, mechanically-induced neuroinflammation in these cultures requires priming with LPS prior to injury. Mechanical injury alone, as delivered by piston compression, failed to produce the expected inflammatory response. In its current state, this system cannot be said to be an *in vitro* model of TBI-induced neuroinflammation as the only aspect of TBI that has been successfully and consistently represented is acute cell death directly induced by the injury mechanism. The design of the system may be inherently incapable of recapitulating the *in vivo* inflammation response simply because it is lacking too many of the peripheral physiological cues. The model lacks circulating macrophages and cells of the immune system that would be present in the event of a BBB breach. Possible incorporation of a pseudo-BBB into this culture system was discussed, but never successfully implemented. Potentially, a simulation of BBB breach could be achieved through the addition of blood or blood products to the culture immediately following mechanical injury. However, despite the lack of these components, there are

modifications that could be made to the system as it is to promote the induced inflammation response.

Possible explanations as to why the expected microglial behavior was not observed or detected have been alluded to throughout this chapter. The complex effects that the ECM has on microglial differentiation and response points to a need to re-evaluate the hydrogel chosen for this system. If the presence of laminin and growth factors is indeed behaving in a neuroprotective manner, then any inflammatory response occurring may be masked. Another consideration is the fact that the cells used in the 3-D multitypic neural cultures are sourced from prenatal and postnatal tissues. The immaturity of the cells may affect the expected response to injury. Finally, the two-phase nature of the 3-D culture system (cell-seeded scaffold and medium) may be preventing the formation of signaling gradients within the culture. The existence of an injury penumbra was visualized using the NO-sensitive dye (see Figure 5.7). However, the fact that released factors diffuse into the medium as well as through the gel creates a situation that is hardly different than if the factors (i.e. ATP) had been introduced to the culture through the medium. In this case, there would be no gradients to elicit the expected microglial response. Indeed, it has been demonstrated *in vivo* that exogenous ATP prevents microglial chemotaxis toward the site of injury, presumably due to the elimination of the local ATP gradient [65]. All of these factors should be taken into consideration before moving forward with this injury model.

6.4.1.2 Future directions for modeling secondary injury processes in TBI

Taking into consideration the described limitations of the injury system, a number of modifications could potentially evolve this into a model of TBI-induced

neuroinflammation. Implementing a more defined 3-D culture scaffold would be ideal; provided that the cells exhibited process extension and that the microglia exhibited process extension. To address the immaturity of the cultured cells, adult cells could be incorporated into the system. While this is not feasible for neurons as culturing dissociated adult neurons has been largely unsuccessful, the microglia and possibly the astrocytes could be considered. Incorporation of adult mouse microglia has already been demonstrated in these cultures (see Figure 5.10). It is possible that the method for harvesting these cells would translate to rat brain, but this has not been attempted. To address the lack of formation of signaling gradients, a number of approaches can be considered. At the simplest level, the addition of medium following injury could be eliminated. The scaffold is composed primarily of aqueous medium and should remain sufficiently hydrated in a humidified incubator for acute time point studies. For longer time points, evaporation could be prevented through the use of gas permeable FEP membrane to cover the culture wells [199]. Should this fail to elicit a response from the microglia, the cell density of the cultures could be increased. At 4,000 cells/mm^3, the 3-D cultures are near the maximum density for which high (>90%) viability was sustained throughout culture. In order to increase the density, a system of continuous medium perfusion would likely need to be implemented to assure sufficient diffusion of oxygen and nutrients. Any or all of these modifications to the injury or culture method could feasibly allow for the formation of signaling gradients that would induce the expected microglial response.

6.4.2 Applications of the culture system

The culture system itself has a number of applications beyond its incorporation into the mechanical injury system. For example, given the immaturity of the cells, the system could potentially be used to model diseases of early development including fetal alcohol syndrome. The 3-D multitypic neural cultures have already been utilized for other purposes. The cultures were successfully incorporated into a novel *in vitro* microsampling device for mass spectrometry which is capable of continuous, spatially resolved detection of biomarkers [200]. The cultures were also used in an unpublished pilot study of *in vitro* blast injury. Modified cultures chambers were used in which a flexible silicone membrane rather than a rigid glass slide formed the surface of the wells. A blast wave was propagated, and the resulting reduction in cell viability was assessed. These same flexible-bottom culture chambers could also be implemented in another injury model that more closely resembles the 2-D membrane stretch method. The 3-D multitypic neural cultures would also be valuable for toxicity assessment, and should the inflammatory response be consistently potentiated, for assessment of materials designed for neural implantation.

The redesigned culture chamber for the generation of flat 3-D cultures described in Chapter 5 could be used in a variety of culture applications separate from neural tissue. The cultures could be created using Matrigel™ as described here or using a hydrogel more appropriate for the tissue type. The ability to reliably create a 3-D gel with uniform thickness has great potential for use in applications such as invasion assays. Further development of the chamber to include multiple concentric levels would allow for stratified plating of 3-D cultures with varying cellular content for tissues where this

organization is relevant. In the realm of neuroscience research, neurons harvested from different brain regions could be cultured in separate layers or cell types could be spatially separated. Such versatility in recreating tissue-like spatial cellular arrangements *in vitro* is a major advantage of this custom-made culture chamber.

6.5 Alternative approaches for studying microglia-driven neuroinflammation

The integration of the 3-D multitypic neural culture system into the compression injury model of TBI was performed with the goal of studying inflammation-based secondary injury mechanisms *in vitro*. The novel incorporation of microglia into a 3-D culture formerly consisting solely of neurons and astrocytes was meant to create a more complete representation of the complex signaling pathways associated with mechanical injury of neural tissue. This dissertation has detailed the iterative development of this culture model and its implementation in neuroinflammation studies. Attempts to induce an inflammatory response to mechanical deformation ultimately fell short in the absence of additional pro-inflammatory stimulation. Possible explanations for this based on system design have already been explored in this chapter. However, taking a step back and re-evaluating the manner in which the overall problem was addressed is merited. Through the lens of the knowledge gained through the characterization of the culture system, an exploration of alternative methods of studying the microglial response to TBI may point to better paths for future research.

The cellular composition of the 3-D cultures has already been discussed as a target of system modification in the context of incorporating adult, rather than perinatal microglia. Also discussed was the possibility of introducing blood or blood products to the cultures to provide a more complete, *in vivo*-like inflammatory response to injury.

Since LPS priming prior to mechanical injury was demonstrated as a successful method for inducing IL-1β release, an alternative 3-D model to that presented here could consist of cells acquired from animals that have already been exposed to a pro-inflammatory challenge. Specifically, prior to P0 glial harvest, pregnant dams could be subjected to LPS injection to initiate inflammatory cascades in the developing embryos. By pre-conditioning the animals in this manner, the inflammatory response of the intact animals would serve to prime the cells intended for culture. Subjecting cultures consisting of cells harvested from these or control-injected animals to mechanical injury may reveal a differential response based on pre-harvest treatment. Pre-conditioning with LPS or with other treatments such as hypoxia or possibly even *in utero* TBI could result in a 3-D culture model of neuroinflammation that is responsive to mechanical injury.

Along the same lines, microglia from adult injured and uninjured rats could be incorporated into 3-D cultures of neurons to study the mechanisms by which the injury-activated microglia interact with the healthy neurons. Again, the use of cells from animals exposed to insult would address the issue of the absence of peripheral interaction in the current model and thus improve its physiological relevance. This would effectively combine the advantages of a well-characterized *in vivo* injury (such as CCI) with the control and ease of manipulation of an *in vitro* model. Since this method would eliminate the need to mechanically injure cultures, studies could also be conducted using 2-D cultures. Setting aside for a moment the advantages of 3-D culture, a major simplification to the system could be a reversion to 2-D cultures. The aforementioned pre-conditioned cell experiments could provide insight into the microglial response to TBI in 2-D as the profiles of differential cytokine regulation and release should not be much different.

Additionally, *in vitro* stretch injury experiments could be performed on cultures consisting of neurons and astrocytes to which microglia from either normal or injury-conditioned animals could later be added.

The disadvantages of dissociated cell culture could be avoided by studying microglia-driven neuroinflammation using slice cultures. Organotypic slice cultures from rat cortex, hippocampus, or other brain regions could be cultured in such a way that they would be compatible with the CCD described here. The retention of the neuroanatomy in this *ex vivo* preparation would address the issues of cell density and signaling gradient formation characteristic of the dissociated 3-D cultures. The experimental design would be along the same lines as the research presented here. Slice cultures would be exposed to compression injuries of various severities and the resulting inflammatory response could be measured using the same outcome measures as those used for the 3-D multitypic neural cultures. Should a response not be detected using these methods, the previously discussed addition of microglia derived from a pre-conditioned animal could be implemented. Alternatively, the *in vitro* injury could be eliminated and slices from injured and uninjured animals could be cultured and studied directly.

Each of these alternatives to the system described here has inherent advantages and disadvantages. While slice cultures have the distinct advantage of preserving the tissue architecture, sufficient nutrient delivery to prevent culture degradation is a constant concern. 2-D cultures have the benefits of ease and convenience, but they limit both the culture density and complex cell-matrix interactions. The culture of cells derived from animals pre-conditioned with LPS, hypoxia, or injury would address some of the limitations of the model presented here. However, it could be argued that rather than

going to the trouble of culturing those cells, the proposed experiments should be carried out *in vivo*.

The novelty of the 3-D multitypic neural cell culture model is its integration of the three cell types most directly affected by TBI. Neurons are the most vulnerable population to mechanical deformation. Astrocytes are vulnerable as well, but typically have a higher survival rate and are an integral part of the post-injury response. Microglia as the immune effectors of the CNS, are a required component for recreating post-injury inflammation *in vitro*. The goal of this research was to create a model of injury-induced neuroinflammation. The reasoning behind using healthy tissue as the cell source for the 3-D cultures was to make the *in vitro* injury the sole source of insult so that the complete injury response could be captured. While this may have been altruistic, the research presented here describes a system that nearly achieves this goal. Implementation of some of the proposed culture modifications could push this system further toward reaching that goal. However, if this research were to be undertaken again informed by the data gleaned from the experiments described here, one or more of the alternative approaches described would be carried out in parallel with the studies using the 3-D multitypic neural cultures. Preparations of slice cultures, 2-D cultures, or alternatively sourced 3-D cultures would allow for critical comparison with this *in vitro* model. Additionally, parallel *in vivo* injury studies would provide a benchmark for the expected inflammatory response to TBI. Admittedly, much of this research was focused on attempting to elicit a response from the 3-D culture system that may not be feasible. Comparison studies would have possibly indicated the shortcomings of the culture system earlier and facilitated optimization to create more complete *in vitro* model of mechanically-induced neuroinflammation.

6.6 Conclusions

The research presented in this dissertation demonstrated the development of a novel 3-D multitypic neural culture system in which rodent neurons, astrocytes, and microglia were maintained with high viability for weeks *in vitro*. The cultures, and specifically the microglia within them, responded to LPS stimulation with the expected elevation of key markers of neuroinflammation. A unique culture chamber was devised that permits the generation of 3-D cultures with a uniform geometry. A mechanical compression injury system was modified and successfully imparted a focused insult to the 3-D cultures. The hypothesized microglial secondary injury responses to the mechanical injury were not observed consistently enough to claim support for the hypothesis. However, implemented manipulations of the system such as LPS priming ultimately showed positive results. Further, proposed manipulations to promote gradient development are believed to be an avenue by which the model may be validated without the need for pre-stimulation. Overall, these investigations have successfully yielded a novel 3-D culture environment with numerous potential applications both within the area of neuroscience research and beyond.

APPENDIX A

3-D MULTITYPIC NEURAL CELL CULTURE METHODS

A.1 Generation of 3-D multitypic neural cell cultures

Any pipetting step of or into Matrigel™ should be performed using ice-cold pipet tips.

A.1.1 Preparation for 3-D culture

A.1.1.1 Stock Matrigel™ preparation

- 10 mL vial arrives on dry ice
- Thaw **on ice** in the refrigerator overnight (will be very viscous, but free-flowing)
- Dilute to 15 mg/mL with ice-cold HBSS; swirl to mix
- Aliquot (2.0 mL) into cold 50 mL conical tubes and store at -20°C
  (NOTE: When preparing aliquots, draw up and expel Matrigel one time before transferring to coat the inside of the tip. Otherwise, the delivered volume will be low.)

A.1.1.2 Culture preparation (day before plating)

- Thaw aliquot(s) of Matrigel™ **on ice** in the refrigerator overnight
- Pre-coat sterile culture vessels (culture wells, glass coverslips, etc) with 100 µg/mL (in sterile, de-ionized water) poly-D-lysine overnight at 37°C.

A.1.1.3 Acquisition of cells

- All animals are from Charles River Laboratories and arrive on Tuesdays
- Embryonic day 19 (E19) dams are ordered for glial cells; harvest on day litter is born (postnatal day 0 (P0) which is usually on E22) (Friday)
- Embryonic day 16 (E16) dams are ordered for neurons; harvest on E18 (13 days after E19 harvest) (Thursday)
- Acquire glial cells from P0 tissue as described in "P0 cortical dissociation" protocol (below)
- 13 days after plating glial cells, perform harvest of brains from E18 rat embryos as described in the "E18 cortical dissociation" protocol (below)

A.1.2 3-D plating

- Rinse coated culture vessels twice with sterile, de-ionized water
- Aspirate second rinse thoroughly and allow vessels to dry in hood while preparing cultures
- Perform dissociation of E18 cortices as described in Section A.1.4
- Agitate a T75 flask of mixed glial cells generated as described in Section A.1.3
- Remove and reserve medium in a 50mL conical tube
- Rinse with 10 mL of PBS
- Add 3 mL of room temperature trypsin-EDTA and incubate at 37 °C for 5 minutes or until cells have loosened from flask surface
- Add 7 mL of reserved medium to the flask
- Using a 10 mL serological pipet, transfer cells from the flask to the conical tube, making sure to use the cell suspension to rinse the surface of the flask to maximize yield
- Centrifuge at 200 rcf for 5 min
- Remove supernatant and resuspend pellet with 2 mL of 3-D multitypic culture plating medium
- Dilute 10 µL of cell suspension in 190 µL HBSS and count using hemacytometer (microglia will stick to surface, include these in total count; typically, they comprise ~15% of the total cells present in the suspension, but this is just an estimate and is quite variable)
- Count neurons from E18 dissociation as described in Section A.1.4
- The ultimate desired concentration of all cells in the 3-D culture is 4,000 cells/µL ($4x10^6$ cells/mL)
- For a 2:1 ratio of neurons to glia, dilute neurons to $10.67x10^6$ cells/mL and dilute glia to $5.33x10^6$ cells/mL
- For a 1:1 ratio of neurons to glia, dilute both suspensions to $8x10^6$ cells/mL
- To a 2.0 mL aliquot of Matrigel™, add 1mL of each cell suspension using ice-cold pipet tips
- Swirl tube to mix
- Using ice-cold pipet tips, gently plate the 3-D cultures using in a circular fashion, using the tip to guide the formation of the layer of gel (200 µL in a 2 cm^2 culture well will produce a ~1mm thick culture)
- Gently transfer cultures to incubator and allow to incubate for 90 min
- Gently add warmed culture medium to the cultures (250 µL per cm^2 of culture surface)
- Feed cultures by replacing half of the medium after 24 hours
- Feed every 2-3 days thereafter using Neuronal medium (**without** G-5 supplement) (3-D multitypic culture maintenance medium)

A.1.3 P0 cortical dissociation (mixed glia)

- Dissect cortices from brains of P0-P1 rat pups (2 whole brains/4 hemi-cortices per T75 flask) in cold HBSS (or L-15 which seems to lead to a dissociation with fewer clumps)
- Mince the cortices into 1-2 mm chunks using dissecting knives
- Transfer tissue to a 15 mL (if plating one flask) or 50 mL conical tube and carry out dissociation in laminar flow hood
- Remove supernatant HBSS
- Add 3.6 mL room temperature trypsin
- Swirl to mix and place tube into water bath for 20 minutes; agitate periodically (~every 5 min)
- Add 400 µL DNase and swirl to mix
- Add 4 mL of Glial medium
- Mix gently with 5 mL serological pipet to begin breaking up tissue
- Triturate with 5 mL serological pipet
- Mix gently with flame-narrowed Pasteur pipet
- Triturate with flame-narrowed Pasteur pipet
- Allow any remaining clumps of tissue to settle and remove using Pasteur pipet
- Centrifuge at 200 rcf for 5 min
- Remove supernatant
- Resuspend with 8 mL of medium
- Mix gently and triturate with 5 mL serological pipet
- Mix gently and triturate with flame-narrowed Pasteur pipet
- Allow any clumps to settle and remove using Pasteur pipet
- Dilute with medium up to appropriate volume (final volume is 10 mL for every T75 flask)
- Plate into T75 flask(s)
- Replace medium after 3 days and every 2-3 days for one week
- DO NOT change medium for the second week leading up to 3-D plating

A.1.4 E18 cortical dissociation (neurons)

- 13 days after plating glial cells, perform harvest of brains from E18 rat embryos
- Dissect cortices from brains in cold HBSS (or L-15 which seems to lead to a dissociation with fewer clumps)
- Transfer tissue to a 15 mL conical tube and carry out dissociation in laminar flow hood or store in 2 mL of L-15 + B-27 supplement at 4°C for up to 24 hours.
- Rinse 2X with cold HBSS
- Add 5 mL room temperature trypsin
- Swirl to mix and place tube into water bath for 11 minutes; swirl every 3 minutes
- Rinse 3X with cold HBSS
- Add cold HBSS up to ~3.6mL
- Add 400 µL DNase swirl to mix at room temperature or warming gently in hands for 1-2 minutes until the cortices begin to separate from each other
- Mix gently with 10 mL serological pipet to begin breaking up tissue
- Mix gently and triturate with a 5 mL serological pipet
- Mix gently and triturate with flame-narrowed Pasteur pipet
- Allow any remaining clumps of tissue to settle and remove using Pasteur pipet
- Centrifuge at 200 rcf for 5 min
- Remove supernatant
- Resuspend with 2 mL of 3-D multitypic culture plating medium
- Mix and triturate with 2 mL serological pipet
- Mix and triturate with flame-narrowed Pasteur pipet
- Allow any clumps to settle and remove using Pasteur pipet
- Dilute 10 µL of cell suspension into 190 µL HBSS; vortex to mix
- Add 200 µL of trypan blue to diluted cells; vortex to mix
- Count cells using hemacytometer
- Determine viability (90% and higher is acceptable) and viable yield (should be 3-5 x 10^6 cells per cortical hemisphere)
- Dilute and plate at desired density

A.1.5 Media formulations

Glial medium

- 50 mL fetal bovine serum
- 450 mL DMEM/F12

Neuronal medium (also 3-D multitypic culture maintenance medium)

- 2 mL B-27 supplement
- 250 µL GlutaMAX
- Dilute to 100 mL with Neurobasal medium

3-D multitypic culture plating medium

- 2 mL B-27 supplement
- 1 mL G-5 supplement
- 250 µL GlutaMAX
- Dilute to 100 mL with Neurobasal medium

*For inflammation studies, B-27 (Minus AO) and Neurobasal medium without phenol red are used.

Table A.1. List of reagents used in 3-D culture preparation

Name	Company (Catalog Number)	Stock Concentration
Poly-D-lysine (MW >300,000)	Sigma-Aldrich (P7405)	100 µg/mL in sterile, de-ionized H_2O
DNase	Sigma-Aldrich (DN25)	1.5 mg/mL in HBSS containing 2.5 mg/mL $MgSO_4$
Growth Factor-Reduced, High Concentration Matrigel™	BD Biosciences/VWR (354263)	Dilute to 15 mg/mL with ice-cold HBSS
Trypsin-EDTA 0.25%	Invitrogen (25200-056)	0.25%
DMEM/F12	Invitrogen (10565-018)	*n/a*
Fetal Bovine Serum (Premium Select)	Atlanta Biologicals (S11550)	*n/a*
Neurobasal Medium	Invitrogen (21103-049)	*n/a*
Neurobasal Medium (minus phenol red)	Invitrogen (12348-017)	*n/a*
L-15 Medium	Invitrogen (11415-064)	*n/a*
B-27 Supplement	Invitrogen (17504-044)	50X stock
B-27 Supplement Minus AO (w/o antioxidants)	Invitrogen (10889-038)	50X stock
G-5 Supplement	Invitrogen (17503-012)	100X stock
GlutaMAX	Invitrogen (35050-061)	use as 400X stock

A.1.6 Example 3-D culture calendar

Sunday	Monday	Tuesday	Wednesday	Thursday	Friday	Saturday
		E19 timed pregnant rat arrives			DISSECTION P0 pups for astrocytes and microglia	
	FEED mixed glial cultures		FEED mixed glial cultures		FEED mixed glial cultures	
		E16 timed pregnant rat arrives		DISSECTION E18 embryos for neurons 3-D PLATING	FEED 3-D cultures	
	FEED 3-D cultures		FEED 3-D cultures		FEED 3-D cultures	
	FEED 3-D cultures		FEED 3-D cultures	INJURIES		

A.2 Preparation of custom-made culture chambers for 3-D plating

- Clean culture chamber slides:
    - Rinse with tap water and remove any large debris remaining in chamber
    - Soak in tap water with Alconox for 30 min. to overnight
    - Soak in de-ionized water for 10 min.
    - Soak in 70% ethanol for 10 min.
    - Soak in acetone for 10 min.
    - Use a cotton swab to wipe the inside of each culture well
    - Soak in 70% ethanol for 10 min.
    - Soak in de-ionized water for 10 min.
- Transfer culture chamber slides to an autoclavable container or bag
- Seal and autoclave
- In a laminar flow hood, transfer chamber slides to culture dish(es)
- Once completely cooled, add 0.5 mL of Poly-D-lysine (100 μg/mL in water) to each well and place in an incubator at least overnight and preferably 2X overnight (the hydrophilicity of the glass surface improves with repeated use in culture)
- Rinse wells twice with 0.5 mL sterile, de-ionized water and allow to dry prior to plating 3D cultures

A.3 Manufacture and preparation of shear injury chambers

The previous injury chamber system was designed such that the frame and lid were machined from polycarbonate plastic. PDMS culture chambers were glued to coverslips which were, in turn glued to the bottom of the plastic frame. The current model can be used with PDMS chambers mounted to slides or coverslips (although slides are much easier to use). Cells are grown in the culture chambers by themselves which is advantageous as they are readily sterilized by autoclaving. For injuries, the culture chambers can be inserted into the rapid prototyped (Fullcure 720 material) injury chamber, injured, and then returned to the incubator. The same injury chamber can be used for all of the culture chambers.

A.3.1 PDMS/glass culture chamber construction

- Cast 3-well PDMS chamber in mold
    - Weigh out an appropriate amount of Sylgard 184 bulk polymer (~10 g per chamber)
    - Add catalyst (10:1 bulk polymer:catalyst ratio w/w)
    - Mix well by stirring with a plastic transfer pipet
    - De-gas to remove bubbles
    - Cast PDMS into mold made of wax or other material that does not inhibit PDMS curing
    - Use a syringe needle to pop any bubbles
    - Cure on a level surface 2X overnight at RT, remove from mold and place in 70-80 °C oven for 1 hour

- Adhere chamber to glass slide or coverslip
    - Slides should be 25mm x 75mm and 1mm thick (VWR plain: 48300-025)
    - Clean slide with ethanol and/or acetone
    - Insert slide into injury chamber frame and mark rectangular outline corresponding to PDMS mold using permanent marker
    - Remove slide and set on a flat surface, with the marked side down
    - Apply a thin layer of Dow Corning 734 flowable sealant to the smooth side (the side which was exposed to air) of the PDMS chamber and allow the sealant to self-level briefly
    - Press the PDMS chamber onto the slide within the outlined area
    - Allow to set overnight at room temperature

- Permanent marker can be wiped off using ethanol
- Use X-Acto knives to remove excess sealant from edges of PDMS wells (inside and outside)
- The PDMS inserts for the injury chamber lid (see below) are generated in a similar fashion

A.3.2 Shear injury chamber construction

- All parts of the injury chamber are printed from CAD files on an Objet Eden 250 printer using Fullcure 720 material. The parts consist of:
    - A **frame** into which the culture chamber slide can be inserted
    - An **insert** which is placed in the frame after the chamber slide is in place to prevent movement of the slide assembly along the injury axis
    - A **lid** which has 'C'-shaped feet into which PDMS inserts are adhered (Dow Corning 734 flowable sealant) such that when placed on top of the frame the PDMS makes gentle contact with the 3D culture
    - A **bracket** which attaches to actuator arm of the injury device on one side and to the injury chamber lid on the other side
- Clean printed parts using a water jet
- Soak the parts in a solution of 2% NaOH in water for 1-2 hours at room temperature. This removes excess support material and induces uncured monomer to leach out of the part.
- Rinse the parts with tap water and clean using a water jet

A.3.3 Compression injury device construction

- All parts of the injury chamber are printed from CAD files on an Objet Eden 250 printer using Fullcure 720 material. The parts consist of:
    - A frame into which the culture chamber slide can be inserted
    - Pistons of various diameters with 1 mm PDMS pads
- Clean printed parts using a water jet
- Soak the parts in a solution of 2% NaOH in water for 1-2 hours at room temperature. This removes excess support material and induces uncured monomer to leach out of the part.
- Rinse the parts with tap water and clean using a water jet

A.3.4 Injury preparation (shear injury chamber)

- Rinse the frame and lid to be used in the injury device with de-ionized water
- Spray them with 70% ethanol, pat the outside dry and place into 15cm culture dishes in a laminar flow hood
- Expose to UV light for 2+ hours
- Transfer culture chambers to injury chamber using sterile technique in a laminar flow hood
- Between injuries, wipe the PDMS feet on the lid with a Kimwipe dampened with 70% ethanol and then perform a rolling dip into sterile medium in a 150 mm dish

A.3.5 Injury preparation (compression injury device)

- Clean piston and frame with 70% ethanol
- Between each injury, swab piston with 70% ethanol and dry with a Kimwipe

A.4 Immunocytochemistry for 3-D cultures

A.4.1 Culture sectioning

- Remove medium
- Fix cultures with 2% paraformaldehyde in phosphate buffer for 30 min at RT
- Rinse 5X with PBS
- Cryoprotect cultures with 30% sucrose in PBS at 4°C overnight
- Freeze cultures in OCT™ using isopentane and liquid nitrogen
- Cut 30 µm sections using cryostat and mount on gelatin-coated slides
- Store at -20°C until ready to perform immunocytochemistry (or -80°C for long-term)
- When ready to use for immunohistochemistry:
    - Allow slides to come to room temperature
    - Draw boundaries around culture slices using a hydrophobic pen

A.4.2 Immunocytochemistry protocol (sectioned or intact cultures)

- **Block** - 0.1% Triton X-100; 10% Horse Serum (HS); 0.05% saponin in PBS for 1 hour at RT
- Rinse 2X with PBS + 0.05% saponin (PBSS)
- **Primary** - Incubate with antibody diluted in 1% HS in PBSS overnight at 4°C
- Rinse 5X with PBSS
- **Secondary** - Incubate with Donkey anti-primary species antibody (1:200 of 1:1 glycerol-diluted stock, Jackson) in 1% HS in PBSS for 2 hours at RT
- Rinse 2X with PBSS; 1X with PBSS + Hoechst 33342 (1:1,000); 2X with PBSS
- Coverslip using Fluoromount-G

REFERENCES

1. Faul M, X.L., Wald MM, Coronado VG, *Traumatic brain injury in the United States: emergency department visits, hospitalizations, and deaths.*, 2010, Centers for Disease Control and Prevention, National Center for Injury Prevention and Control: Atlanta (GA).

2. Janowitz, T. and D.K. Menon, *Exploring new routes for neuroprotective drug development in traumatic brain injury.* Sci Transl Med, 2010. **2**(27): p. 27rv1.

3. Kabadi, S.V. and A.I. Faden, *Neuroprotective strategies for traumatic brain injury: improving clinical translation.* Int J Mol Sci, 2014. **15**(1): p. 1216-36.

4. Hanisch, U.K., *Microglia as a source and target of cytokines.* Glia, 2002. **40**(2): p. 140-55.

5. Holbourn, A.H.S., *MECHANICS OF HEAD INJURIES.* The Lancet, 1943. **242**(6267): p. 438-441.

6. Shuck, L.Z. and S.H. Advani, *Rheological Response of Human Brain-Tissue in Shear.* Journal of Basic Engineering, 1972. **94**(4): p. 905-911.

7. Enriquez, P. and R. Bullock, *Molecular and cellular mechanisms in the pathophysiology of severe head injury.* Current Pharmaceutical Design, 2004. **10**(18): p. 2131-2143.

8. De Pitta, M., N. Brunel, and A. Volterra, *Astrocytes: Orchestrating synaptic plasticity?* Neuroscience, 2015.

9. Jha, M.K. and K. Suk, *Glia-based biomarkers and their functional role in the CNS.* Expert Rev Proteomics, 2013. **10**(1): p. 43-63.

10. Raghupathi, R., *Cell death mechanisms following traumatic brain injury.* Brain Pathol, 2004. **14**(2): p. 215-22.

11. Doppenberg, E.M., S.C. Choi, and R. Bullock, *Clinical trials in traumatic brain injury: lessons for the future.* J Neurosurg Anesthesiol, 2004. **16**(1): p. 87-94.

12. Narayan, R.K., M.E. Michel, B. Ansell, A. Baethmann, A. Biegon, M.B. Bracken, M.R. Bullock, S.C. Choi, G.L. Clifton, C.F. Contant, W.M. Coplin, W.D. Dietrich, J. Ghajar, S.M. Grady, R.G. Grossman, E.D. Hall, W. Heetderks, D.A. Hovda, J. Jallo, R.L. Katz, N. Knoller, P.M. Kochanek, A.I. Maas, J. Majde, D.W. Marion, A. Marmarou, L.F. Marshall, T.K. McIntosh, E. Miller, N. Mohberg, J.P. Muizelaar, L.H. Pitts, P. Quinn, G. Riesenfeld, C.S. Robertson, K.I. Strauss, G. Teasdale, N. Temkin, R. Tuma, C. Wade, M.D. Walker, M. Weinrich, J. Whyte, J.

Wilberger, A.B. Young, and L. Yurkewicz, *Clinical trials in head injury.* J Neurotrauma, 2002. **19**(5): p. 503-57.

13. Cassidy, J.D., L.J. Carroll, P.M. Peloso, J. Borg, H. von Holst, L. Holm, J. Kraus, V.G. Coronado, and W.H.O.C.C.T.F.o.M.T.B. Injury, *Incidence, risk factors and prevention of mild traumatic brain injury: results of the WHO Collaborating Centre Task Force on Mild Traumatic Brain Injury.* J Rehabil Med, 2004(43 Suppl): p. 28-60.

14. Ling, H., J. Hardy, and H. Zetterberg, *Neurological consequences of traumatic brain injuries in sports.* Mol Cell Neurosci, 2015.

15. Gubata, M.E., E.R. Packnett, C.D. Blandford, A.L. Piccirillo, D.W. Niebuhr, and D.N. Cowan, *Trends in the Epidemiology of Disability Related to Traumatic Brain Injury in the US Army and Marine Corps: 2005 to 2010.* J Head Trauma Rehabil, 2014. **29**(1): p. 65-75.

16. Weiner, M.W., K.E. Friedl, A. Pacifico, J.C. Chapman, M.S. Jaffee, D.M. Little, G.T. Manley, A. McKee, R.C. Petersen, R.K. Pitman, K. Yaffe, H. Zetterberg, R. Obana, L.J. Bain, and M.C. Carrillo, *Military risk factors for Alzheimer's disease.* Alzheimers Dement, 2013. **9**(4): p. 445-51.

17. Jordan, B.D., *The clinical spectrum of sport-related traumatic brain injury.* Nat Rev Neurol, 2013. **9**(4): p. 222-30.

18. Sahler, C.S. and B.D. Greenwald, *Traumatic brain injury in sports: a review.* Rehabil Res Pract, 2012. **2012**: p. 659652.

19. Gentleman, S.M., P.D. Leclercq, L. Moyes, D.I. Graham, C. Smith, W.S. Griffin, and J.A. Nicoll, *Long-term intracerebral inflammatory response after traumatic brain injury.* Forensic Sci Int, 2004. **146**(2-3): p. 97-104.

20. Smith, C., *Review: the long-term consequences of microglial activation following acute traumatic brain injury.* Neuropathol Appl Neurobiol, 2013. **39**(1): p. 35-44.

21. Johnson, V.E., J.E. Stewart, F.D. Begbie, J.Q. Trojanowski, D.H. Smith, and W. Stewart, *Inflammation and white matter degeneration persist for years after a single traumatic brain injury.* Brain, 2013. **136**(Pt 1): p. 28-42.

22. Breunig, J.J., M.V. Guillot-Sestier, and T. Town, *Brain injury, neuroinflammation and Alzheimer's disease.* Front Aging Neurosci, 2013. **5**: p. 26.

23. Johnson, V.E., W. Stewart, and D.H. Smith, *Widespread tau and amyloid-beta pathology many years after a single traumatic brain injury in humans.* Brain Pathol, 2012. **22**(2): p. 142-9.

24. Fakhran, S. and L. Alhilali, *Neurodegenerative changes after mild traumatic brain injury.* Prog Neurol Surg, 2014. **28**: p. 234-42.

25. Ma, J., S. Huang, S. Qin, and C. You, *Progesterone for acute traumatic brain injury.* Cochrane Database Syst Rev, 2012. **10**: p. CD008409.

26. Stein, D.G. and D.W. Wright, *Progesterone in the clinical treatment of acute traumatic brain injury.* Expert Opin Investig Drugs, 2010. **19**(7): p. 847-57.

27. Skolnick, B.E., A.I. Maas, R.K. Narayan, R.G. van der Hoop, T. MacAllister, J.D. Ward, N.R. Nelson, N. Stocchetti, and S.T. Investigators, *A clinical trial of progesterone for severe traumatic brain injury.* N Engl J Med, 2014. **371**(26): p. 2467-76.

28. Wright, D.W., S.D. Yeatts, R. Silbergleit, Y.Y. Palesch, V.S. Hertzberg, M. Frankel, F.C. Goldstein, A.F. Caveney, H. Howlett-Smith, E.M. Bengelink, G.T. Manley, L.H. Merck, L.S. Janis, W.G. Barsan, and N. Investigators, *Very early administration of progesterone for acute traumatic brain injury.* N Engl J Med, 2014. **371**(26): p. 2457-66.

29. Saatman, K.E., A.C. Duhaime, R. Bullock, A.I. Maas, A. Valadka, and G.T. Manley, *Classification of traumatic brain injury for targeted therapies.* J Neurotrauma, 2008. **25**(7): p. 719-38.

30. Zink, B.J., J. Szmydynger-Chodobska, and A. Chodobski, *Emerging concepts in the pathophysiology of traumatic brain injury.* Psychiatr Clin North Am, 2010. **33**(4): p. 741-56.

31. Li, L.M., D.K. Menon, and T. Janowitz, *Cross-sectional analysis of data from the u.s. Clinical trials database reveals poor translational clinical trial effort for traumatic brain injury, compared with stroke.* PLoS One, 2014. **9**(1): p. e84336.

32. Cernak, I., *Animal models of head trauma.* NeuroRx, 2005. **2**(3): p. 410-22.

33. Xiong, Y., A. Mahmood, and M. Chopp, *Animal models of traumatic brain injury.* Nat Rev Neurosci, 2013. **14**(2): p. 128-42.

34. Feeney, D.M., M.G. Boyeson, R.T. Linn, H.M. Murray, and W.G. Dail, *Responses to cortical injury: I. Methodology and local effects of contusions in the rat.* Brain Res, 1981. **211**(1): p. 67-77.

35. Namjoshi, D.R., W.H. Cheng, K.A. McInnes, K.M. Martens, M. Carr, A. Wilkinson, J. Fan, J. Robert, A. Hayat, P.A. Cripton, and C.L. Wellington, *Merging pathology with biomechanics using CHIMERA (Closed-Head Impact Model of Engineered Rotational Acceleration): a novel, surgery-free model of traumatic brain injury.* Mol Neurodegener, 2014. **9**: p. 55.

36. Lighthall, J.W., *Controlled cortical impact: a new experimental brain injury model.* J Neurotrauma, 1988. **5**(1): p. 1-15.

37. Lindgren, S. and L. Rinder, *Experimental studies in head injury. I. Some factors influencing results of model experiments.* Biophysik, 1965. **2**(5): p. 320-9.

38. Johnson, V.E., D.F. Meaney, D.K. Cullen, and D.H. Smith, *Animal models of traumatic brain injury.* Handb Clin Neurol, 2015. **127**: p. 115-28.

39. O'Connor, W.T., A. Smyth, and M.D. Gilchrist, *Animal models of traumatic brain injury: a critical evaluation.* Pharmacol Ther, 2011. **130**(2): p. 106-13.

40. Morrison, B., 3rd, B.S. Elkin, J.P. Dolle, and M.L. Yarmush, *In vitro models of traumatic brain injury.* Annu Rev Biomed Eng, 2011. **13**: p. 91-126.

41. Morrison, B., 3rd, H.L. Cater, C.D. Benham, and L.E. Sundstrom, *An in vitro model of traumatic brain injury utilising two-dimensional stretch of organotypic hippocampal slice cultures.* J Neurosci Methods, 2006. **150**(2): p. 192-201.

42. Morrison, B., 3rd, H.L. Cater, C.C. Wang, F.C. Thomas, C.T. Hung, G.A. Ateshian, and L.E. Sundstrom, *A tissue level tolerance criterion for living brain developed with an in vitro model of traumatic mechanical loading.* Stapp Car Crash J, 2003. **47**: p. 93-105.

43. Cater, H.L., D. Gitterman, S.M. Davis, C.D. Benham, B. Morrison, 3rd, and L.E. Sundstrom, *Stretch-induced injury in organotypic hippocampal slice cultures reproduces in vivo post-traumatic neurodegeneration: role of glutamate receptors and voltage-dependent calcium channels.* J Neurochem, 2007. **101**(2): p. 434-47.

44. Staal, J.A., S.R. Alexander, Y. Liu, T.D. Dickson, and J.C. Vickers, *Characterization of cortical neuronal and glial alterations during culture of organotypic whole brain slices from neonatal and mature mice.* PLoS One, 2011. **6**(7): p. e22040.

45. Geddes, D.M. and R.S. Cargill, 2nd, *An in vitro model of neural trauma: device characterization and calcium response to mechanical stretch.* J Biomech Eng, 2001. **123**(3): p. 247-55.

46. Geddes-Klein, D.M., K.B. Schiffman, and D.F. Meaney, *Mechanisms and consequences of neuronal stretch injury in vitro differ with the model of trauma.* J Neurotrauma, 2006. **23**(2): p. 193-204.

47. LaPlaca, M.C. and L.E. Thibault, *An in vitro traumatic injury model to examine the response of neurons to a hydrodynamically-induced deformation.* Ann Biomed Eng, 1997. **25**(4): p. 665-77.

48. Balgude, A.P., X. Yu, A. Szymanski, and R.V. Bellamkonda, *Agarose gel stiffness determines rate of DRG neurite extension in 3D cultures.* Biomaterials, 2001. **22**(10): p. 1077-84.

49. Rowley, J.A., G. Madlambayan, and D.J. Mooney, *Alginate hydrogels as synthetic extracellular matrix materials.* Biomaterials, 1999. **20**(1): p. 45-53.

50. Beniash, E., J.D. Hartgerink, H. Storrie, J.C. Stendahl, and S.I. Stupp, *Self-assembling peptide amphiphile nanofiber matrices for cell entrapment.* Acta Biomater, 2005. **1**(4): p. 387-97.

51. Gelain, F., D. Bottai, A. Vescovi, and S. Zhang, *Designer self-assembling Peptide nanofiber scaffolds for adult mouse neural stem cell 3-dimensional cultures.* PLoS ONE, 2006. **1**: p. e119.

52. Genove, E., C. Shen, S. Zhang, and C.E. Semino, *The effect of functionalized self-assembling peptide scaffolds on human aortic endothelial cell function.* Biomaterials, 2005. **26**(16): p. 3341-51.

53. Hucknall, A.M., *A Self-Assembling Peptide Scaffold Functionalized for Use With Neural Stem Cells*, in *Materials Science and Engineering*2005, Massachusetts Institute of Technology. p. 35.

54. Kim, U.J., J. Park, C. Li, H.J. Jin, R. Valluzzi, and D.L. Kaplan, *Structure and properties of silk hydrogels.* Biomacromolecules, 2004. **5**(3): p. 786-92.

55. Lv, Q., K. Hu, Q. Feng, and F. Cui, *Fibroin/collagen hybrid hydrogels with crosslinking method: preparation, properties, and cytocompatibility.* J Biomed Mater Res A, 2008. **84**(1): p. 198-207.

56. Baldwin, S.P., C.E. Krewson, and W.M. Saltzman, *PC12 cell aggregation and neurite growth in gels of collagen, laminin and fibronectin.* Int J Dev Neurosci, 1996. **14**(3): p. 351-64.

57. Kleinman, H.K., M.L. McGarvey, L.A. Liotta, P.G. Robey, K. Tryggvason, and G.R. Martin, *Isolation and characterization of type IV procollagen, laminin, and heparan sulfate proteoglycan from the EHS sarcoma.* Biochemistry, 1982. **21**(24): p. 6188-93.

58. Potter, W., R.E. Kalil, and W.J. Kao, *Biomimetic material systems for neural progenitor cell-based therapy.* Front Biosci, 2008. **13**: p. 806-21.

59. Cullen, D.K. and M.C. LaPlaca, *Neuronal response to high rate shear deformation depends on heterogeneity of the local strain field.* J Neurotrauma, 2006. **23**(9): p. 1304-19.

60. Cullen, D.K., C.M. Simon, and M.C. LaPlaca, *Strain rate-dependent induction of reactive astrogliosis and cell death in three-dimensional neuronal-astrocytic co-cultures.* Brain Res, 2007. **1158**: p. 103-15.

61. LaPlaca, M.C., D.K. Cullen, J.J. McLoughlin, and R.S. Cargill, 2nd, *High rate shear strain of three-dimensional neural cell cultures: a new in vitro traumatic brain injury model.* J Biomech, 2005. **38**(5): p. 1093-105.

62. Cullen, D.K., V.N. Vernekar, and M.C. LaPlaca, *Trauma-induced plasmalemma disruptions in three-dimensional neural cultures are dependent on strain modality and rate.* J Neurotrauma, 2011. **28**(11): p. 2219-33.

63. Ransohoff, R.M. and M.A. Brown, *Innate immunity in the central nervous system.* J Clin Invest, 2012. **122**(4): p. 1164-71.

64. Morganti-Kossmann, M.C., L. Satgunaseelan, N. Bye, and T. Kossmann, *Modulation of immune response by head injury.* Injury, 2007. **38**(12): p. 1392-400.

65. Davalos, D., J. Grutzendler, G. Yang, J.V. Kim, Y. Zuo, S. Jung, D.R. Littman, M.L. Dustin, and W.B. Gan, *ATP mediates rapid microglial response to local brain injury in vivo.* Nat Neurosci, 2005. **8**(6): p. 752-8.

66. Wake, H., A.J. Moorhouse, S. Jinno, S. Kohsaka, and J. Nabekura, *Resting microglia directly monitor the functional state of synapses in vivo and determine the fate of ischemic terminals.* J Neurosci, 2009. **29**(13): p. 3974-80.

67. Loane, D.J. and K.R. Byrnes, *Role of microglia in neurotrauma.* Neurotherapeutics, 2010. **7**(4): p. 366-77.

68. Gehrmann, J., Y. Matsumoto, and G.W. Kreutzberg, *Microglia: intrinsic immuneffector cell of the brain.* Brain Res Brain Res Rev, 1995. **20**(3): p. 269-87.

69. Allan, S.M. and N.J. Rothwell, *Cytokines and acute neurodegeneration.* Nat Rev Neurosci, 2001. **2**(10): p. 734-44.

70. Kuno, K. and K. Matsushima, *The IL-1 receptor signaling pathway.* J Leukoc Biol, 1994. **56**(5): p. 542-7.

71. Scheller, J., A. Chalaris, D. Schmidt-Arras, and S. Rose-John, *The pro- and anti-inflammatory properties of the cytokine interleukin-6.* Biochim Biophys Acta, 2011. **1813**(5): p. 878-88.

72. Ziebell, J.M. and M.C. Morganti-Kossmann, *Involvement of pro- and anti-inflammatory cytokines and chemokines in the pathophysiology of traumatic brain injury.* Neurotherapeutics, 2010. **7**(1): p. 22-30.

73. Woodcock, T. and M.C. Morganti-Kossmann, *The role of markers of inflammation in traumatic brain injury.* Front Neurol, 2013. **4**: p. 18.

74. Rothwell, N.J. and G.N. Luheshi, *Interleukin 1 in the brain: biology, pathology and therapeutic target.* Trends Neurosci, 2000. **23**(12): p. 618-25.

75. Woodroofe, M.N., G.S. Sarna, M. Wadhwa, G.M. Hayes, A.J. Loughlin, A. Tinker, and M.L. Cuzner, *Detection of interleukin-1 and interleukin-6 in adult rat brain, following mechanical injury, by in vivo microdialysis: evidence of a role for microglia in cytokine production.* J Neuroimmunol, 1991. **33**(3): p. 227-36.

76. Yao, J. and R.W. Johnson, *Induction of interleukin-1 beta-converting enzyme (ICE) in murine microglia by lipopolysaccharide.* Brain Res Mol Brain Res, 1997. **51**(1-2): p. 170-8.

77. Ferrari, D., C. Pizzirani, E. Adinolfi, R.M. Lemoli, A. Curti, M. Idzko, E. Panther, and F. Di Virgilio, *The P2X7 receptor: a key player in IL-1 processing and release.* J Immunol, 2006. **176**(7): p. 3877-83.

78. Grahames, C.B., A.D. Michel, I.P. Chessell, and P.P. Humphrey, *Pharmacological characterization of ATP- and LPS-induced IL-1beta release in human monocytes.* Br J Pharmacol, 1999. **127**(8): p. 1915-21.

79. Mingam, R., V. De Smedt, T. Amedee, R.M. Bluthe, K.W. Kelley, R. Dantzer, and S. Laye, *In vitro and in vivo evidence for a role of the P2X7 receptor in the release of IL-1 beta in the murine brain.* Brain Behav Immun, 2008. **22**(2): p. 234-44.

80. Joosten, L.A., M.G. Netea, and C.A. Dinarello, *Interleukin-1beta in innate inflammation, autophagy and immunity.* Semin Immunol, 2013. **25**(6): p. 416-24.

81. Denes, A., G. Lopez-Castejon, and D. Brough, *Caspase-1: is IL-1 just the tip of the ICEberg?* Cell Death Dis, 2012. **3**: p. e338.

82. Perez-Polo, J.R., H.C. Rea, K.M. Johnson, M.A. Parsley, G.C. Unabia, G. Xu, S.K. Infante, D.S. Dewitt, and C.E. Hulsebosch, *Inflammatory consequences in a rodent model of mild traumatic brain injury.* J Neurotrauma, 2013. **30**(9): p. 727-40.

83. Sanchez Mejia, R.O., V.O. Ona, M. Li, and R.M. Friedlander, *Minocycline reduces traumatic brain injury-mediated caspase-1 activation, tissue damage, and neurological dysfunction.* Neurosurgery, 2001. **48**(6): p. 1393-9; discussion 1399-401.

84. O'Callaghan, J.P., K. Sriram, and D.B. Miller, *Defining "neuroinflammation".* Ann N Y Acad Sci, 2008. **1139**: p. 318-30.

85. Choi, B.Y., B.G. Jang, J.H. Kim, B.E. Lee, M. Sohn, H.K. Song, and S.W. Suh, *Prevention of traumatic brain injury-induced neuronal death by inhibition of NADPH oxidase activation.* Brain Res, 2012. **1481**: p. 49-58.

86. Peterson, P.K., S. Hu, W.R. Anderson, and C.C. Chao, *Nitric oxide production and neurotoxicity mediated by activated microglia from human versus mouse brain.* J Infect Dis, 1994. **170**(2): p. 457-60.

87. Mander, P. and G.C. Brown, *Activation of microglial NADPH oxidase is synergistic with glial iNOS expression in inducing neuronal death: a dual-key mechanism of inflammatory neurodegeneration.* J Neuroinflammation, 2005. **2**: p. 20.

88. Kamm, K., W. Vanderkolk, C. Lawrence, M. Jonker, and A.T. Davis, *The effect of traumatic brain injury upon the concentration and expression of interleukin-1beta and interleukin-10 in the rat.* J Trauma, 2006. **60**(1): p. 152-7.

89. Li, B., A. Mahmood, D.Y. Lu, H.T. Wu, Y. Xiong, C.S. Qu, and M. Chopp, *Simvastatin Attenuates Microglial Cells and Astrocyte Activation and Decreases Interleukin-1b Level after Traumatic Brain Injury.* Neurosurgery, 2009. **65**(1): p. 179-186.

90. Kinoshita, K., K. Chatzipanteli i, E. Vitarbo, J.S. Truettner, O.F. Alonso, and W.D. Dietrich, *Interleukin-1beta messenger ribonucleic acid and protein levels after fluid-percussion brain injury in rats: importance of injury severity and brain temperature.* Neurosurgery, 2002. **51**(1): p. 195-203; discussion 203.

91. Gresa-Arribas, N., C. Vieitez, G. Dentesano, J. Serratosa, J. Saura, and C. Sola, *Modelling neuroinflammation in vitro: a tool to test the potential neuroprotective effect of anti-inflammatory agents.* PLoS One, 2012. **7**(9): p. e45227.

92. Fahlenkamp, A.V., M. Coburn, M. Czaplik, Y.M. Ryang, M. Kipp, R. Rossaint, and C. Beyer, *Expression analysis of the early chemokine response 4 h after in vitro traumatic brain injury.* Inflamm Res, 2010.

93. An, Y., Q. Chen, and N. Quan, *Interleukin-1 exerts distinct actions on different cell types of the brain in vitro.* J Inflamm Res, 2011. **2011**(4): p. 11-20.

94. Lull, M.E. and M.L. Block, *Microglial activation and chronic neurodegeneration.* Neurotherapeutics, 2010. **7**(4): p. 354-65.

95. Aloisi, F., *Immune function of microglia.* Glia, 2001. **36**(2): p. 165-79.

96. Kettenmann, H., U.K. Hanisch, M. Noda, and A. Verkhratsky, *Physiology of microglia.* Physiol Rev, 2011. **91**(2): p. 461-553.

97. Fischer, H.G. and G. Reichmann, *Brain dendritic cells and macrophages/microglia in central nervous system inflammation.* J Immunol, 2001. **166**(4): p. 2717-26.

98. Hetier, E., J. Ayala, P. Denefle, A. Bousseau, P. Rouget, M. Mallat, and A. Prochiantz, *Brain macrophages synthesize interleukin-1 and interleukin-1 mRNAs in vitro.* J Neurosci Res, 1988. **21**(2-4): p. 391-7.

99. Ginhoux, F., M. Greter, M. Leboeuf, S. Nandi, P. See, S. Gokhan, M.F. Mehler, S.J. Conway, L.G. Ng, E.R. Stanley, I.M. Samokhvalov, and M. Merad, *Fate*

mapping analysis reveals that adult microglia derive from primitive macrophages. Science, 2010. **330**(6005): p. 841-5.

100. Kierdorf, K., D. Erny, T. Goldmann, V. Sander, C. Schulz, E.G. Perdiguero, P. Wieghofer, A. Heinrich, P. Riemke, C. Holscher, D.N. Muller, B. Luckow, T. Brocker, K. Debowski, G. Fritz, G. Opdenakker, A. Diefenbach, K. Biber, M. Heikenwalder, F. Geissmann, F. Rosenbauer, and M. Prinz, *Microglia emerge from erythromyeloid precursors via Pu.1- and Irf8-dependent pathways.* Nat Neurosci, 2013. **16**(3): p. 273-80.

101. Neumann, H. and H. Wekerle, *Brain microglia: watchdogs with pedigree.* Nat Neurosci, 2013. **16**(3): p. 253-5.

102. Prinz, M. and A. Mildner, *Microglia in the CNS: immigrants from another world.* Glia, 2011. **59**(2): p. 177-87.

103. Byrnes, K.R., J. Garay, S. Di Giovanni, A. De Biase, S.M. Knoblach, E.P. Hoffman, V. Movsesyan, and A.I. Faden, *Expression of two temporally distinct microglia-related gene clusters after spinal cord injury.* Glia, 2006. **53**(4): p. 420-33.

104. Ekdahl, C.T., Z. Kokaia, and O. Lindvall, *Brain inflammation and adult neurogenesis: The dual role of microglia.* Neuroscience, 2009. **158**(3): p. 1021-9.

105. Morganti-Kossmann, M.C., M. Rancan, P.F. Stahel, and T. Kossmann, *Inflammatory response in acute traumatic brain injury: a double-edged sword.* Curr Opin Crit Care, 2002. **8**(2): p. 101-5.

106. Burnstock, G., *Physiology and pathophysiology of purinergic neurotransmission.* Physiol Rev, 2007. **87**(2): p. 659-797.

107. Koizumi, S., Y. Shigemoto-Mogami, K. Nasu-Tada, Y. Shinozaki, K. Ohsawa, M. Tsuda, B.V. Joshi, K.A. Jacobson, S. Kohsaka, and K. Inoue, *UDP acting at P2Y6 receptors is a mediator of microglial phagocytosis.* Nature, 2007. **446**(7139): p. 1091-5.

108. Ohsawa, K., Y. Irino, T. Sanagi, Y. Nakamura, E. Suzuki, K. Inoue, and S. Kohsaka, *P2Y12 receptor-mediated integrin-beta1 activation regulates microglial process extension induced by ATP.* Glia, 2010. **58**(7): p. 790-801.

109. Burnstock, G. and V. Alexei, *Purinergic Signalling and the Nervous System*. 2012: Springer.

110. Nicke, A., *Homotrimeric complexes are the dominant assembly state of native P2X7 subunits.* Biochem Biophys Res Commun, 2008. **377**(3): p. 803-8.

111. North, R.A., *Molecular physiology of P2X receptors.* Physiol Rev, 2002. **82**(4): p. 1013-67.

112. Di Virgilio, F., P. Chiozzi, S. Falzoni, D. Ferrari, J.M. Sanz, V. Venketaraman, and O.R. Baricordi, *Cytolytic P2X purinoceptors.* Cell Death Differ, 1998. **5**(3): p. 191-9.

113. Ferrari, D., P. Chiozzi, S. Falzoni, S. Hanau, and F. Di Virgilio, *Purinergic modulation of interleukin-1 beta release from microglial cells stimulated with bacterial endotoxin.* J Exp Med, 1997. **185**(3): p. 579-82.

114. Monif, M., C.A. Reid, K.L. Powell, M.L. Smart, and D.A. Williams, *The P2X7 receptor drives microglial activation and proliferation: a trophic role for P2X7R pore.* J Neurosci, 2009. **29**(12): p. 3781-91.

115. Skaper, S.D., L. Facci, A.A. Culbert, N.A. Evans, I. Chessell, J.B. Davis, and J.C. Richardson, *P2X(7) receptors on microglial cells mediate injury to cortical neurons in vitro.* Glia, 2006. **54**(3): p. 234-42.

116. Sanz, J.M. and F. Di Virgilio, *Kinetics and mechanism of ATP-dependent IL-1 beta release from microglial cells.* J Immunol, 2000. **164**(9): p. 4893-8.

117. Kim, Y.J., S.Y. Hwang, E.S. Oh, S. Oh, and I.O. Han, *IL-1beta, an immediate early protein secreted by activated microglia, induces iNOS/NO in C6 astrocytoma cells through p38 MAPK and NF-kappaB pathways.* J Neurosci Res, 2006. **84**(5): p. 1037-46.

118. Pelegrin, P. and A. Surprenant, *Pannexin-1 mediates large pore formation and interleukin-1beta release by the ATP-gated P2X7 receptor.* EMBO J, 2006. **25**(21): p. 5071-82.

119. Silverman, W.R., J.P. de Rivero Vaccari, S. Locovei, F. Qiu, S.K. Carlsson, E. Scemes, R.W. Keane, and G. Dahl, *The pannexin 1 channel activates the inflammasome in neurons and astrocytes.* J Biol Chem, 2009. **284**(27): p. 18143-51.

120. Collo, G., S. Neidhart, E. Kawashima, M. Kosco-Vilbois, R.A. North, and G. Buell, *Tissue distribution of the P2X7 receptor.* Neuropharmacology, 1997. **36**(9): p. 1277-83.

121. Skaper, S.D., P. Debetto, and P. Giusti, *The P2X7 purinergic receptor: from physiology to neurological disorders.* FASEB J, 2010. **24**(2): p. 337-45.

122. Takenouchi, T., K. Sekiyama, A. Sekigawa, M. Fujita, M. Waragai, S. Sugama, Y. Iwamaru, H. Kitani, and M. Hashimoto, *P2X7 receptor signaling pathway as a therapeutic target for neurodegenerative diseases.* Arch Immunol Ther Exp (Warsz), 2010. **58**(2): p. 91-6.

123. Choo, A.M., W.J. Miller, Y.C. Chen, P. Nibley, T.P. Patel, C. Goletiani, B. Morrison, 3rd, M.K. Kutzing, B.L. Firestein, J.Y. Sul, P.G. Haydon, and D.F.

Meaney, *Antagonism of purinergic signalling improves recovery from traumatic brain injury.* Brain, 2013. **136**(Pt 1): p. 65-80.

124. Dalmau, I., J.M. Vela, B. Gonzalez, B. Finsen, and B. Castellano, *Dynamics of microglia in the developing rat brain.* J Comp Neurol, 2003. **458**(2): p. 144-57.

125. Amat, J.A., H. Ishiguro, K. Nakamura, and W.T. Norton, *Phenotypic diversity and kinetics of proliferating microglia and astrocytes following cortical stab wounds.* Glia, 1996. **16**(4): p. 368-82.

126. Nimmerjahn, A., F. Kirchhoff, and F. Helmchen, *Resting microglial cells are highly dynamic surveillants of brain parenchyma in vivo.* Science, 2005. **308**(5726): p. 1314-8.

127. Szabo, M. and K. Gulya, *Development of the microglial phenotype in culture.* Neuroscience, 2013. **241**: p. 280-95.

128. Giulian, D. and T.J. Baker, *Characterization of ameboid microglia isolated from developing mammalian brain.* J Neurosci, 1986. **6**(8): p. 2163-78.

129. Floden, A.M. and C.K. Combs, *Microglia repetitively isolated from in vitro mixed glial cultures retain their initial phenotype.* J Neurosci Methods, 2007. **164**(2): p. 218-24.

130. Carson, M.J., J. Crane, and A.X. Xie, *Modeling CNS microglia: the quest to identify predictive models.* Drug Discov Today Dis Models, 2008. **5**(1): p. 19-25.

131. Bianco, F., E. Pravettoni, A. Colombo, U. Schenk, T. Moller, M. Matteoli, and C. Verderio, *Astrocyte-derived ATP induces vesicle shedding and IL-1 beta release from microglia.* J Immunol, 2005. **174**(11): p. 7268-77.

132. Orr, A.G., A.L. Orr, X.J. Li, R.E. Gross, and S.F. Traynelis, *Adenosine A(2A) receptor mediates microglial process retraction.* Nat Neurosci, 2009. **12**(7): p. 872-8.

133. Ohsawa, K. and S. Kohsaka, *Dynamic motility of microglia: purinergic modulation of microglial movement in the normal and pathological brain.* Glia, 2011. **59**(12): p. 1793-9.

134. Hernandez-Ontiveros, D.G., N. Tajiri, S. Acosta, B. Giunta, J. Tan, and C.V. Borlongan, *Microglia activation as a biomarker for traumatic brain injury.* Front Neurol, 2013. **4**: p. 30.

135. Ramlackhansingh, A.F., D.J. Brooks, R.J. Greenwood, S.K. Bose, F.E. Turkheimer, K.M. Kinnunen, S. Gentleman, R.A. Heckemann, K. Gunanayagam, G. Gelosa, and D.J. Sharp, *Inflammation after trauma: microglial activation and traumatic brain injury.* Ann Neurol, 2011. **70**(3): p. 374-83.

136. Wang, P., N.J. Rothwell, E. Pinteaux, and D. Brough, *Neuronal injury induces the release of pro-interleukin-1beta from activated microglia in vitro.* Brain Res, 2008. **1236**: p. 1-7.

137. Dichter, M.A., *Rat cortical neurons in cell culture: culture methods, cell morphology, electrophysiology, and synapse formation.* Brain Res, 1978. **149**(2): p. 279-93.

138. Jones, E.V., D. Cook, and K.K. Murai, *A neuron-astrocyte co-culture system to investigate astrocyte-secreted factors in mouse neuronal development.* Methods Mol Biol, 2012. **814**: p. 341-52.

139. Saura, J., *Microglial cells in astroglial cultures: a cautionary note.* J Neuroinflammation, 2007. **4**: p. 26.

140. McCarthy, K.D. and J. de Vellis, *Preparation of separate astroglial and oligodendroglial cell cultures from rat cerebral tissue.* J Cell Biol, 1980. **85**(3): p. 890-902.

141. Tanaka, J. and N. Maeda, *Microglial ramification requires nondiffusible factors derived from astrocytes.* Exp Neurol, 1996. **137**(2): p. 367-75.

142. Brewer, G.J. and C.W. Cotman, *Survival and Growth of Hippocampal-Neurons in Defined Medium at Low-Density - Advantages of a Sandwich Culture Technique or Low Oxygen.* Brain Research, 1989. **494**(1): p. 65-74.

143. Bottenstein, J., *Growth and Differentiation of Neural Cells in Defined Media*, in *Cell Culture in the Neurosciences*, J. Bottenstein and G. Sato, Editors. 1985, Springer US. p. 3-43.

144. Ponomarev, E.D., M. Novikova, K. Maresz, L.P. Shriver, and B.N. Dittel, *Development of a culture system that supports adult microglial cell proliferation and maintenance in the resting state.* J Immunol Methods, 2005. **300**(1-2): p. 32-46.

145. Azevedo, F.A., L.R. Carvalho, L.T. Grinberg, J.M. Farfel, R.E. Ferretti, R.E. Leite, W. Jacob Filho, R. Lent, and S. Herculano-Houzel, *Equal numbers of neuronal and nonneuronal cells make the human brain an isometrically scaled-up primate brain.* J Comp Neurol, 2009. **513**(5): p. 532-41.

146. Kloss, C.U., M. Bohatschek, G.W. Kreutzberg, and G. Raivich, *Effect of lipopolysaccharide on the morphology and integrin immunoreactivity of ramified microglia in the mouse brain and in cell culture.* Exp Neurol, 2001. **168**(1): p. 32-46.

147. abd-el-Basset, E. and S. Fedoroff, *Effect of bacterial wall lipopolysaccharide (LPS) on morphology, motility, and cytoskeletal organization of microglia in cultures.* J Neurosci Res, 1995. **41**(2): p. 222-37.

148. Aderem, A. and R.J. Ulevitch, *Toll-like receptors in the induction of the innate immune response.* Nature, 2000. **406**(6797): p. 782-7.

149. Alexander, C. and E.T. Rietschel, *Bacterial lipopolysaccharides and innate immunity.* J Endotoxin Res, 2001. **7**(3): p. 167-202.

150. De Castro, C., O. Holst, R. Lanzetta, M. Parrilli, and A. Molinaro, *Bacterial lipopolysaccharides in plant and mammalian innate immunity.* Protein Pept Lett, 2012. **19**(10): p. 1040-4.

151. Sasaki, E., H. Kojima, H. Nishimatsu, Y. Urano, K. Kikuchi, Y. Hirata, and T. Nagano, *Highly sensitive near-infrared fluorescent probes for nitric oxide and their application to isolated organs.* J Am Chem Soc, 2005. **127**(11): p. 3684-5.

152. Kaur, C., S.T. Dheen, and E.A. Ling, *From blood to brain: amoeboid microglial cell, a nascent macrophage and its functions in developing brain.* Acta Pharmacol Sin, 2007. **28**(8): p. 1087-96.

153. Dawson, T.M., V.L. Dawson, and S.H. Snyder, *A novel neuronal messenger molecule in brain: the free radical, nitric oxide.* Ann Neurol, 1992. **32**(3): p. 297-311.

154. Kaur, C., V. Sivakumar, L.S. Ang, and A. Sundaresan, *Hypoxic damage to the periventricular white matter in neonatal brain: role of vascular endothelial growth factor, nitric oxide and excitotoxicity.* J Neurochem, 2006. **98**(4): p. 1200-16.

155. Vincent, V.A., F.J. Tilders, and A.M. Van Dam, *Production, regulation and role of nitric oxide in glial cells.* Mediators Inflamm, 1998. **7**(4): p. 239-55.

156. Amor, S., L.A. Peferoen, D.Y. Vogel, M. Breur, P. van der Valk, D. Baker, and J.M. van Noort, *Inflammation in neurodegenerative diseases--an update.* Immunology, 2014. **142**(2): p. 151-66.

157. Amor, S., F. Puentes, D. Baker, and P. van der Valk, *Inflammation in neurodegenerative diseases.* Immunology, 2010. **129**(2): p. 154-69.

158. You, Y. and C. Kaur, *Expression of induced nitric oxide synthase in amoeboid microglia in postnatal rats following an exposure to hypoxia.* Neurosci Lett, 2000. **279**(2): p. 101-4.

159. Zhao, W., W. Xie, W. Le, D.R. Beers, Y. He, J.S. Henkel, E.P. Simpson, A.A. Yen, Q. Xiao, and S.H. Appel, *Activated microglia initiate motor neuron injury by a nitric oxide and glutamate-mediated mechanism.* J Neuropathol Exp Neurol, 2004. **63**(9): p. 964-77.

160. Nakamura, Y., Q.S. Si, and K. Kataoka, *Lipopolysaccharide-induced microglial activation in culture: temporal profiles of morphological change and release of cytokines and nitric oxide.* Neurosci Res, 1999. **35**(2): p. 95-100.

161. Defaux, A., M.G. Zurich, P. Honegger, and F. Monnet-Tschudi, *Inflammatory responses in aggregating rat brain cell cultures subjected to different demyelinating conditions.* Brain Res, 2010. **1353**: p. 213-24.

162. Nakamura, Y., *Regulating factors for microglial activation.* Biol Pharm Bull, 2002. **25**(8): p. 945-53.

163. Tamashiro, T.T., C.L. Dalgard, and K.R. Byrnes, *Primary microglia isolation from mixed glial cell cultures of neonatal rat brain tissue.* J Vis Exp, 2012(66): p. e3814.

164. Wilson, J.X., *Antioxidant defense of the brain: a role for astrocytes.* Can J Physiol Pharmacol, 1997. **75**(10-11): p. 1149-63.

165. Ma, D., S. Jin, E. Li, Y. Doi, B. Parajuli, M. Noda, Y. Sonobe, T. Mizuno, and A. Suzumura, *The neurotoxic effect of astrocytes activated with toll-like receptor ligands.* J Neuroimmunol, 2013. **254**(1-2): p. 10-8.

166. Bandeira, F., R. Lent, and S. Herculano-Houzel, *Changing numbers of neuronal and non-neuronal cells underlie postnatal brain growth in the rat.* Proc Natl Acad Sci U S A, 2009. **106**(33): p. 14108-13.

167. Giulian, D., *Ameboid microglia as effectors of inflammation in the central nervous system.* J Neurosci Res, 1987. **18**(1): p. 155-71, 132-3.

168. Sasaki, Y., M. Hoshi, C. Akazawa, Y. Nakamura, H. Tsuzuki, K. Inoue, and S. Kohsaka, *Selective expression of Gi/o-coupled ATP receptor P2Y12 in microglia in rat brain.* Glia, 2003. **44**(3): p. 242-50.

169. Geddes, D.M., R.S. Cargill, 2nd, and M.C. LaPlaca, *Mechanical stretch to neurons results in a strain rate and magnitude-dependent increase in plasma membrane permeability.* J Neurotrauma, 2003. **20**(10): p. 1039-49.

170. Skotak, M., F. Wang, and N. Chandra, *An in vitro injury model for SH-SY5Y neuroblastoma cells: effect of strain and strain rate.* J Neurosci Methods, 2012. **205**(1): p. 159-68.

171. Allen, J.W., S.M. Knoblach, and A.I. Faden, *Combined mechanical trauma and metabolic impairment in vitro induces NMDA receptor-dependent neuronal cell death and caspase-3-dependent apoptosis.* FASEB J, 1999. **13**(13): p. 1875-82.

172. Glass, T.F., B. Reeves, and F.R. Sharp, *Modeling both the mechanical and hypoxic features of traumatic brain injury in vitro in rats.* Neurosci Lett, 2002. **328**(2): p. 133-6.

173. Frantseva, M.V., L. Kokarovtseva, C.G. Naus, P.L. Carlen, D. MacFabe, and J.L. Perez Velazquez, *Specific gap junctions enhance the neuronal vulnerability to brain traumatic injury.* J Neurosci, 2002. **22**(3): p. 644-53.

174. Adembri, C., A. Bechi, E. Meli, E. Gramigni, L. Venturi, F. Moroni, A.R. De Gaudio, and D.E. Pellegrini-Giampietro, *Erythropoietin attenuates post-traumatic injury in organotypic hippocampal slices.* J Neurotrauma, 2004. **21**(8): p. 1103-12.

175. Schoeler, M., P.D. Loetscher, R. Rossaint, A.V. Fahlenkamp, G. Eberhardt, S. Rex, J. Weis, and M. Coburn, *Dexmedetomidine is neuroprotective in an in vitro model for traumatic brain injury.* BMC Neurol, 2012. **12**: p. 20.

176. Berthois, Y., J.A. Katzenellenbogen, and B.S. Katzenellenbogen, *Phenol red in tissue culture media is a weak estrogen: implications concerning the study of estrogen-responsive cells in culture.* Proc Natl Acad Sci U S A, 1986. **83**(8): p. 2496-500.

177. Bindal, R.D., K.E. Carlson, B.S. Katzenellenbogen, and J.A. Katzenellenbogen, *Lipophilic impurities, not phenolsulfonphthalein, account for the estrogenic activity in commercial preparations of phenol red.* J Steroid Biochem, 1988. **31**(3): p. 287-93.

178. Welshons, W.V., M.F. Wolf, C.S. Murphy, and V.C. Jordan, *Estrogenic activity of phenol red.* Mol Cell Endocrinol, 1988. **57**(3): p. 169-78.

179. Baker, A.E., V.M. Brautigam, and J.J. Watters, *Estrogen modulates microglial inflammatory mediator production via interactions with estrogen receptor beta.* Endocrinology, 2004. **145**(11): p. 5021-32.

180. Vegeto, E., C. Bonincontro, G. Pollio, A. Sala, S. Viappiani, F. Nardi, A. Brusadelli, B. Viviani, P. Ciana, and A. Maggi, *Estrogen prevents the lipopolysaccharide-induced inflammatory response in microglia.* J Neurosci, 2001. **21**(6): p. 1809-18.

181. Cerciat, M., M. Unkila, L.M. Garcia-Segura, and M.A. Arevalo, *Selective estrogen receptor modulators decrease the production of interleukin-6 and interferon-gamma-inducible protein-10 by astrocytes exposed to inflammatory challenge in vitro.* Glia, 2010. **58**(1): p. 93-102.

182. Imamura, H., S. Takao, and T. Aikou, *A modified invasion-3-(4,5-dimethylthiazole-2-yl)-2,5-diphenyltetrazolium bromide assay for quantitating tumor cell invasion.* Cancer Res, 1994. **54**(13): p. 3620-4.

183. Lee, J.K. and M.G. Tansey, *Microglia isolation from adult mouse brain.* Methods Mol Biol, 2013. **1041**: p. 17-23.

184. Kundu, K., S.F. Knight, N. Willett, S. Lee, W.R. Taylor, and N. Murthy, *Hydrocyanines: a class of fluorescent sensors that can image reactive oxygen species in cell culture, tissue, and in vivo.* Angew Chem Int Ed Engl, 2009. **48**(2): p. 299-303.

185. Lundberg, J.O., E. Weitzberg, and M.T. Gladwin, *The nitrate-nitrite-nitric oxide pathway in physiology and therapeutics.* Nat Rev Drug Discov, 2008. **7**(2): p. 156-67.

186. Moykkynen, T., R. Liebkind, J. Sjoberg, E.R. Korpi, and P. Liesi, *The neuroprotective KDI domain of gamma 1-laminin is a universal and potent inhibitor of ionotropic glutamate receptors.* J Neurosci Res, 2005. **81**(6): p. 797-804.

187. Vaananen, A.J., P. Rauhala, R.K. Tuominen, and P. Liesi, *KDI tripeptide of gamma1 laminin protects rat dopaminergic neurons from 6-OHDA induced toxicity.* J Neurosci Res, 2006. **84**(3): p. 655-65.

188. Menezes, K., J.R. de Menezes, M.A. Nascimento, S. Santos Rde, and T. Coelho-Sampaio, *Polylaminin, a polymeric form of laminin, promotes regeneration after spinal cord injury.* FASEB J, 2010. **24**(11): p. 4513-22.

189. Tang-Schomer, M.D., J.D. White, L.W. Tien, L.I. Schmitt, T.M. Valentin, D.J. Graziano, A.M. Hopkins, F.G. Omenetto, P.G. Haydon, and D.L. Kaplan, *Bioengineered functional brain-like cortical tissue.* Proc Natl Acad Sci U S A, 2014. **111**(38): p. 13811-6.

190. Pottler, M., S. Zierler, and H.H. Kerschbaum, *An artificial three-dimensional matrix promotes ramification in the microglial cell-line, BV-2.* Neurosci Lett, 2006. **410**(2): p. 137-40.

191. Liesi, P., D. Dahl, and A. Vaheri, *Laminin is produced by early rat astrocytes in primary culture.* J Cell Biol, 1983. **96**(3): p. 920-4.

192. Chamak, B. and M. Mallat, *Fibronectin and laminin regulate the in vitro differentiation of microglial cells.* Neuroscience, 1991. **45**(3): p. 513-27.

193. Milner, R. and I.L. Campbell, *The extracellular matrix and cytokines regulate microglial integrin expression and activation.* J Immunol, 2003. **170**(7): p. 3850-8.

194. Tate, C.C., M.C. Tate, and M.C. LaPlaca, *Fibronectin and laminin increase in the mouse brain after controlled cortical impact injury.* J Neurotrauma, 2007. **24**(1): p. 226-30.

195. Milner, R. and I.L. Campbell, *Cytokines regulate microglial adhesion to laminin and astrocyte extracellular matrix via protein kinase C-dependent activation of the alpha6beta1 integrin.* J Neurosci, 2002. **22**(5): p. 1562-72.

196. Summers, L., C. Kielty, and E. Pinteaux, *Adhesion to fibronectin regulates interleukin-1 beta expression in microglial cells.* Mol Cell Neurosci, 2009. **41**(2): p. 148-55.

197. Summers, L., K. Kangwantas, L. Nguyen, C. Kielty, and E. Pinteaux, *Adhesion to the extracellular matrix is required for interleukin-1 beta actions leading to reactive phenotype in rat astrocytes.* Mol Cell Neurosci, 2010. **44**(3): p. 272-81.

198. Roche, M., P. Rondeau, N.R. Singh, E. Tarnus, and E. Bourdon, *The antioxidant properties of serum albumin.* FEBS Lett, 2008. **582**(13): p. 1783-7.

199. Potter, S.M. and T.B. DeMarse, *A new approach to neural cell culture for long-term studies.* J Neurosci Methods, 2001. **110**(1-2): p. 17-24.

200. Olivero, D., M. LaPlaca, and P.A. Kottke, *Ambient nanoelectrospray ionization with in-line microdialysis for spatially resolved transient biochemical monitoring within cell culture environments.* Anal Chem, 2012. **84**(4): p. 2072-5.